

**The Effect of Genistein on Thyroid
Hormone-dependent Tail Regression in the *Rana catesbeiana*
Tadpole**

by

Lan Ji

B.Sc., Shanghai Second Medical University, 1993

A Thesis Submitted in Partial Fulfillment of the Requirements for the Degree of

MASTER OF SCIENCE

In the Department of Biochemistry and Microbiology

© Lan Ji, 2005
University of Victoria

All rights reserved. This thesis may not be reproduced in whole or in part, by photocopying or by other means, without the permission of the author.

Supervisor: Dr. Caren C. Helbing

Abstract

Thyroid hormone (TH) regulated gene expression is mediated by TH binding to thyroid hormone nuclear receptors (TRs). Despite extensive studies in mammalian cells that showed that signaling pathways, such as the mitogen-activated protein kinase, cyclin-dependent-kinase, and tyrosine kinase signaling are involved in the regulation of diverse and important TH functions, little is known about their regulation and functional roles *in vivo* during development. Anuran metamorphosis is a postembryonic process that is absolutely dependent upon the presence of TH. Tadpole tail resorption is one of the last changes during anuran natural metamorphosis and is entirely controlled by TH. This process can be precociously induced by exogenous administration of 3,5,3'-triiodothyronine (T_3). In this study, it is shown that genistein inhibits T_3 -induced tail regression in the *Rana catesbeiana* tadpole. This inhibition is *via* inhibition of tyrosine kinase action rather than through genistein's classic estrogenic action. Quantitative polymerase chain reaction analysis demonstrates that genistein significantly attenuates T_3 -induced up-regulation of $TR\beta$ mRNA but not $TR\alpha$ mRNA. Further evidence shows that genistein affects T_3 -induced phosphorylation of $TR\alpha$, which indicates that phosphorylation is an important factor in establishing T_3 -dependent gene expression programs. Partial sequences of two inhibitor of growth (ING)1 variants were cloned from the tail (*rING1_{tail}*) and brain (*rING1_{brain}*) of *Rana catesbeiana*. *rING1_{brain}* mRNA is a T_3 -responsive gene and is down-regulated by genistein during the T_3 -induced tail regression program. cDNA array analysis suggests that gelatinase B may also require tyrosine kinase signaling during T_3 -dependent tadpole tail regression. Taken together, these findings demonstrate that genistein affects T_3 signaling in the context of normal cells *in*

vivo and indicate that phosphorylation is important for the establishment of T₃-dependent gene expression programs.

Table of contents

Abstract	ii
Table of Contents	iv
List of Tables	viii
List of Figures	viii
Acknowledgments	xii
List of Abbreviations	xiii
Chapter 1. INTRODUCTION	
I. Thyroid Hormone and Genistein Overview	1
II. Thyroid Hormone Background	2
i. Thyroid hormone synthesis and regulation	2
ii. Deiodinase enzymes involved in thyroid hormone activation and inactivation.....	4
III. Thyroid Hormone Classical Genomic Effects	8
i. Thyroid hormone receptor isoforms	10
ii. Thyroid hormone response elements	16
iii. Thyroid hormone receptor co-regulators	16
iv. Thyroid hormone receptor phosphorylation	20
IV. Thyroid Hormone Non-classical Effects	21
V. Thyroid Hormone Classical and Non-classical Effects – A Complex Model of Actions	27
VI. Thyroid Hormone Receptors and Estrogen Receptors Cross-talk	27
i. Estrogen action	27

ii. TR cross-talk with ER	28
VII. The Amphibian Model	32
VIII. Genistein	36
i. Genistein and soy formula	36
ii. Genistein and tyrosine kinase signaling pathway	38
iii. Estrogenic activity of genistein and breast cancer	39
iv. Genistein and thyroid hormone metabolism	41
IX. Research Hypothesis and Thesis Outline	42
Chapter 2. The Effect of Genistein on Thyroid Hormone-dependent Tadpole Tail Regression in <i>Rana catesbeiana</i>	
1. Introduction	44
2. Material and Methods	47
2.1 Experimental animals	47
2.2 Tail organ culture	47
2.3 <i>In vivo</i> T ₃ tadpole treatment	48
2.4 Tail measurement and analysis	49
2.5 Tissue homogenization for protein phosphorylation analysis	51
2.6 Preparation of RNA	51
2.7 Preparation of amplified RNA (aRNA)	52
2.8 Target preparation and labeling for cDNA array analysis.....	52
2.9 Multi-species analysis of gene expression cDNA hybridization	53
2.10 Array data analysis	55
2.11 Statistical analysis	58

2.12 Preparation of cDNA	58
2.13 Real-time quantitative polymerase chain reaction (QPCR)	59
2.14 Cloning and sequence analysis of ING1 (Rana inhibitor of growth 1) from <i>Rana catesbeiana</i> brain and tail	60
2.15 RT-PCR and densitometry analysis for <i>rING1_{brain}</i> transcripts expression in <i>Rana catesbeiana</i> tail	61
2.16 Immunoprecipitation (IP)	62
2.17 Immunoblotting	62
3. Results	63
3.1 Induction of T ₃ -dependent tadpole tail regression in serum-free organ culture	63
3.2 Genistein inhibits T ₃ -induced tadpole tail regression	64
3.3 Genistein reduces steady state levels of a 75 kDa protein phosphorylation during T ₃ -induced tail regression	69
3.4 Genistein blocks tail regression up to hours to days after T ₃ -treatment	69
3.5 cDNA array analysis to examine the effects of genistein on T ₃ -induced gene expression profiles	71
3.5.1 Determining stable normalizer genes for array data analysis	74
3.5.2 Identification T ₃ -responsive genes	79
3.5.3 T ₃ -responsive transcripts modulated by genistein during T ₃ -induced tail regression	83
3.6 Using reverse transcriptase quantitative real-time PCR (RT-QPCR) to examine effects of genistein on T ₃ -induced TR α , TR β , and HSP30	

gene expression profiles	88
3.6.1 T ₃ -induced TR α transcript levels are not affected by genistein	88
3.6.2 Genistein affects T ₃ -induced T ₃ -induced up-regulation of TR β	91
3.6.3 T ₃ up-regulated HSP30 expression is not affected by genistein	94
3.7 Isolation and determination of T ₃ -and genistein sensitivity of two <i>Rana</i> <i>catesbeiana</i> INGI (inhibitor of growth) genes	96
3.8 TR α steady state level of phosphorylation is reduced by genistein during T ₃ -induced tail regression	102
4. Discussion	102
5. Conclusions and future directions	111
Literature cited	113
Appendices cDNA Array Data Process	
Appendix 2.1 Variance analysis of twelve candidate normalizer genes	125
Appendix 2.2 Calculation of geometric mean and normalization factor (NF) based on the six normalizer genes.....	126
Appendix 2.3 Floor determination	127
Appendix 2.4 Intraclass correlation coefficient analysis sample integrity	128
Appendix 2.5.1 The normalized and floor adjusted final data applied for determination relative gene expression for 24 h injection set	129
Appendix 2.5.2 The normalized and floor adjusted final data applied for determination relative gene expression for 48 h injection set	135
Appendix 2.6.1 Fold change for all good data in the 24 h injection set	141
Appendix 2.6.2 Fold change for all good data in the 48 h injection set	144

Appendix 2.7 24 h set T ₃ -responsive genes variance analysis.....	147
Appendix 2.8 48 h set T ₃ -responsive genes variance analysis.....	148

List of Tables

Table 1.1 Characteristics of the human iodothyronine deiodinases	9
Table 1.2 Comparison of thyroid hormone classical and non-classical actions	23
Table 2.1 Descriptive statistics of twelve candidate normalizer genes based on their crossing point (CP) values	76
Table 2.2 Pair-wise correlation analysis of candidate normalizer genes.....	77
Table 2.3 T ₃ -induced gene expression profiles in the tail of <i>Rana catesbeiana</i> tadpoles in the 24 h injection set.....	80
Table 2.4 T ₃ -induced gene expression profiles in the tail of <i>Rana catesbeiana</i> tadpoles in the 48 h injection set.....	81
Table 2.5 Transcripts modulated by genistein during T ₃ -induced tail regression in <i>Rana catesbeiana</i> in the 24 h injection set	86
Table 2.6 Transcripts modulated by genistein during T ₃ -induced tail regression in <i>Rana catesbeiana</i> in the 48 h injection set	87

List of Figures

Figure 1.1 Structure of genistein in relation to estradiol	3
Figure 1.2 The steps of thyroid hormone biosynthesis and release	5
Figure 1.3 Structure of tyrosine, 3-monoiodotyrosine (MIT), 3,5-diiiodotyrosine (DIT), 3,5,3'-triiodothyronine (T ₃), and 3,5,3',5'-tetraiodothyronine (T ₄ , thyroxine).....	6
Figure 1.4 Regulation of thyroid hormone synthesis and secretion	7

Figure 1.5 General model for thyroid hormone action in the nucleus	11
Figure 1.6 A schematic representation of the four functional domains of the thyroid hormone receptor is shown in (a). The protein products of the thyroid hormone receptor alpha and beta genes (<i>THRA</i> and <i>THRB</i>) are shown in (b)	12
Figure 1.7 DNA-binding domain of human TR α	13
Figure 1.8 TR α -1 ligand-binding domain (LBD) crystal structure	15
Figure 1.9 Half-site orientation and optimal nucleotide spacing between half-sites of thyroid hormone response element (TRE)	17
Figure 1.10 A molecular model for (a) basal repression by corepressors in the absence of T ₃ and (b) transcriptional activation by coactivators in the presence of T ₃	18
Figure 1.11 Schematic representation of the proposed mechanism by which thyroid hormone activates the MAPK (mitogen activated protein kinase) and STAT (signal transducer and activators of transcription) signaling pathways	25
Figure 1.12 A schematic representation of the four functional domains of the estrogen receptor protein is shown in (a). The protein products of the estrogen receptor alpha and beta are shown in (b).....	29
Figure 1.13 The role of ER coregulators in gene transcription regulation.....	30
Figure 1.14 Thyroid hormones are the central trigger for tadpole metamorphosis.....	33
Figure 1.15 Structure of genistein in relation to tamoxifen	37
Figure 2.1 Experimental design of effects of genistein on T ₃ -induced tadpole tail	

regression	50
Figure 2.2 100 nM T ₃ and 10 nM T ₃ induce T ₃ -dependent tadpole tail regression	
serum-free organ culture.....	65
Figure 2.3 100 μM genistein inhibits T ₃ -induced tadpole tail regression	66
Figure 2.4 Genistein inhibits protein phosphotyrosine level during T ₃ -induced	
tail regression	70
Figure 2.5 Genistein inhibits T ₃ -induced tail regression in serum-free organ culture	
within 24 h	72
Figure 2.6 Expression of six normalizer genes and their geometric	
mean across all 24 arrays	78
Figure 2.7 Cluster analysis of transcripts responsive to T ₃ in the tadpole tail tissue of	
<i>Rana catesbeiana</i>	84
Figure 2.8 T ₃ -dependent TRα expression is not affected by genistein	90
Figure 2.9 Genistein affects T ₃ -induced up-regulation of TRβ	92
Figure 2.10 T ₃ -dependent increase in HSP30 expression is not affected	
by genistein.....	95
Figure 2.11 Sequence alignments of transcripts variants for <i>rING1_{brain}</i> and <i>rING1_{tail}</i>	
and their putative encoded proteins	97
Figure 2.12 Expression of the <i>rING1_{brain}</i> transcript during natural and T ₃ -precocious	
metamorphosis in the <i>Rana catesbeiana</i> tail	98
Figure 2.13 Relative expression levels of <i>rING1_{brain}</i> in the tadpole injection	
followed by genistein inhibition study	101
Figure 2.14 Genistein inhibition T ₃ -induced TRα phosphorylation	103

Figure 2.15 Summary of effects of genistein on T₃-induced TR α and TR β , HSP30, and *rING1_{brain}* mRNA expression levels in the 24 h injection set (A) and in the 48 h injection set (B)106

ACKNOWLEDGMENTS

I am grateful to thank my supervisor, Dr. Helbing, for her unwavering support and faith in my abilities. She introduced and help me transition from a clinical doctor to a scientific researcher. I wish to thank my committee members, Dr. J. Ausio and Dr. W. Hintz, for their encouragement and scientific support. I also thank Dr. Nik Veldhoen for his advice on all topics. I am very appreciative of Mary Wagner in providing primers and her advice on my cross species cloning of rING. I thank Dominik Domanski for his invaluable discussion for my protein work. Rachel Skirrow deserves high praise for giving so much her time to the pursuit of my organ culture work, and Carmen Bailey, for her excellent technical assistance of my microarray work. I thank D. Brown provide TR α antibodies. To my past and present lab members, Dr. Fang Zhang, Dr. Mark Gunderson, and Maki Tabuchi, I thank you for your generous help during the process. My husband, Wei Ding, gave me invaluable support in the completion of this work. I would also like to thank my parents who took care of my daughter in my difficult time.

List of Abbreviations

5'-D	5'-deiodinase
5'-D-I	5'-deiodinase-I
5'-D-II	5'-deiodinase-II
°C	Degree Celsius
aRNA	Amplified RNA
AIB	Amplified in breast cancer-1 protein
ATP	Adenosine triphosphate
bp	Base pair
C/EBP	CCAAT/enhancer core binding protein
CAT	TRE-chloramphenicol acetyltransferase
CBP	CREB-binding protein
Cdk	Cyclin-dependent-kinase
cDNA	Complementary deoxyribonucleic acid
Ci	Curie
CP	Cross points
CREB	cyclic adenosine monophosphate-response element-binding protein
CTD	Carboxy-terminal domain
d	Day
DAD-1	Defender against cell death 1
dATP	Deoxyadenosinetriphosphate
DBD	DNA-binding domain
D-D	Tadpole injected with DMSO and tail tip incubated in DMSO-containing medium

DMBA	7,12-dimethylbenzanthracene
DEPC	Diethyl pyrocarbonate
D-G	Tadpole injected with DMSO and tail tip incubated in genistein-containing medium
DIT	Diiodotyrosine
DLL4	Distal-less 4
DMSO	Dimethyl sulfoxide
DNA	Deoxyribonucleic acid
dNTP	Deoxynucleotidetriphosphate
DRIPs	Vitamin D receptor interactin proteins
DRs	Direct repeats
DTT	Dithiothreitol
E ₂	17 β -estradiol
EGFR	Epidermal growth factor receptor
EMSA	Electrophoretic mobility shift assays
ER	Estrogen receptor
ERE	Estrogen response elements
ERK	Extracellular regulated protein kinase
EtBr	Ethidium bromide
EtOH	Ethanol
G	Genistein
GAPDH	Glyceraldehyde-3-phosphate dehydrogenase
GM	Geometric mean
GPCR	G protein-coupled receptor

GSK-3	Glycogen synthase kinase 3
GTF	General transcription factor
h	hour
HATs	Histone acetyl transferase
HBD	Hormone binding domain
HDAC1	Histone deacetylase 1
HPT	Hypothalamic/pituitary/thyroid axis
HRE	Hormone response elements
HSP	Heat shock protein
IFN- γ	Human interferon- γ
IGFR	Insulin-like growth factor receptor
ING1	Inhibitor of growth 1
IP	Immunoprecipitation
IPs	Inverted palindromes
K _d	Dissociation constant
LB medium	Luria-Bertani medium
LBD	Ligand-binding-domain
Lyz	Lysozyme
m	Milli
μ	Micro
M	Molarity
MAGEX	Multispecies analysis of gene expression
MAPK	Mitogen-activated protein kinase

μCi	microCurie
MEK	MAPK/ERK activating kinase
mg	Milligram
MHC	Major histocompatibility complex
MIT	3-monoiodotyrosine
ml	Millitre
μl	Microlitre
mm	Milmetre
mM	Millimolar
mRNA	messenger RNA
mSin3A	Mammalian Sin3
mtPPAR	Mitochondrial peroxisome proliferator activator receptor
mtRXR	Mitochondrial retinoid X receptor
NCoR	Nuclear receptor co-repressor
NF	Normalization factor
nm	Nanometre
P/CAF	p300/CBP-associated factor
p160/SRCs	Steroid receptor co-activators
p300/CBP	cAMP-response element-binding protein
pal	Palindromes
PCR	Polymerase chain reaction
PDGFR	Platelet-derived growth factor receptor
PHD finger	Plant homeodomain finger

PI3K	Phosphoinositide-3 kinase
PKA	Protein kinase A
PKC	Protein kinase C
PLC	Phospholipase C
PLD	Phospholipase D
pmol	picomole
PTK	Protein tyrosine kinase
QPCR	Quantitative PCR
RARs	Retinoic acid receptors
RNA	Ribonucleic acid
rT ₃	Reverse T ₃
RT-PCR	Reverse transcription-PCR
RXR	Retinoid X receptor
RXR _s	Retinoid X receptors
SD	Standard deviation
SDS	Sodium dodecyl sulfate
SDS-PAGE	SDS-polyacrylamide gel electrophoresis
SMRT	Silencing mediator of retinoid and thyroid hormone receptors
SPARC	Secreted protein acidic and rich in cysteine
SPI+	Soy protein isolate
SRC-1	Steroid receptor coactivator-1
SSC	Sodium chloride and sodium citrate
ST3	Stromelysin 3

STAT	Signal transducers and activators of transcription
T ₃	3,5,3'-triiodothyronine
T ₄	Thyroxine
TAF	TBP associated factor
Taq	DNA <i>Thermus aquaticus</i> DNA polymerase
TBG	Thyroxine binding globulin
TBP	TATA box binding protein
T ₃ -D	Tadpole injected with T ₃ and tail tip incubated in DMSO-containing medium
TF	Transcription factor
Tg	Thyroglobulin
T ₃ -G	Tadpole injected with T ₃ and tail tip incubated in genistein-containing medium
TGF	Transforming growth factor
TH	Thyroid hormone
TH/bZIP	TH-induced basic leucine-zipper containing transcription factor gene
TK stage	Taylor and Kollros stage
TMEM	Tadpole minimal essential medium
TPO	Thyroid peroxidase
TR	Thyroid hormone receptor
TRAPs	Thyroid receptor associated proteins
TRE	Thyroid hormone response element
TRH	Thyrotropin releasing hormone
TSH	Thyroid stimulating hormone or pituitary thyrotropin

Chapter 1. Introduction

I. Thyroid Hormone and Genistein Overview

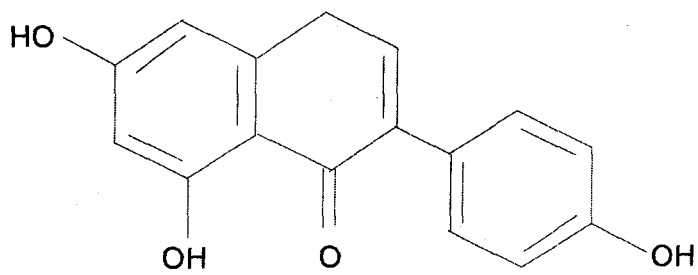
The thyroid hormones (THs), 3,5,3'-triiodothyronine (T_3) and 3,5,3',5'-tetraiodothyronine (T_4 , thyroxine), play critical roles in the growth, metabolism, differentiation, and apoptosis of nearly all tissues in a variety of organisms such as fish, amphibia, and higher vertebrates [1]. During the past century, advances in clinical medicine, physiology, biochemistry, and molecular genetics have greatly enhanced our understanding of TH action. In humans, thyroid gland disorders are one of the most common endocrine diseases. For example, endemic cretinism (caused by iodine deficiency and subsequent lack of TH synthesis) is still a huge public health problem in developing countries. In North America, about 7% of the population has thyroid disease making this the most common endocrine disorder. Neonatal hypothyroidism can cause mental retardation and permanent neurological defects because TH is responsible for myelin basic protein synthesis and myelination of axons in the brain [1]. TH is required for the homeostasis of nearly all organs in the human body, including brain, bone, heart, and liver. The study of TH action has great biological and medical implications. Molecular genetics has provided insight into our understanding of the mechanisms of TH action in normal and disease states. Recent studies at the molecular level have demonstrated that TH regulates target gene expression through genomic effects by binding thyroid hormone nuclear receptors (TRs) [1]. However, there is increasing

evidence of signaling transduction and membrane receptors [2] or transporters [3-5] that could affect TH genomic action [6-10].

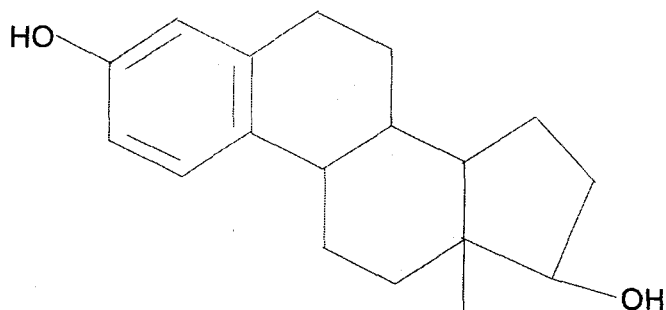
Genistein (4',5,7—trihydroxyisoflavone) is a precursor of phytoalexins in legumes and an important nutraceutical molecule found in soybean seeds [11]. Genistein, a phytoestrogen, has structural similarity to 17β estradiol (**Figure 1.1**) and a wide variety of pharmacological effects on animal cells [11]. In the last 10 years, two important observations have significantly shaped research on genistein. Since 1991, many epidemiological studies have reported that Asian women who consume traditional diets (high in soy products) have low incidences of breast cancer [12]. This finding suggests a possible correlation between soy diet and morbidity of breast cancer. Based on both epidemiological and animal model studies, genistein has been linked with a variety of potential beneficial health effects, which include: chemoprevention of breast [12, 13] and prostate cancers [14], cardiovascular disease [15], osteoporosis [16] and relief of menopausal symptoms [17]. Most of these effects are associated with genistein's estrogenic activity. Moreover, *in vitro* research has demonstrated that genistein can act as a specific inhibitor of tyrosine kinases [18] affecting different growth factor signaling pathways in cells [7, 19, 20]. Further, a series of *in vitro* and *in vivo* studies has demonstrated that genistein can also inhibit thyroid peroxidase (TPO) [7, 19-24] and 5'-deiodinase (5'-D) [25], two important enzymes involved in the synthesis and metabolism of TH. It is not known whether genistein can affect TH signaling at the cellular level leading to a change in biological consequence.

II Thyroid Hormone Background

i. Thyroid hormone synthesis and regulation.



Genistein



Estradiol

Figure 1.1. Structure of genistein in relation to estradiol.

Modified from Dixon *et al.* [11].

Thyroid hormones are synthesized in the follicular cells of the thyroid gland under the regulation of pituitary thyrotropin (TSH) [26, 27]. Initially, thyroglobulin (Tg), a large globular glycoprotein containing tyrosine residues, is synthesized in the follicular cells and transported to the cell surface (**Figure 1.2**). Once at the surface, thyroglobulin is iodinated by thyroid peroxidase (TPO), a membrane-bound heme-protein enzyme located at the apical surface, which activates I^- and couples iodinated tyrosines to form thyronines. The iodinated Tg containing 3-monoiodotyrosine (MIT), 3,5-diiodotyrosine (DIT), T_3 , and T_4 (thyroxine) (**Figure 1.3**) is transported to the lumen of thyroid follicles as a component of colloid. With the stimulation of TSH, the iodinated Tg, stored in the lumen of follicles is endocytosed into the follicular cells and hydrolyzed. Tg hydrolysis occurs within the endolysosome and releases MIT, DIT, T_3 and T_4 . Only T_3 and T_4 diffuse from the cell into the capillary network surrounding the follicles.

TH synthesis and secretion is accurately regulated by a negative-feedback system that involves the hypothalamus, pituitary, and thyroid gland (hypothalamic/pituitary/thyroid (HPT) axis) (**Figure 1.4**). TH negatively regulates both thyrotropin releasing hormone (TRH) and TSH secretion [26, 27] in mammals. However, in anuran amphibian, instead of TRH, it is corticotrophin releasing factor (CRF) that acts as a stimulator to release TSH from the pituitary gland [28].

ii. Deiodinase enzymes involved in thyroid hormone activation and inactivation.

Most of the circulating thyroid hormones (about 99%) are bound reversibly to plasma carrier proteins, such as thyroxine binding globulin (TBG), albumin, and thyroid binding prealbumin (also called transthyretin). Only the free TH enters target cells to exert biological effects [27]. In most cases, T_4 is the major circulating thyroid hormone

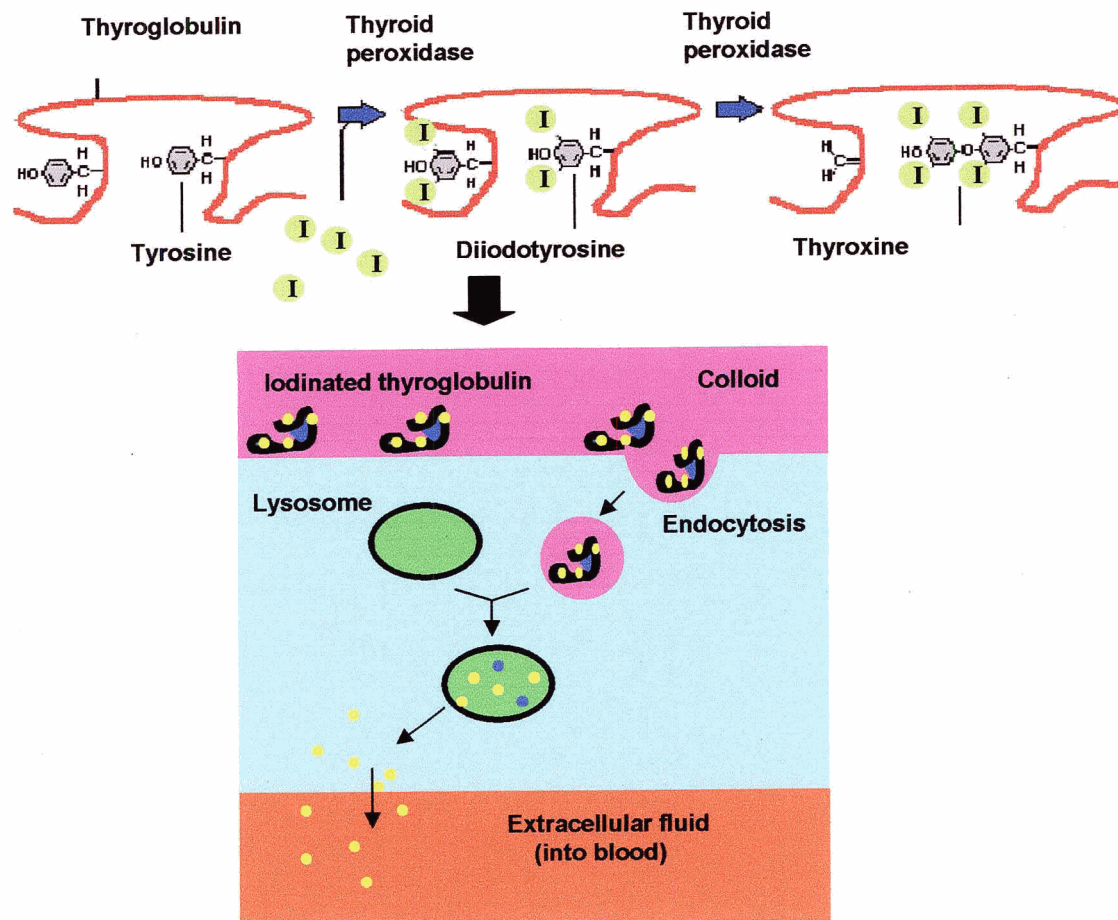


Figure 1.2. The steps of thyroid hormone biosynthesis and release.

The yellow circles represent 3,5,3'-triiodothyronine (T₃) and 3,5,3',5'-tetraiodothyronine (T₄, thyroxine). The blue circles denote 3-monoiodotyrosine (MIT) and 3,5-diiodotyrosine (DIT).

Modified from

<http://arbl.cvmb.colostate.edu/hbooks/pathphys/endocrine/thyroid/physio.html>

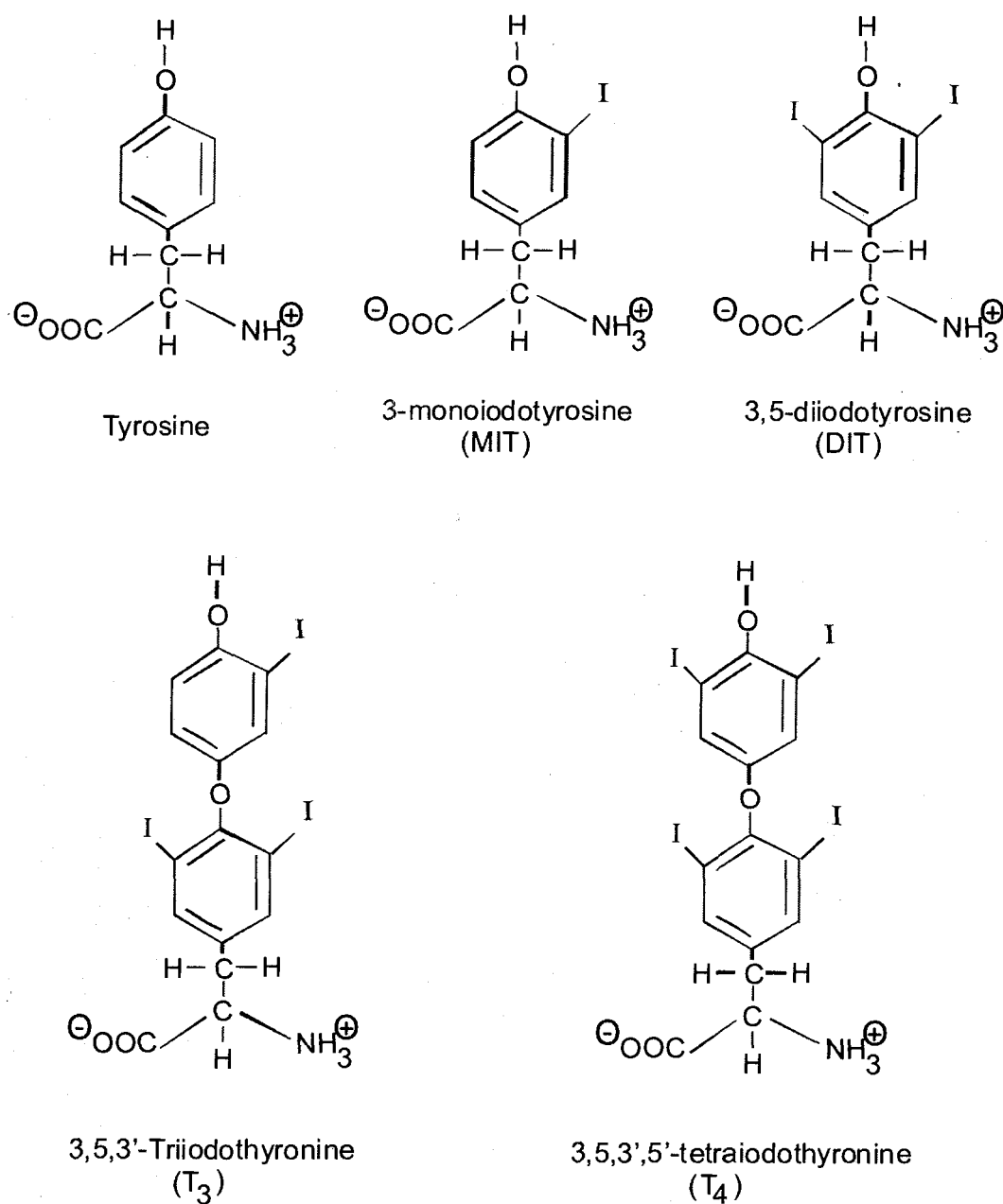


Figure 1.3. Structure of tyrosine, 3-monoiodotyrosine (MIT), 3,5-diiodotyrosine (DIT), 3,5,3'-triiodothyronine (T₃), and 3,5,3',5'-tetraiodothyronine (T₄, thyroxine).

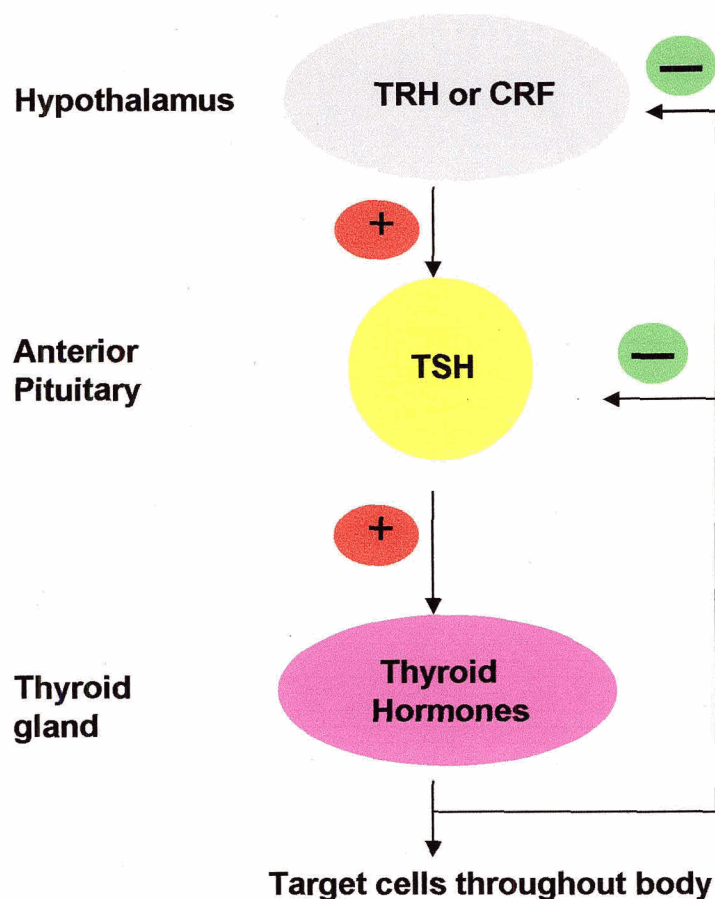


Figure 1.4. Regulation of thyroid hormone synthesis and secretion.

The thyroid gland is part of the hypothalamic-pituitary-thyroid axis, and control of thyroid hormone secretion is exerted by classical negative feedback. Thyroid-releasing hormone (TRH) (in mammals) or corticotrophin releasing factor (CRF) (in anuran amphibian) from the hypothalamus stimulates TSH from the pituitary, which stimulates thyroid hormone release. As blood concentrations of thyroid hormones increase, they inhibit both TSH and TRH or CRF, leading to "shutdown" of thyroid epithelial cells. Later, when blood levels of thyroid hormone have decayed, the negative feedback signal fades, and the system wakes up again. Modified from <http://arbl.cvmb.colostate.edu/hbooks/pathphys/endocrine/thyroid/physio.html>

(in mammals, total serum T_4 is 40-fold higher than serum T_3) and is converted to T_3 by 5'-deiodinase (5'-D) at peripheral tissues [1]. There are two types of 5'-deiodinases known in mammals, 5'-deiodinase-I (5'D-I) which is found primarily in the liver, kidney, and thyroid and 5'-deiodinase II (5'D-II) which is found in the brain, pituitary, and placenta (Table 1.1). A third deiodinase, 5-deiodinase-III (5 D-III), found in the brain and placenta, can convert T_3 to T_2 . Free T_3 is the most biologically active form of the hormone [1].

III. Thyroid Hormone Classical Genomic Effects

T_3 and T_4 are hydrophobic, and their mechanisms of action are similar to those of steroid hormones. TH, like steroid hormones that have a lipophilic nature, is thought to enter target cells by passive diffusion. However, there is some evidence to support the concept that a carrier system is important for both steroid and thyroid hormones to enter cells. For example, Ritchie *et al.* [3] using *Xenopus* oocytes demonstrated that System L serves as a plasma membrane transporter of T_3 to the nucleus and enhances transcriptional activation by TRs. Conversely, specific inhibitors blocking System L activity decreases both T_3 uptake and TR function.

Early studies showed that the effects of TH at the genomic level are mediated by the binding of TH to nuclear TRs. In the nucleus, TH binds to TRs with high affinity and specificity. The K_d (dissociation constant) of T_3 is about 10^{-10} M [29]. TRs, which have 10-fold greater affinity for T_3 than T_4 [29], function as monomers, homodimers, and heterodimers [1]. The heterodimer is commonly formed between TRs and retinoid X receptors (RXRs). RXR heterodimerization with TR enhances the specificity and efficiency of the receptor interaction with the thyroid response elements (TREs) thereby

Table 1.1. Characteristics of the human iodothyronine deiodinases. Adapted from Griffin *et al.* [29].

	Type I	Type II	Type III
Deiodination site	5' and 5	5'	5
Physiologic roles	<ul style="list-style-type: none"> ● Provide T₃ for the circulation ● Inactivate T₄ and T₃ ● Degrade rT₃ 	<ul style="list-style-type: none"> ● Provide intracellular T₃ in pituitary, brain, and brown adipose tissue ● Provide T₃ for the circulation 	<ul style="list-style-type: none"> ● Inactivate T₄ and T₃
Tissue location	Liver, kidney, thyroid, brain	Pituitary, brain, brown adipose tissue, placenta, thyroid, skeletal and cardiac muscle	Brain, placenta, skin

modulating transcriptional activity [1]. TRs regulate gene expression by binding to specific TREs in the promoters of T₃-target genes then activate or repress transcription in response to hormone [30-32]. In unliganded state, TRs associate with co-repressors and then actively repress transcription. In the presence of T₃, TRs dissociate from co-repressors and bind to co-activators and activate transcription (**Figure 1.5**). These nuclear actions (called the classical genomic effects) of T₃ are sensitive to inhibitors of transcription and translation and have a considerable latency with response times in hours to days [1].

i. Thyroid hormone receptor isoforms.

Vennstrom and Evans first cloned TR in 1986 from embryonic chicken (TR α) and human placental (TR β) cDNA libraries [33, 34], respectively, and showed that TRs are the cellular homologues of *v-erb A*, a known viral oncogene. Presently, TRs belong to a large superfamily of nuclear hormone receptors including steroid, vitamin D, retinoic acid receptors, and “orphan” receptors, which have no known ligand or function [1].

The two different genes *THRA* and *THRB* encode eight nuclear TR isoforms due to alternative splicing or alternative promoter usage (**Figure 1.6b**). TR α and TR β are encoded on human chromosomes 17 and 3 respectively. All isoforms of TR share a similar domain organization (**Figure 1.6a**): an amino-terminal A/B domain, a central DNA-binding domain (DBD) containing two “zinc fingers” (**Figure 1.7**), a hinge region (lysine-rich sequence that is highly conserved among TRs) containing the nuclear localization signal, and a carboxyl-terminal ligand-binding domain (LBD). The DBD is localized N-terminal to these domains and the two zinc-fingers are responsible for the

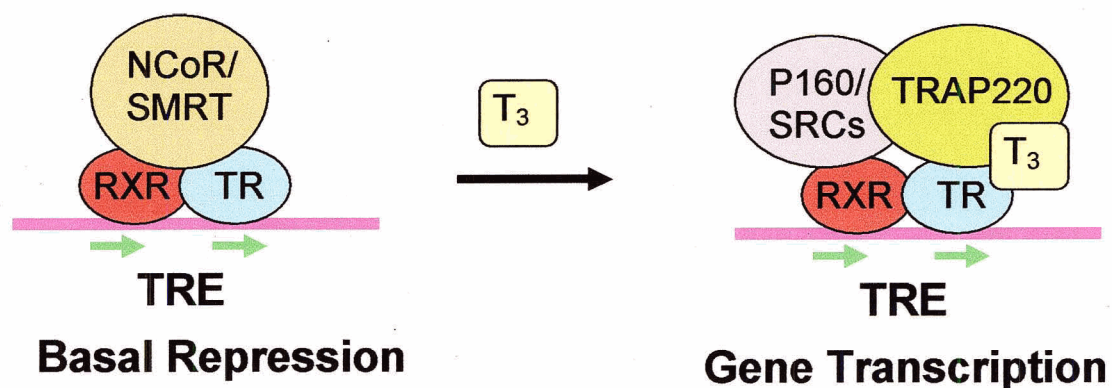


Figure 1.5. General model for thyroid hormone action in the nucleus.

In the nucleus, unliganded TR associates with co-repressors NCoR (nuclear receptor co-repressor) and SMRT (silencing mediator of retinoid and TH receptors) and then actively represses transcription. T₃ binding of the TR leads to dissociation of co-repressors and binding of co-activators p160/ SRCs (steroid receptor co-activators) and TRAPs (thyroid receptor associated proteins). This results in the relief of basal transcriptional repression and induction of transcription. The green arrows denote direct repeats of TRE half-sites. Abbreviations: thyroid hormone receptor (TR), retinoid X receptors (RXR), thyroid hormone responsive element (TRE). Modified from Bassett *et al.* [30].

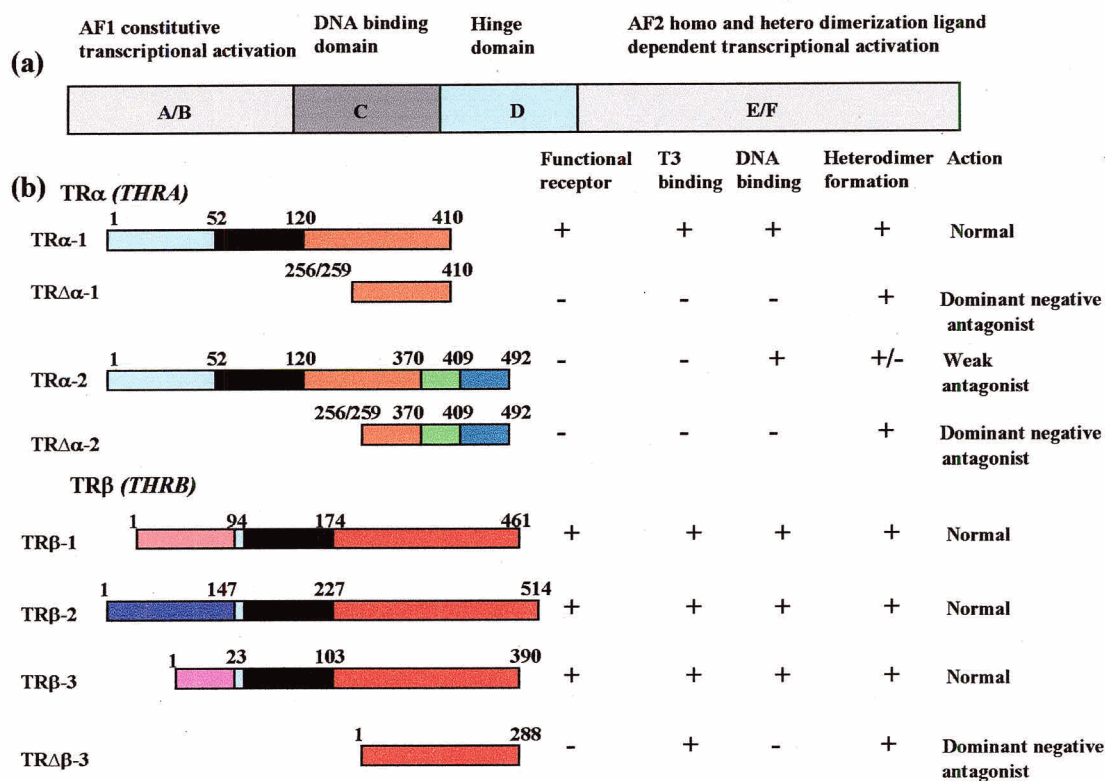


Figure 1.6. A schematic representation of the four functional domains of the thyroid hormone receptor protein is shown in (a). The protein products of the thyroid hormone receptor alpha and beta genes (*THRA* and *THRB*) are shown in (b).

The TR isoforms are generated by alternative splicing or alternative promoter usage of the two TR genes encoding TR α and TR β . Colours represent identical or divergent regions that result from alternative mRNA splicing. The filled black region represents the DNA binding domain. Modified from Bassett *et al.* [30].

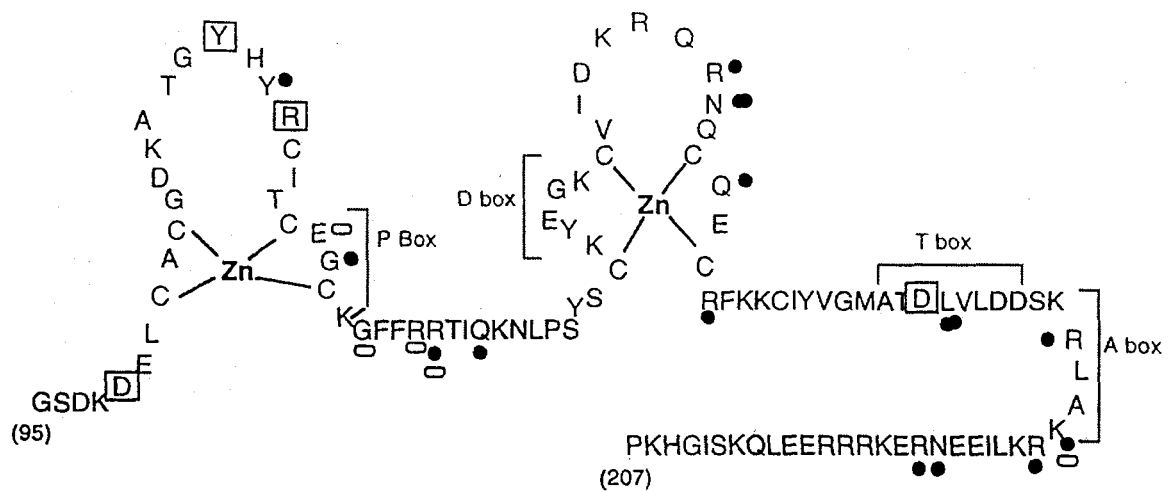


Figure 1.7. The DNA-binding domain of human TR α .

Schematic drawing of the two zinc fingers of human TR α and the various subregions within the DNA-binding domains. Squares, TR/RXR heterodimerization contacts; ovals, direct base contacts; solid circles, direct phosphate contacts. Adapted from Yen *et al.* [1].

binding to TREs and also for dimerization. The LBD is not only critical for TH binding but also necessary for dimerization, transactivation, and basal repression by unliganded TRs [1]. The LBD consists of 12 α -helices that are arranged to create a pocket for ligand binding (**Figure 1.8**). The helix 12 is essential for the switch of the receptor from a silencer to an activator. In the absence of TH, helix 12 protrudes away from the core structure of the LBD and allows corepressor binding. TH binding induces helix 12 to contact to the LBD core, which results in corepressor release and coactivator association [35]. Deletion of helix 12 leads to constitutive silencing even in the presence of ligand [36]. This indicates that helix 12 is involved in the coordination of repression and activation.

Five out of eight TR isoforms (**Figure 1.6b**) TR α 1, and TR β 1, TR β 2, TR β 3 and TR Δ β 3 can bind T₃. Three isoforms TR α 2, TR Δ α 1, TR Δ α 2, which are derived from the TR α locus, are not able to bind T₃ and act as TR inhibitors [37]. TR Δ α 1 and TR Δ α 2 lack the DBD. TR α 2 cannot bind T₃ because its carboxyl-terminal replaces a region (122-amino acids) in TR α 1 that is critical for TH binding [1].

TR α 1, TR α 2, TR β 1 and TR β 3 are expressed ubiquitously in all tissues, whereas TR β 2 is predominantly restricted to the hypothalamic/pituitary axis. TR β 2 acts as a negative regulator of thyroid stimulating hormone (TSH) α - and β - subunit transcription [30]. Selective generation of transgenic and knockout mouse models has shed light on the roles of TRs in the regulation of specific target genes and development. These studies indicated that TR α is responsible for postnatal development, heart rate and temperature regulation. The TR β seems to be mainly involved in the appropriate maturation of cochlear and retinal cells and the regulation of liver metabolism [38].

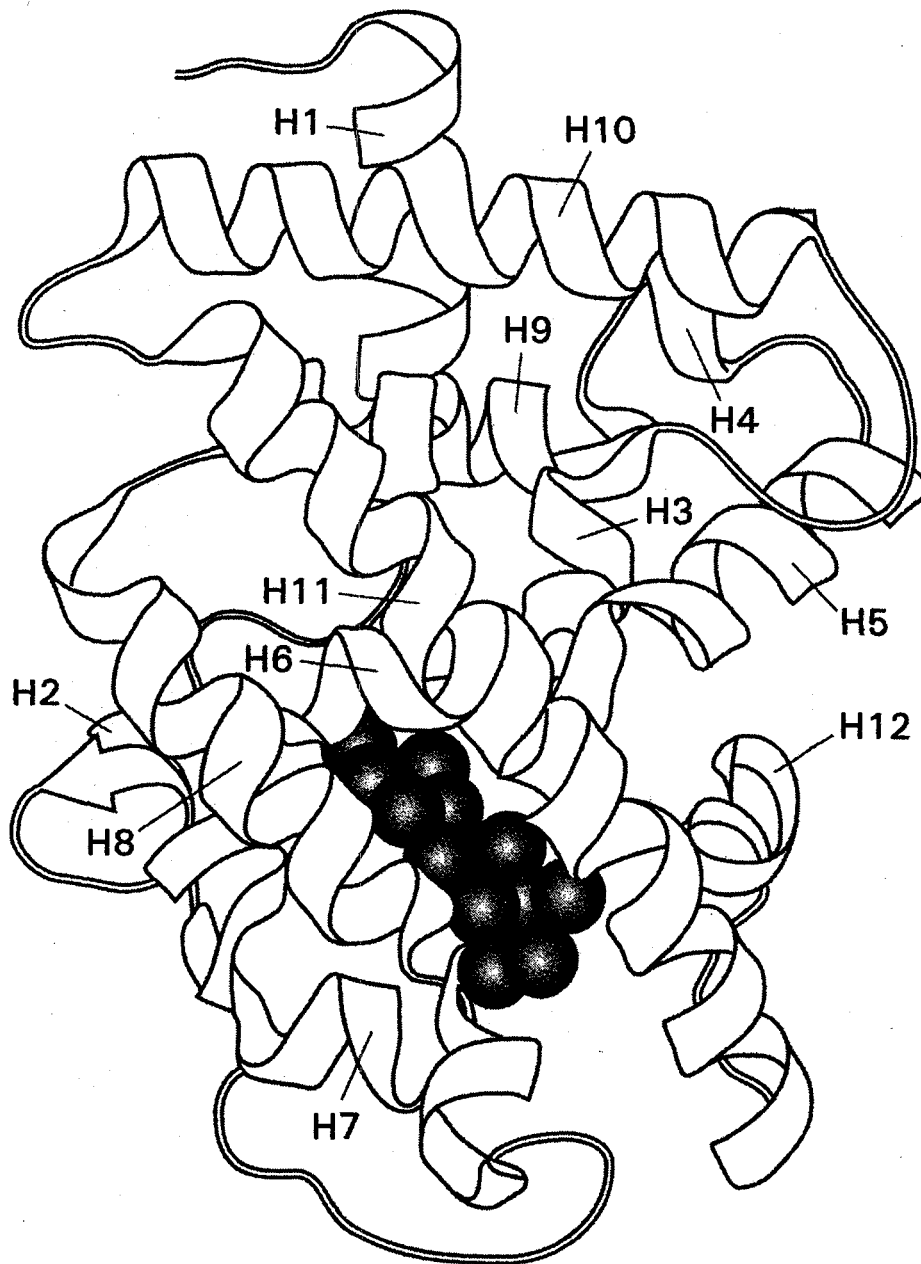


Figure 1.8. TR α -1 ligand-binding domain (LBD) crystal structure.

α -Helices (H) are indicated and the T₃ ligand is represented as a series of dark spheres.

Adapted from Yen *et al.* [1]

ii. Thyroid hormone response elements.

TRs bind to the thyroid hormone response elements (TREs), which contain consensus hexamer half-site sequences (G/A)GGT(C/G)A, as monomers, homodimers, and heterodimers. Most TREs are located upstream of the promoter. There is considerable variation in the nucleotide sequences, number, spacing, and orientation of TRE half-sites. Half-sites are arranged as palindromes (TREpal), direct repeats (DRs), and inverted palindromes (IPs). Among 30 known natural TREs, DRs are more common than IPs which are more common than TREpal [1]. The optimal spacing for these half-site arrangements is zero, four, and six nucleotides, respectively (TREpal0, DR4, and IP6) (Figure 1.9).

iii. Thyroid hormone receptor co-regulators.

The classical genomic model of steroid hormone action dictates that ligand binding leads to a conformational change in the nuclear receptor, which results an exchange of co-activators/accessory proteins. In the nucleus, the ligand/receptor complex binds DNA at hormone response elements (HREs) in the promoters of target genes leading to chromatin modification and regulation of gene transcription [39]. *In vitro* and *in vivo* studies in *Xenopus laevis* have shown that co-repressor/co-activators recruited to unliganded or liganded TRs bind to TREs regulating target gene transcription [32, 40].

In the absence of TH (Figure 1.10a), the corepressor complexes, which contain histone deacetylases (HDACs), bind to helices three and five of the unliganded TR LBD [30]. This TR/RXR/corepressor complexes leads to histone deacetylation and gene repression. There are two well-characterized corepressors: nuclear receptor corepressor

CONSENSUS TRE HALF-SITE

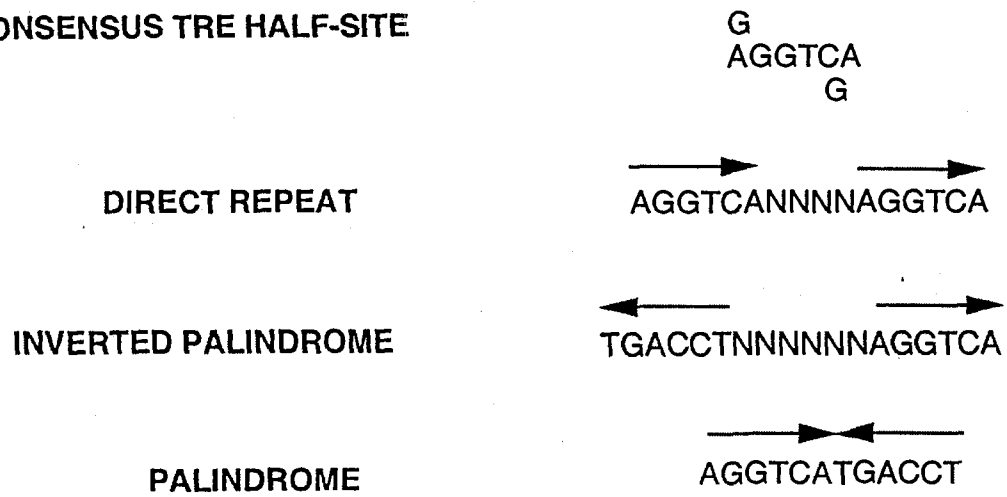


Figure 1.9. Half-site orientation and optimal nucleotide spacing between half-sites of thyroid hormone response element (TRE).

N refers to nucleotides, and arrows show direction of half-sites on the sense strand.

Adapted from Yen *et al.* [1].

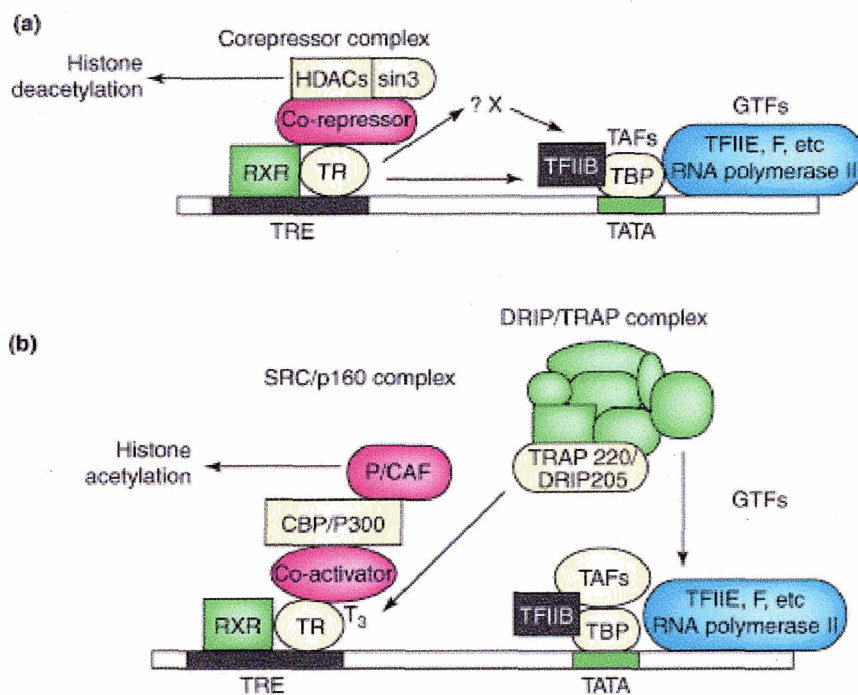


Figure 1.10. A molecular model for (a) basal repression by corepressors in the absence of T_3 and (b) transcriptional activation by coactivators in the presence of T_3 .

Abbreviations: cAMP-response element-binding protein (CBP), vitamin D receptor-interacting protein (DRIP), general transcription factor (GTF), histone deacetylase (HDAC), p300/CBP-associated factor (P/CAF), retinoid X receptor (RXR), steroid receptor coactivator (SRC), TATA-binding protein-associated factor (TAF), TATA-binding protein (TBP), transcription factor (TF), thyroid hormone receptor (TR), TR-associated protein (TRAP), thyroid hormone-response element (TRE). Adapted from Yen *et al.* [41].

(NCoR) and silencing mediator of retinoid and TH receptors (SMRT). NCoR, a 270-kDa protein, can interact with both RXRs and retinoic acid receptors (RARs). NCoR also interacts with preinitiation transcriptional complex II members, TFIIB, TAFII32, and TAFII7. Therefore, part of its ability to repress transcription may be due to its ability to interact with the preinitiation transcriptional complex. SMRT, containing sequence homology to NCoR, is able to modulate basal repression of TRs and RARs in cotransfection studies [42, 43]. Moreover, corepressors can complex with other repressors, such as Sin3 and histone deacetylase 1 (HDAC1). Thus histone deacetylation, which helps maintain local chromatin structure in a repressive state, may play a critical role in basal repression by nuclear hormone receptors [1, 40].

When TH is present (**Figure 1.10b**), corepressor complexes dissociate from TR/RXR heterodimers. Coactivator complexes, which often contain histone acetyltransferase (HATs) activity, can then bind to TR/RXR heterodimers, leading to histone acetylation and gene expression. So, it is hypothesized that TH activates gene transcription in part by increasing local acetylation of histone [1]. Steroid receptor coactivator (p160/SRC1) is an example of a co-activator having intrinsic HAT activity. The SRC1-associated protein, cAMP-response element-binding protein (p300/CBP), directly binds RNA polymerase II thus acting as an adaptor protein for liganded TR/RXR and the basal transcriptional machinery [30]. In addition to coactivator complexes having histone acetyltransferase activities, other coactivator complexes have been identified. TR associated proteins (TRAPs) or Vitamin D receptor interacting proteins (DRIPs) are other well characterized co-activators which lack HAT activity. The critical co-activator

TRAP220 anchors a TRAP/DRIP complex of proteins that mediates RNA polymerase II binding [44].

A two-stage process of liganded TR/RXR mediate transcriptional activation has been proposed [30]. First, the p160/SRC proteins initially recruit HAT activity leading to chromatin remodeling. This process may then be followed by recruitment of TRAP220 and the TRAP/DRIP complex of proteins to promote gene transcription in a hormone-dependent fashion.

iv. Thyroid hormone receptor phosphorylation.

Phosphorylation has been reported to modulate TR-mediated regulation of transcription both *in vitro* and *in vivo*. Sugawara *et al.* [45] assessed the effect of phosphorylation on the binding of TR β 1 to a TRE by using an electrophoretic mobility shift assay *in vitro*. They expressed human TR β 1 (hTR β 1) in bacteria and phosphorylated it with ATP (the ratio of phosphoserine to phosphothreonine was 5:1) in HeLa cytosolic extract, which lacks endogenous TRs. They found that phosphorylation of hTR β 1 selectively increases binding of the TR homodimer, but not the TR/RXR heterodimer, to TRE. Addition of alkaline phosphatase to phosphorylated hTR β 1 eliminates this increase in TRE binding. However, Bhat *et al.* [46] demonstrated *in vitro* that phosphorylation of TR β 1 enhances TR/RXR heterodimer binding to three different TREs: i) the chicken lysozyme (lyz) gene TRE, ii) Direct repeats of a half-site separated by four gaps (DR4), and iii) a palindromic (Pal) TRE. Furthermore, they cotransfected hTR β 1, RXR β and TRE-chloramphenicol acetyltransferase (CAT) expression plasmid into CV-1 cells. Using the CAT reporter gene in the absence or presence of okadaic acid, an inhibitor of phosphatases, they showed that okadaic acid enhances hTR β 1-mediated CAT activity.

Although the mechanism of this enhanced transcriptional activation is unknown, these findings suggest that phosphorylation, in addition to ligand binding, may modulate TR-mediated transcription. It is hypothesized that phosphorylation regulates the transcriptional activity of hTR β 1 at several levels [46]. Phosphorylation affects the DNA-binding of both homodimers and heterodimers. It increases the ability of homodimers to bind DNA. As for heterodimers, unphosphorylated hTR β 1/RXR heterodimers bind weakly in the order of DR4 > lyz > Pal. After phosphorylation, not only the binding ability of the heterodimers were enhanced, but also the order of binding activity changes to lyz > DR4 > Pal. Therefore, the extent of TRE binding enhancement depends on the orientation of the half-site binding motifs, suggesting that this increase is mediated by phosphorylation-induced conformational change. The above studies have focused on TR β . There are limited studies on TR α phosphorylation. One study showed that phosphorylation of rat TR α enhances its nuclear localization [47], but its functional and biological roles are unclear. Thus phosphorylation may be one of the mechanisms by which TRs achieve their diverse biological functions. However, the biological relevance of this phosphorylation *in vivo* remains to be determined.

IV. Thyroid Hormone Non-classical Effects

Most thyroid hormone effects are thought to be primarily mediated *via* binding of the TRs to the TRE in the nucleus. However, non-classical actions for thyroid hormone (T₃ and T₄) have been recognized recently. It is hypothesized that the mechanism of these non-classical effects involves TH binding to putative specific membrane receptors, thereby exerting biological effects through signal transduction pathways including cAMP, calmodulin, phosphatidylinositol, and protein kinase pathways [1, 48]. The recent

identification of novel seven-transmembrane receptors for progestins and estrogens [49-51] and integrin $\alpha_v\beta_3$ as a cell surface receptor for T_4 [2] has highlighted the potential importance of non-classical actions of TH. The putative non-classical effects of TH are diverse and the biological mechanisms are still under investigation.

The major difference between classical genomic and non-classical effects is the time of action [48]. Genomic effects are characterized by their delayed onset, usually more than 10 min. This longer delay may be due to the time required for *de novo* synthesis and processing of proteins, processes that are sensitive to the effects of transcriptional and translational inhibitors (e.g. actinomycin D and cycloheximide). For example, genomic action resulting from mineralocorticoid stimulation takes about 30-min [48]. On the other hand, there is a short delay for non-classical actions, which are insensitive to the inhibitors of transcription or protein synthesis. For example, estrogens have been shown to influence intracellular signaling and vasoregulation within 1-2 min upon administration [48]. Schmidt *et al.* [9] conducted a clinical experiment with T_3 and showed that T_3 treatments cause a significant increase in cardiac output and a decrease in systemic vascular resistance in healthy male volunteers. The time interval of the action was within 3 min of T_3 administration. This short time clearly excludes a genomic effect. **Table 1.2** compares the classical/genomic with non-classical/non-genomic actions of thyroid hormones.

These non-classical responses are frequently associated with the modulation of Na^+ , K^+ , Ca^{2+} and glucose transport, activation of protein kinase C (PKC), cyclic AMP dependent kinase (PKA) and extracellular signal-regulated protein kinase

Table 1.2. Comparison of thyroid hormone classical and non-classical actions.

	Classical/ genomic actions, Nuclear transcription	Non-classical/non-genomic actions, Cell surface receptor
Ligand	T ₃ (hours to days)	T ₄ /T ₃ (seconds to minutes)
Receptor	TR α and TR β	Putative GPCR
Dimerization partners	RXR, TRs	
Associated factors or signaling pathways	<ul style="list-style-type: none"> • NCoR/SMRT • SRC/p160/TRAPs 	Raf1/MEK/MAPK
Actions	<ul style="list-style-type: none"> • Basal transcriptional repression • Transcriptional activation • Transcriptional repression 	<ul style="list-style-type: none"> • TR phosphorylation and altered transcriptional activity • p53 phosphorylation and altered transcriptional activity • Increased STAT mediated transcription

Abbreviations: thyroxine (T₄), triiodothyronine (T₃), retinoid X receptor (RXR), thyroid hormone receptor (TR), G protein coupled receptor (GPCR), nuclear receptor co-repressor (NCoR), silencing mediator of RAR and TR (SMRT), steroid receptor coactivator (SRC), thyroid receptor associated protein (TRAPs), Raf serine/threonine kinase (Raf1), mitogen activated protein kinase kinase (MEK), MAPK mitogen -activated protein kinase (MAPK), signal transducers and activators of transcription (STAT).

Modified from Bassett *et al.* [30].

(ERK)/mitogen-activated protein kinase (MAPK) and regulation of phospholipid metabolism by activation of phospholipase C (PLC) and phospholipase D (PLD).

Bassett *et al.* [30] proposed a non-classical action model of TH in mammalian cells. In this model (**Figure 1.11**), T_4 or T_3 initially bind a putative G protein coupled receptor (GPCR). TH binding results in activation of PLC and PKC, the PKA may also be involved. Then PKC activates PLD sustaining the non-classical response and also activates the Raf serine/threonine kinase (Raf1) leading to MAPK phosphorylation *via* the mitogen activated protein kinase kinase (MEK). Tyrosine phosphorylation of MAPK results in its nuclear translocation and its phosphorylation of TRs, signal transducer and activator of transcription (STAT) and p53 (a tumor suppressor gene). Serine phosphorylation of TRs induces dissociation from the co-repressors NCoR and SMRT and increase transcriptional activity following binding of ligand, RXR and the co-activators p160/SRCs and TRAPs. In the cytoplasm, activated MEK also tyrosine phosphorylates STAT1 α and STAT3 resulting in their activation and nuclear translocation, further serine phosphorylation of these STATs by the nuclear MAPK maximizes the STAT transcriptional activity.

More recent studies described below suggest some possible mechanisms for the non-classical effects of TH. Using whole-cell recording methods and fluorescence microscopy, Wang *et al.* [10] demonstrated that when cat atrial myocytes are acutely exposed to T_3 , the inward Na^+ current and cardiac contraction strength are significantly increased. However, treatment with either reverse T_3 (rT_3) or T_4 has no effect on Na^+ movement. This suggests that acute T_3 exposure increases Na^+ influx and thereby stimulates reverse-mode, Na^+-Ca^{2+} exchange, to increase intracellular Ca^{2+} concentration

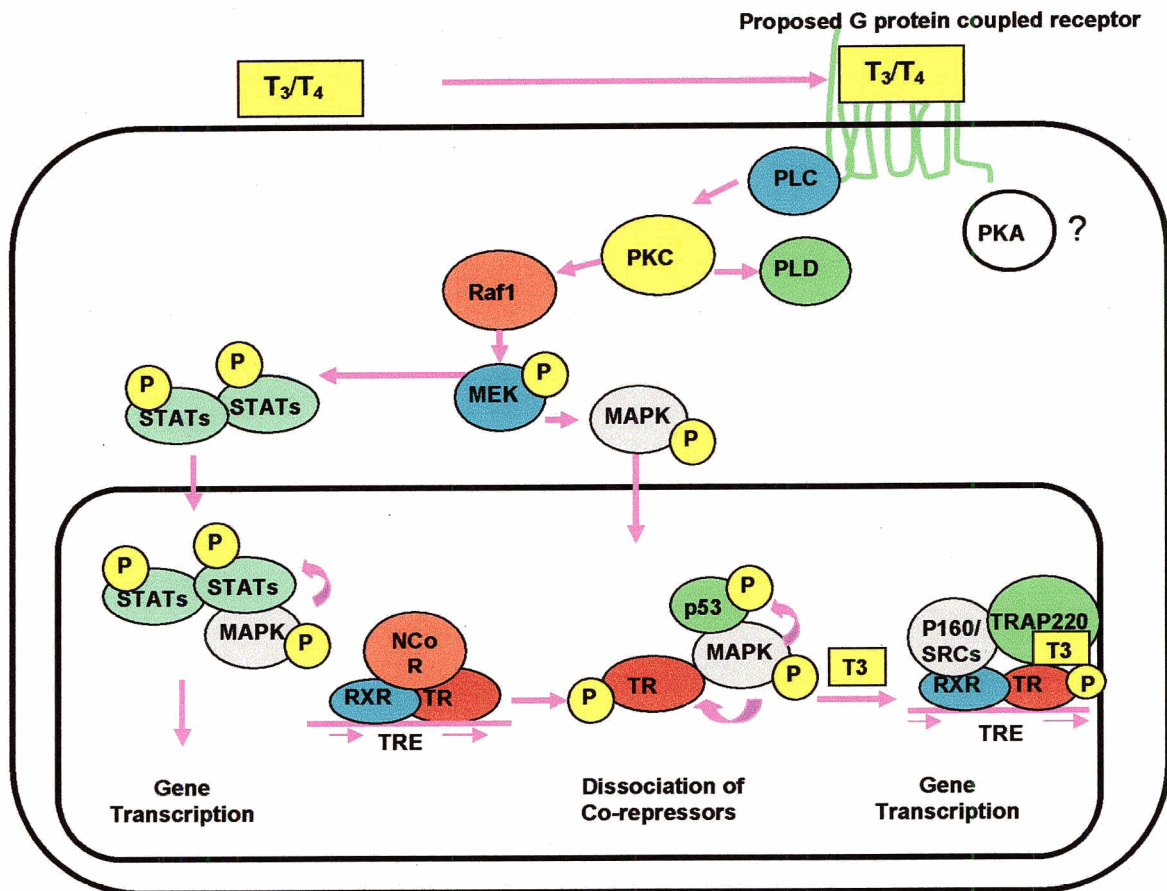


Figure 1.11. Schematic representation of the proposed mechanism by which thyroid hormone activates the MAPK (mitogen activated protein kinase) and STAT (signal transducer and activators of transcription) signaling pathways.

Modified from Bassett *et al.*[30].

resulting in enhancement of cardiac output. There is also evidence that showed that TH can exert its effects independently of nuclear TRs and that this effect can be abrogated by kinase inhibitors. Lin *et al.* [8] observed that the antiviral activity of human interferon- γ (IFN- γ) can be potentiated by T₄ and T₃ in HeLa cells that lack endogenous TRs. These effects are blocked by inhibitors of PKC and PKA, but not by 5'-deiodinase inhibitor. Lin *et al.* [7] also investigated IFN- γ induced human leukocyte antigen (HLA)-DR expression in HeLa and CV-1 cells, which both lack TRs. HLA-DR, the major histocompatibility complex (MHC) class II antigen, is usually expressed on B lymphocytes, monocytes, macrophages, and is induced by IFN- γ in HeLa and CV-1 cells. They found that T₄ potentiates IFN- γ -induced HLA-DR expression, but that effect is blocked by PKC inhibitors and genistein. Furthermore, Lin *et al.* [6] examined T₄ induced tyrosine phosphorylation and STAT3 nuclear translocation. This effect occurs in as little as 10-20 min. They also found that the activation of STAT3 in HeLa and CV-1 cells is similar to that in BG-9 cells (the human skin fibroblasts which do have TRs). This effect is reproduced by T₄-agarose, which prevents T₄ from entering the cell, and is blocked by genistein as well as the inhibitors of PKC and MAPK kinase. This suggests that T₄-induced the activation of STAT3 is mediated *via* non-classical mechanisms that require PKC, protein tyrosine kinase (PTK), and the MAPK pathway. These observations suggest that the rapid non-classical effects of thyroid hormone are widespread and may be involved in multiple physiological processes in many different cell types.

The identification of a progestin membrane receptor and the sub-cellular targeted nuclear receptor isoforms estrogen receptor α (ER) [52], mitochondrial retinoid X receptor α isoform mtRXR (mtRXR), mitochondrial peroxisome proliferator activator

receptor γ^2 associated protein (mtPPAR) [49-51], demonstrate that membrane receptors do exist for hormones previously defined for their genomic action. The recent finding that integrin, $\alpha_v\beta_3$ [2] as a cell surface receptor for T_4 in mammalian cells, lends credence to non-classical actions TH.

V. Thyroid Hormone Classical and Non-classical Effects – A Complex Model of Actions

The data presented so far has made a clear distinction between classical and non-classical effects of TH. However, it is more plausible that the two effects are interconnected to elicit a cellular response. For example, by non-classical mechanisms, TH can facilitate serine or/and threonine phosphorylation, which alters transcriptional activity of TR in the nucleus [45, 46, 53]. Davis and others [53-55] proposed a two-step model. This model (also see **Figure 1.11**) suggests that TH first binds to putative membrane receptors such as G protein coupled receptor, which induces second messengers including PKC, Ras, Raf1, MEK and electrolyte movements. These results in tyrosine phosphorylation, activation and nuclear translocation of MAPK, which in turn phosphorylates a serine residue in the second zinc finger of TR. This phosphorylation results in dissociation of TR from the co-repressors SMRT and NCoR, and association with co-activators to induce transcriptional activity. Although these data suggest that phosphorylation may be important in TH-mediated regulation of gene expression, its relative importance is not clear, particularly as it relates to biological outcome.

VI. Thyroid Hormone Receptors and Estrogen Receptors Cross-talk

i. Estrogen action.

Estrogen binds to estrogen receptors (ERs), which bind to estrogen response elements (EREs) as homodimers [52]. ERs have two isoforms ER α and ER β (**Figure 1.12**) that are encoded on human chromosomes 6 and 14, respectively [56]. Although there is high degree of sequence homology (only three amino acids differ) in the ER α and ER β DNA-binding domain, the ligand-binding domain shows only 53% homology. ER α is primarily expressed in the mammary gland and in the uterus and is mainly involved in reproductive events. While, ER β is very important in the central nervous system and the cardiovascular system [56]. For example, using ER α $-/-$ mice, Iafrati *et al.* [57] showed that 17 β -estradiol (E₂) can protect against vascular injury to a similar degree in both wide-type and ER α $-/-$ mice. This suggests that this effect of estrogens is mainly mediated *via* ER β .

Similar to TRs, in the presence of estrogen or tamoxifen, liganded ERs bind to EREs and recruit specific co-regulators with HATs or HDACs activity to remodel chromatin (**Figure 1.13**). The net agonist/antagonist activity of ER and ligands depends on ligand-induced conformational changes of the receptor. The receptor isoform as well as the specific coregulatory and promoter sequences also contribute to the functional specificity of the receptor down to the gene expression level [58]. The remodeling and “opening” up of the chromatin structure leads to gene activation [52]. However, unlike TRs, ERs cannot regulate transcription in the absence of ligand and are cytoplasmic until ligand binding allows for the translocation of the ER to the nucleus [1].

ii. TR cross-talk with ER.

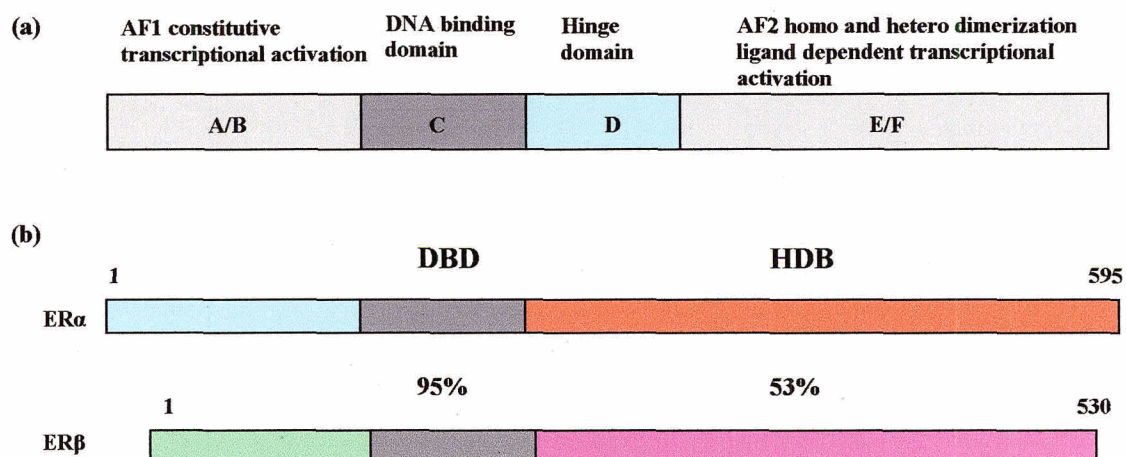


Figure 1.12. A schematic representation of the four functional domains of the estrogen receptor protein is shown in (a). The protein products of the estrogen receptor alpha and beta are shown in (b).

ER α contains 595 amino acids and ER β is somewhat shorter than ER α , containing 530 amino acids. ER α and ER β consists with a central DNA-binding domain (DBD), along with a carboxy-terminal hormone-binding domain (HBD). The region of highest homology between ER α and ER β is in the DBD (95%). Whereas, there is less homology (53%) in the crucial HBD. Their functional domains have been designated AF. Modified from Osborne *et al.* [58].

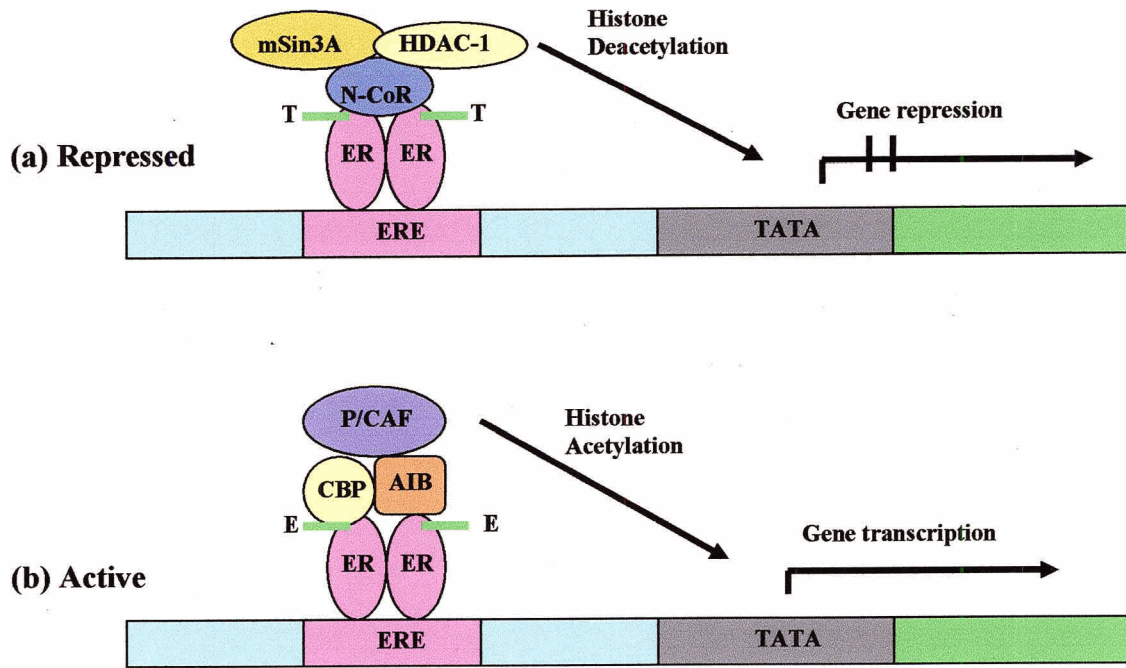


Figure 1.13. The role of ER coregulators in gene transcription regulation.

(a) When tamoxifen (T) binds to ER, it antagonizes the effect of estrogen by the recruitment of corepressors to the receptor complex. The corepressors possess histone deacetylase activity, and this activity silences transcription by allowing DNA to wrap more tightly around the core histone proteins. (b) Ligand estrogen (E) binding then releases the corepressors from the transcription complex, enabling the receptor to recruit coactivators and cointegrators with their associated histone acetylase activity. These acetyl transferases add acetyl groups to histones, thereby loosening their interaction with DNA, which then exposes important residues to the basal transcriptional machinery.

Abbreviation: estrogen receptor (ER), estrogen response element (ERE), mammalian Sin3 (mSin3A), histone deacetylase 1 (HDAC-1), nuclear receptor co-repressor (N-CoR), p300/CBP-associated factor (P/CAF), CREB-binding protein (CBP), amplified in breast cancer-1 protein (AIB). Modified from Osborne *et al.* [58].

TRs and ERs can each modulate the transcriptional activity of the other as both TRs and ERs have identical “P boxes” within the first finger of their DBDs (**Figure 1.7**) [59]. This “P box” is important in the recognition of hormone response elements. The “P box” of the TRs and ERs recognizes the same consensus HRE half-site sequence (AGGTCA). ERs bind as homodimers to EREs, which are arranged as palindromes separated by three nucleotides; while, TRs bind to TREs as monomers, homodimers, or heterodimers. Therefore, it is possible that competition between the two receptors may lead to antagonism. This crosstalk can occur by either competition for half-site binding or by squelching of coactivators.

TRs can block ER-mediated transcription. Using electrophoretic mobility shift assays (EMSA), Zhun *et al.* [60] demonstrated that both ER α and TR (α 1 and β 1) can bind rat preproenkephalin (PPE) gene promoter ERE. Furthermore, Zhun *et al.* [61] transiently cotransfected ER α and TR α 1 into CV-1 cells, which have low endogenous ERs and TRs, and assessed the activity of 437 bp of the rat PPE gene promoter fused to the CAT reporter gene. After pretreatment with exogenous 17 β -estradiol and/or T₃, they showed that estrogen-induced PPE promoter activity is significantly inhibited by liganded TR α 1, suggesting TR antagonism of the ERE. However, when they performed transient cotransfection assays with a P-box mutated TR α 1 (TR α 1p), which is unable to bind the AGGTCA TRE consensus sequence, treatment with T₃ also significantly inhibits estrogen-induced increase in CAT activity. This suggests that competition for half-site binding is not the only mechanism for crosstalk between TRs and ERs. Furthermore, Vasudevan *et al.* [62] performed the same transient cotransfection assays with the addition of SRC-1, which can bind the LBD of both ER and TR. They demonstrated that

SRC-1 overexpression can rescue P-box mutated TR α 1 inhibition. This indicates that squelching of common coactivators is another important mechanism of inhibition by TR isoforms.

ERs can also block T₃-regulated transcription by TRs. Using EMSA, Yarwood *et al.* [63] demonstrated that both TR and ER bind the TRE of the human glycoprotein hormone α subunit gene. T₃ is known to be a major negative regulator of α subunit transcription [63]. They performed cotransfection assays with TR β in JEG-3 human choriocarcinoma cells, which produce endogenous α subunit and are deficient in TR. They showed that estradiol inhibits T₃-mediated negative regulation of the glycoprotein hormone α -subunit gene transcription, suggesting that competition between ER and TR for TRE binding may block T₃-mediated negative regulation of this target gene. However, Yen *et al.* [64] observed that two ER mutants that cannot bind TREs or EREs also block T₃-mediated transcriptional activation *via* DR4 (four-nucleotide gap) and IP (six-nucleotide gap), suggesting that these ERs may titrate a critical coactivator (unknown) also required for T₃-mediated transcriptional activation.

VII. The Amphibian Model

The importance of TH in vertebrate postembryonic development was first discovered by Gudernatsch (1912) who fed thyroid glands to frog tadpoles and precociously induced metamorphosis [65]. Amphibian metamorphosis is divided into three periods [66]: premetamorphosis, prometamorphosis, and metamorphic climax. The entire process is under the control of TH which increases in amount throughout prometamorphosis reaching a peak concentration at climax [67] (**Figure 1.14**). During anuran metamorphosis, virtually every tissue exhibits profound morphological and

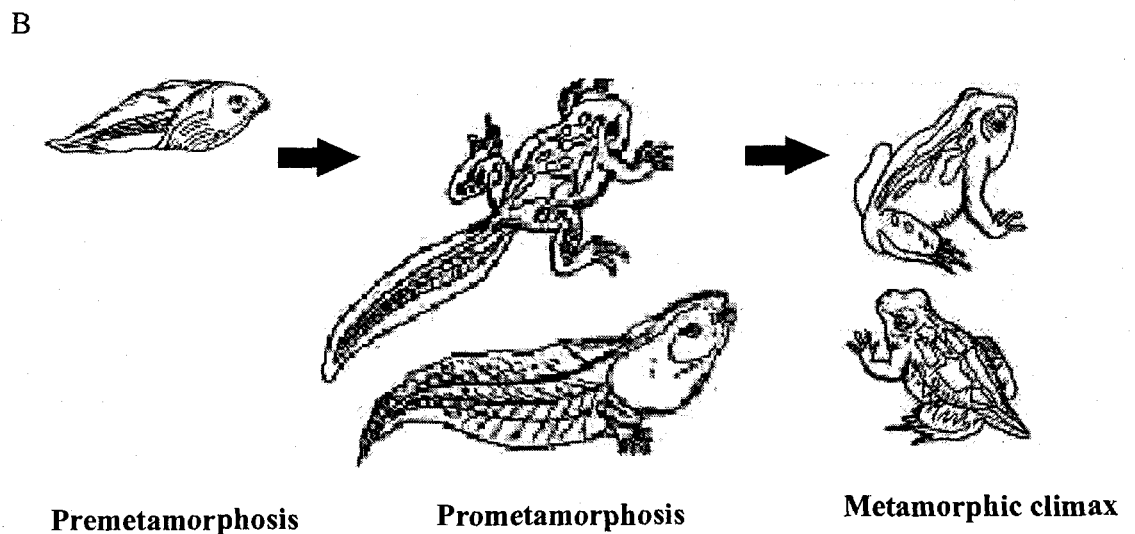
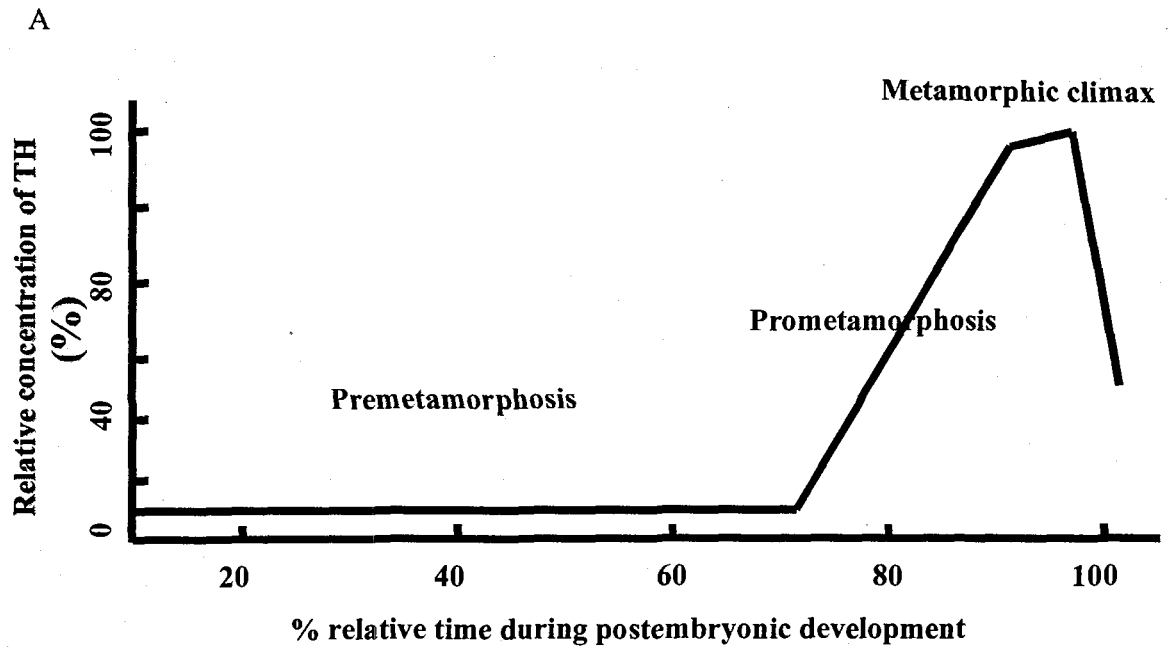


Figure 1.14. Thyroid hormones are the central trigger for tadpole metamorphosis.

Concentrations of T_4 and T_3 in blood plasma in tadpoles are usually undetectable in premetamorphosis stage, rise during prometamorphosis, peak dramatically during metamorphic climax, and then decrease to the suprabasal levels of the frog [67].

biochemical changes. For example, the larval liver and skin undergo genetic reprogramming that leads to synthesis of serum albumin and urea cycle enzymes in the liver and collagen deposition and keratinization of the skin. Among the most dramatic morphological and biochemical changes are the emergences of limbs and the total cell loss in the tail. All these changes could be induced precociously by exogenous TH in organ culture experiments [68-71]. Due to the central role of TH during amphibian metamorphosis, it has become a classic model for the study of TH actions.

Numerous studies have utilized cell lines to investigate the action of TH. However, the postembryonic amphibian presents a better study system, because remodeling of the entire organism during metamorphosis is controlled by a single hormonal signal. Amphibian metamorphosis is a simple and highly reproducible experimental model. At the premetamorphosis stage, the tadpole is euthyroid (has normal thyroid gland) but functionally athyroid (cannot secrete TH). These tadpoles readily take up T_3 from the aqueous rearing solution or cultured medium and respond in a dose dependent and highly stereotypic manner which matches the onset and completion of natural metamorphosis [72, 73]. Thus, amphibian metamorphosis represents a unique opportunity to address important questions regarding the biological actions of TH that may be conserved across all vertebrate species.

Ever since the successful cloning of TRs (1986), there has been an explosion of information on the molecular mechanisms of TH actions. $TR\alpha$ and $TR\beta$ are the two major isoforms of TRs and are differentially regulated in *Xenopus laevis* [74, 75]. The $TR\alpha$ genes are constitutively expressed after the completion of embryogenesis and are required for the initial response to exogenous TH [72, 76]. The $TR\beta$ genes have little

expression prior to metamorphosis and are up-regulated by exogenous T_3 which is critical for the establishment of tissue-specific genetic programs for metamorphosis [72]. Recent studies in *Xenopus laevis* has greatly aided our understanding of the roles of unliganded and liganded TRs in regulating target genes [40]. Further evidence from mammals showed that the nuclear action of TRs is influenced by diverse signaling transduction pathways [6-8, 10, 54]. Therefore, a complex model of TH action has been proposed. The effects of TH are mediated *via* the hormones first binding with nuclear TRs which bind to specific TREs and/or *via* signaling transduction through a putative membrane receptor, which result in the phosphorylation of TRs. These interactions alter the transcription of specific genes, followed by translation to protein, and finally to morphological metamorphic changes.

During amphibian metamorphosis, diverse responses such as tail resorption [72, 73], limb growth and differentiation [77], intestinal remodeling [78], and restructuring and functional differentiation of liver [70, 71, 79] are mediated by TH-regulated gene expression. Each organ or tissue has been programmed to respond to TH in its own specific way. However, how a different gene regulation and signaling cascade occurs in different tissues has yet to be resolved.

Tail resorption is the last change; it occurs rapidly at metamorphic climax. It is easy to manipulate and serves as ideal model system to investigate the mechanisms of action of TH in apoptosis. The TH-induced gene regulation cascade leading to tail resorption has been studied extensively in *Xenopus laevis* [72, 73, 76, 80-82] and *Rana catesbeiana* [83-85]. Given there is increasing evidence showing the potential importance of protein phosphorylation cascades in the action of TH, the question arises as to which

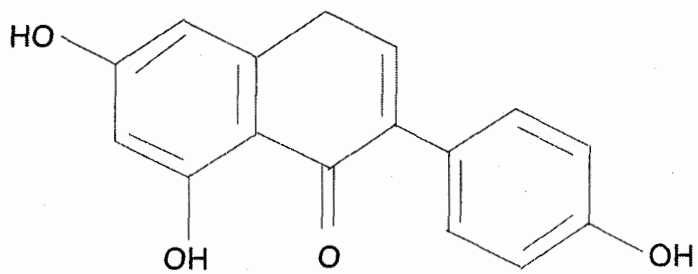
signaling pathway and what precise substrates are involved in TH induced tail regression. The advantage of the tail organ culture system is that it allows one to answer such questions as the involvement of a particular signaling pathway by using specific inhibitors which would otherwise be toxic to the intact tadpoles.

VIII. Genistein

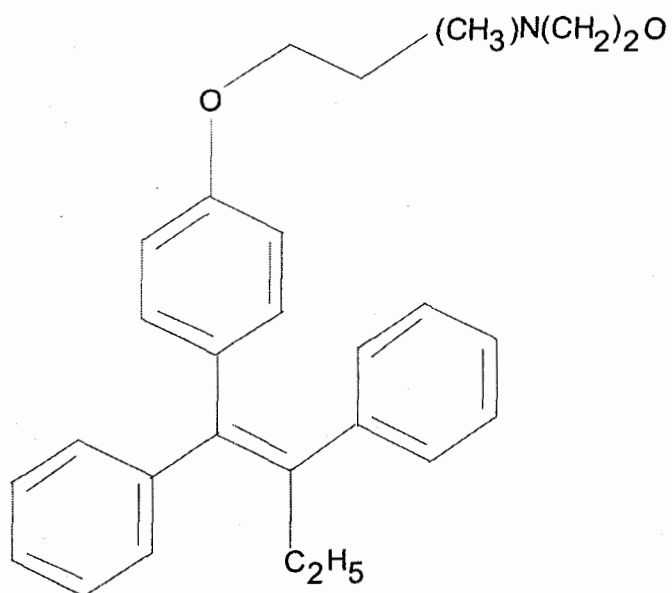
Genistein (4',5,7—trihydroxyisoflavone) is one of major components in soy formula and shares similar structural features with E₂ as well as tamoxifen (**Figure 1.15**), a synthetic anti-estrogen. At low concentrations, genistein can exert either estrogenic or anti-estrogenic effects [86-88]. However, at high concentrations, genistein is a specific inhibitor of tyrosine kinase [18]. Due to its dual function, genistein has been used as a tool to investigate molecular mechanisms in signaling pathways in numerous studies. It has been shown that genistein can disrupt TH action in *in vitro* studies [6-8, 20-25]. Genistein can also regulate transforming growth factor (TGF) β -1 [19], in addition to its estrogenic and tyrosine kinase inhibiting effects.

i. Genistein and soy formula.

In 1929 Hill and Stuart [89] reported the use of soy formula as a replacement for infants with allergies to cow's milk protein. Since then, soy formula has been used for several other related medical indications including postdiarrhea lactose intolerance, galactosemia and primary lactase deficiency [90]. Presently, with the improvement of soy formula quality, the U. S. Food and Drug Administration has established safety and quality standards for infant formulas [91]. Genistein and daidzein are two major components in soy formula [11]. Commercially available baby soy formula marketed in the United States is made with soy protein isolate (SPI+) [91]. Setchell and Cole [92]



Genistein



Tamoxifen

Figure 1.15. Structure of genistein in relation to tamoxifen.

reported that isoflavone levels in SPI+ was 30.2 +/- 5.8 mg/L (Mean +/- SD) and the ratio of genistein to daidzein isoflavone forms was 2.72 +/- 0.24 (Mean +/- SD).

The soyfood habits of Americans differ substantially from those of Asians. Asians are more likely to consume relatively high levels of soyfoods throughout life, except between birth and weaning. Asian infants are fed either cow milk formula or breast milk for the first year of life [91]. In contrast a substantial number of North American infants are exposed to an exclusively soy-based diet. In 1998, marketing data and hospital discharge records of the U. S. showed that ~25% of the nearly 4 million newborns were fed with baby soy formula [90]. The reason for the infant consuming soy formula may be, not only that the American Academy of Pediatrics recommends soy formula as a safe and effective alternative for infants, but also the desire of parents to maintain a vegetarian lifestyle and the increasing belief that soyfoods provide the potential benefits. Before birth and after weaning, most Americans are not exposed to appreciable levels of soyfoods [91].

Genistein is associated with a decreased risk of hormone-dependent cancer initiation later in life (e.g. breast and prostate cancers) and a variety of potential beneficial health effects including chemoprevention of cardiovascular disease, osteoporosis and relief of menopausal symptoms [11]. However, genistein exerts goitrogenic effects at dose of 0.33 mg/kg/day [93] which is three times higher than the amount typically consumed in Japan (0.08 to 0.13 mg/kg/day).

ii. Genistein and the tyrosine kinase signaling pathway.

Tyrosine phosphorylation plays a pivotal role for cell proliferation and cell transformation, because tyrosine-specific protein kinase activity such as Src [94],

epidermal growth factor receptor (EGFR) [95], platelet-derived growth factor receptor (PDGFR) [96], and insulin-like growth factor receptor (IGFR) [97], is strongly correlated with the ability of retroviruses to transform cells. Therefore, a specific inhibitor for tyrosine kinases could be a promising antitumor candidate as well as a tool for elucidating the role of tyrosine phosphorylation in cells. In 1987, Akiyama *et al.* [18] first demonstrated that genistein is a specific inhibitor of tyrosine kinase *in vitro*. It was shown that genistein inhibition of the EGFR kinase activity is competitive with ATP and leads to the formation of nonproductive enzyme-substrate complexes. For the phosphate acceptor, histone H2B, genistein functions as a noncompetitive inhibitor. This finding “unleashed” a great interest in using genistein as a tool to investigate molecular mechanisms of cancer and signaling pathways. For example, genistein, can trigger cancer cell apoptosis in B-cell precursor leukemia [98]. As discussed on page 26, using genistein as a specific tyrosine kinase inhibitor, there was some *in vitro* evidence showing that tyrosine kinase signaling plays a critical role in the action of TH.

iii. Estrogenic activity of genistein and breast cancer.

Genistein has been clinically tested as a chemopreventive agent in women with high risk of breast cancer due to its similar structural features with E₂ and tamoxifen. Genistein, an analog of estrogen, at low concentrations can exert either estrogenic or anti-estrogenic effects [86-88]. These effects may be by competing binding to the ERs.

Using a rat model, it is suggested that exposure to genistein during the perinatal or early juvenile period can induce mammary cell differentiation and suppress the development of mammary cancer [99, 100]. Rats were exposed to genistein only in a limited segment of the early life and yet were apparently protected from chemically-

induced cancer initiation later in life. This latter point is extremely important for possible health benefits of soy infant formula, since genistein is a major component in soy formula.

The mechanism of genistein and soy formula exerting chemoprotective effects has been investigated. Cotroneo *et al.* [101] showed that the protective effect of genistein against 7,12-dimethylbenzanthracene (DMBA)-induced mammary cancer results from its alteration rat mammary cell development by inducing cell differentiation. This effect is through up-regulated expression of EGFRs both at mRNA and protein levels [102] or *via* mimicking ER actions [101]. With the soy formula (the unpurified form of genistein), it was shown although DMBA-induced mammary cancer is reduced, the gross mammary gland morphology (differentiation stage), epithelial cell apoptotic index, expression of estrogen and progesterone receptors, and mammary density of treated animals are the same as control [103]. DMBA is a procarcinogen that must be metabolized to a carcinogen (activation stage) by cytochrome P450 enzymes, primarily those in gene family 1 (CYP1) [91]. The soy formula is working to reduce the incidence of DMBA-induced mammary gland cancer by down-regulating CYP1 and reducing DMBA-DNA adducts [103]. This represents a significant difference between feeding soy formula and a diet to which purified genistein is added.

The perinatal period is the most sensitive window for reproductive tract development and alterations. The safety of genistein and soy formula on animal reproductive systems is the centre of the debate. There are controversial results on reproductive effects of the consumption soy formula and genistein on the rat model [99, 104, 105] and sheep [106]. There is very little research on the reproductive effects of

consumption soy phytoestrogens by human neonates. Setchell *et al.* [107] reported the plasma isoflavone concentrations of infants fed soy formula is ~7000 nM, which is 280-fold higher than milk formula and breast milk fed infants. Soy isoflavones contain high proportions of genistein and daidzein, two well-known estrogenic endocrine disrupters that may alter reproductive development and function. Although the estrogenic potency of isoflavones is lower than that of E₂ (genistein is ~1000 times less potent than E₂ [87, 91]), the plasma isoflavone concentrations are ~50-100 times higher in infants fed soy formula than the E₂ levels achieved by women during pregnancy and nearly 3000 times higher than the E₂ concentrations achieved during the estrogen surge of the menstrual cycle [91]. Since humans do not normally have high concentrations of estrogens until after puberty, this raises great concerns of short- and long-term effects on reproductive systems of consuming soy formula especially in infants. Given that Asians who do have lower incidence of breast and prostate cancer usually do not consume soy formula in the first year of life, the health benefit of infants consuming soy formula should be carefully evaluated. Since large studies focusing on this issue have not been conducted, the adverse effects of soy formula and purified genistein on reproductive systems need to be further monitored and investigated.

iv. Genistein and thyroid hormone metabolism.

There is considerable interest in the putative health benefits from genistein, such as chemoprevention of breast and prostate cancer, relief of postmenopausal symptoms, and osteoporosis amelioration [11]. However, soybean consumption also has a long-standing association with goiter in animals and humans [23]. This suggests that genistein, a major component of soybean, can affect TH metabolism.

Mori *et al.* [25] investigated the role of genistein in the regulation of 5'-deiodinase, an enzyme that converts T_4 to T_3 . They found that the remarkable increase of 5'D-I activity induced by TSH or Bu2cAMP in rat FRTL-5 cell (a thyroid gland cell) is completely inhibited by 100 μ M genistein. Similarly, the same concentration of genistein also blocked Bu2cAMP and hydrocortisone increased activity of 5'D-II in rat astrocytes (brain). Since genistein at high concentrations is a specific tyrosine kinase inhibitor, this finding suggests that tyrosine phosphorylation may play an important role in the regulation of thyroid hormone metabolism in the rat thyroid and brain. Given that TH is important in proper brain development of infants and given that TH levels are critical around the neonatal period [108], consuming large amounts of genistein-rich foods may pose a risk for infant brain development.

In addition, genistein is identified as the component in soy that inhibits TPO-catalyzed iodination and coupling. Doerge *et al.* [21-24] examined the TPO activity in rats fed with genistein-fortified diets, it was shown that TPO activity significantly decreased and this reduction was dose-dependent [24]. The mechanism of this effect is not known.

IX. Research Hypothesis and Thesis Outline

Genistein disrupts non-classical TH action by inhibition of tyrosine kinases [6-8], but it may also act through affecting classical pathways. The mechanism remains unclear, particularly in the context of normal cells. Using genistein as a tool and tadpole metamorphosis as a model for TH action, I address the hypothesis that phosphorylation is important in TH-dependent tadpole tail regression.

The effect of genistein on TH-dependent tadpole tail regression was examined and the evidence indicates that genistein inhibits tail regression *via* inhibition of tyrosine kinase action rather than estrogenic action. The molecular mechanism underlying the biological outcomes is further examined by cDNA array, real-time quantitative polymerase chain reaction (QPCR), and protein analyses. This work demonstrates that genistein affects TH signaling in target tissues directly without the requirement of an intact HPT axis and indicates that phosphorylation is an important factor in establishing TH-dependent gene expression programs.

Chapter 2. The Effect of Genistein on Thyroid

Hormone-dependent Tadpole Tail Regression in *Rana catesbeiana*

1. Introduction

Thyroid hormones (THs) are required for the homeostasis of nearly all organs in the human body, including brain, bone, heart, and liver. The study of TH action has great biological and medical implications. Early studies showed that the effects of TH at the genomic level are mediated by the binding of TH to the nuclear receptors called thyroid hormone receptors (TRs). TRs belong to a large superfamily of nuclear hormone receptors including steroid, vitamin D, retinoic acid receptors, and “orphan” receptors, which have no known ligand or function. In the nucleus, TH binds to TRs with high affinity and specificity (K_d of T_3 is about 10^{-10} M [29]). TRs, which have 10-fold greater affinity for T_3 than T_4 [29], function as monomers, homodimers, and heterodimers. The heterodimers are commonly formed between TRs and retinoid X receptors (RXRs). TRs regulate gene expression by binding to specific DNA sequences in target genes, the TH response elements (TREs), then activation or repression transcription in response to hormone [30-32].

Most TH effects are thought to be primarily mediated *via* binding of the TRs to the TRE in the nucleus. However, non-classical actions for thyroid hormone (T_3 and T_4) have been recognized recently. It is hypothesized that the mechanism of these non-classical effects involves TH binding to putative specific membrane receptors [2], thereby exerting biological effects through signal transduction pathways including cAMP, calmodulin, phosphatidylinositol, and protein kinase pathways [1, 9, 48]. The putative

non-classical effects of TH are diverse and the biological mechanisms are still under investigation.

Despite accumulating evidence showing that signaling pathways, such as the MAPK [6-8, 54], cyclin dependent kinase (Cdk) [109], and tyrosine kinase signaling [20] are involved in the regulation of diverse and important TR functions, the precise substrate, the location of phosphorylation sites, their regulation, and functional roles remain to be elucidated. Moreover, genistein (4',5,7-trihydroxyisoflavone), one of major components in soy formula, disrupts T₄ action by inhibition of tyrosine kinase signal transduction [6-8, 20, 54] and by inhibiting 5'-deiodinase and thyroid peroxidase (TPO) [25], two important enzymes involved in the conversion of T₄ to T₃ and TH synthesis, respectively. This is consistent with the observation that high soybean consumption, which mainly consists of genistein, increases the incidence of goiter in animals and humans [23].

Another possible mechanism of antagonism to TH action for genistein is its known activity as a phytoestrogen at low concentrations [86-88]. Nuclear TRs and estrogen receptors (ERs) are capable of modulating the transcriptional activity of each other. Despite this, little is known regarding its potential effects on T₃ action (which is considered to be the bioactive form) and whether genistein affects target tissues directly.

Most research on TH uses either rats or mammalian cell lines as the experimental model. In both cases, the requirement for TH for healthy cells makes it difficult to accurately delineate the molecular mechanism of TH action by depletion and subsequent replenishment of TH. The tadpole at a premetamorphic stage serves as a better experimental model to investigate the mechanism of TH by exogenous T₃ administration.

Anuran metamorphosis is a postembryonic process that is absolutely dependent upon the presence of TH. Postembryonic development is divided into three phases: premetamorphosis, prometamorphosis, and metamorphic climax. At the premetamorphosis stage, the tadpole is competent to respond to TH, but is functionally athyroid. At this stage tadpoles readily take up TH from the aqueous rearing solution and respond in a dose-dependent highly stereotypical manner. Each tissue in the tadpole is a target for action and the responses include apoptosis, growth, or differentiation [110]. Thus, amphibian metamorphosis presents a unique opportunity to address important questions regarding TH action that is common to all vertebrates.

The purpose of this study is to address the hypothesis that phosphorylation may be important in TH-dependent tadpole tail regression. Resorption of the tadpole tail is one of the last changes during anuran natural metamorphosis and is entirely controlled by TH. This process can be precociously induced by exogenous administration of T_3 [72, 73, 80].

$TR\alpha$ and $TR\beta$ are the two major isoforms of TRs. T_3 binds to $TR\alpha$ and $TR\beta$ eliciting a variety of cellular outcomes (apoptosis, proliferation, or differentiation) during anuran metamorphosis [1]. Their genes are TH-responsive and this response has been well characterized [72]. Previous studies showed that heat shock protein (HSP)30 mRNA expression is T_3 -dependent in the liver of *Rana catesbeiana* during both natural and T_3 -induced precocious metamorphosis [79].

Inhibitor of growth (ING)1 is a negative growth regulator tumor suppressor, which shares many biological functions with p53, such as playing a role in oncogenesis, apoptosis [111, 112], DNA repair [113], and cell cycle regulation [114]. Transcriptional dysregulation of ING1b has been observed in many diverse tumor types and cancer cell

lines [115, 116]. We have previously shown that ING is T_3 -responsive and that its expression correlates with induction of tail regression in *Xenopus laevis* [117, 118]. The molecular basis of how ING is involved in the regulation of gene expression has not been fully elucidated.

In this study, different concentration effects of genistein on the T_3 -dependent tadpole tail regression were investigated. I show that genistein inhibits T_3 -induced tadpole tail regression most likely through its tyrosine kinase inhibitory action. The critical window for this signaling to occur is between 24 and 48 h of T_3 induction, which is coincident with the time required for the establishment genetic program for tail resorption [73]. The molecular mechanisms underlying this biological outcome were further investigated. Given tadpole tail regression requires the modulation of a number of genes [72, 73, 80], I used cDNA array and reverse transcriptase quantitative real-time PCR (RT-QPCR) analysis to identify changes in gene expression. Although many genes were identified as being T_3 -responsive, only one transcript, $TR\beta$ was identified whose expression correlates strongly with genistein's inhibition of T_3 -induced tail regression. Although $TR\alpha$ transcript levels were not affected, I show that genistein affects T_3 -induced phosphorylation of the $TR\alpha$ protein. Since phosphorylation of $TR\alpha$ may be linked to increased transcriptional activity of the $TR\beta$ promoter, this provides the first evidence that changes in phosphorylation are important in T_3 -dependent biological outcomes.

2. Material and Methods

2.1 Experimental animals.

Taylor and Kollros (TK) [119] stage VI-XV *Rana catesbeiana* tadpoles were locally caught (Victoria, BC) or purchased (Ward's Natural Science Ltd., St. Catharines, ON). The care and treatment of animals used in this study were in accordance with the guidelines of the Animal Care Committee, University of Victoria. Animals were housed in the University of Victoria aquatics facility and maintained in charcoal filtered, aerated tap water at 15°C in a constant flow-through system with exposure to natural daylight. Tadpoles were fed daily with spirulina (Aquatic ELO-Systems, Inc., FL).

2.2 Tail organ culture.

The procedure used for tail culture was adapted from procedures described previously [70]. Tadpoles were euthanized in 0.1% tricaine methanesulfonate (MS-222) (Syndel Laboratories, Vancouver, BC). The animals were then rinsed in 100 ml sterile distilled water for 10 seconds, followed by a 5 second immersion in 100 ml 70% ethanol and two subsequent 10 second immersions in 100 ml sterile distilled water. Then 2 cm tail tips were aseptically removed and placed into Tadpole Minimal Essential Medium (TMEM) at a density of 1 tip per 5ml dish media individually. The TMEM consists of a 55% strength solution of Minimal Essential Medium (MEM) (Invitrogen), 25 mM HEPES (Sigma-Aldrich, St. Louis, MO), 3 mM NaHCO₃, 1.2 mM Na₂HPO₄, 1.2 mM NaH₂PO₄, 20 mM NaCl, 2 mM L-glutamine, 50 units/ml penicillin, 50 mg/ml streptomycin, and 50 mg/ml neomycin, and final pH was adjusted to 7.1. Tail tips were incubated for 24 hours at 25°C prior to the addition of treatment reagents except in the *in vivo* T₃ treatment experiments (section 2.3) in which chemical treatments were directly applied after the tail was removed. After 24 hours, equal volumes (10 µl DMSO in 5 ml

medium) of dimethyl sulfoxide (DMSO) solution (ACP chemicals Inc., Montreal, QC), 0.1 μM genistein (Sigma-Aldrich, Canada Ltd), 1 μM genistein, 100 μM genistein, 1 nM T_3 (Sigma, St. Louis, MO), 10 nM T_3 , 100 nM T_3 , or a combination of genistein and T_3 (100 nM T_3 + 100 μM genistein, 100 nM T_3 + 1 μM genistein, 100 nM T_3 + 0.1 μM genistein, 10 nM T_3 + 100 μM genistein, 10 nM T_3 + 1 μM genistein, or 10 nM T_3 + 0.1 μM genistein) were added to the media. Media and chemicals were replenished every 24 h for the duration of the experiment.

2.3 *In vivo* T_3 tadpole treatment.

Prior to T_3 exposure, TK stage [119] VI-XV tadpoles (1 per 2 L water) were collected and maintained at 25°C in dechlorinated water by using an automatic aquarium heater (Warnock Hersey) for 2 days to acclimate to laboratory conditions. After 2 days, the animals were immobilized on ice and injected intraperitoneally through the tail muscle with either DMSO solution or T_3 -containing solution at dose of 3×10^{-10} moles/body weight which equals 3 $\mu\text{l/g}$ 10^{-4} M T_3 (**Figure 2.1**). Animals were continuously maintained at 25°C in dechlorinated water using an automatic aquarium heater for the duration of the experiment and water was changed daily. During the acclimatization and *in vivo* T_3 exposure periods, animals were not fed. At either 24 h (24 h injection set) or 48 h (48 h injection set), animals were sacrificed in MS-222. Tail tips of the animals were aseptically removed for subsequent tail organ culture as described above. Cultured tail tips were treated for 24 h, 48 h, or 72 h with equal volume (10 μl in 5 ml medium) of DMSO or 100 μM (final concentration) genistein. Media and chemical reagents were replenished every 24 h. At the end of the culture treatment time points, tail

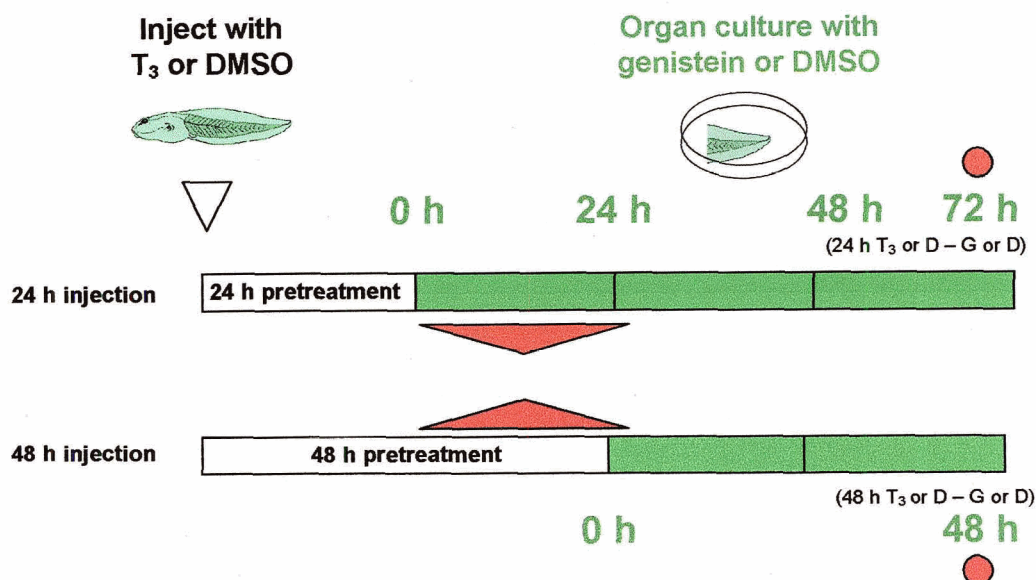


Figure 2.1. Experimental design of effects of genistein on T_3 -induced tadpole tail regression.

TK stage VI-X tadpoles were injected intraperitoneally through the tail muscle with either DMSO (vehicle) or T_3 . Animals were continuously maintained in 25°C water for 24 h (24 h injection set) or 48 h (48 h injection set). Following the exposure time course (either 24 h or 48 h), animals were sacrificed and tail tips of the animals were aseptically removed for tail organ culture. Cultured tail tips were treated for 24 h, 48 h, or 72 h with an equal volume of DMSO or 100 μM (final concentration) genistein. Media and chemical reagents were replenished every 24 h and pictures were taken at same time. At the end of treatment time points (24 h, 48 h, or 72 h) tail tips were collected for molecular analysis. The red circles are the time points selected for cDNA array analysis. The red triangle represents the “time commitment” points, which is an important transition phase in which inhibitors of transcription and translation can prevent tail regression up until 24h but not after 48 h.

tissue was collected and preserved in RNAlater (Ambion Inc., Austin, TX) at 4°C for later RNA isolation.

2.4 Tail measurement and analysis.

Photographs of cultured tails were taken every 24 hours using a digital camera (DVC Company, Austin, TX). Tail area was measured using Northern Eclipse version 5.0 (Empix Imaging Inc., Mississauga, ON) software. Statistical analysis was conducted using SPSS version 11.0 (Chicago, IL) software.

2.5 Tissue homogenization for protein phosphorylation analysis.

Tail tips were homogenized on ice using a Barnant Mixer in a buffer containing 50 mM HEPES, 150 mM NaCl, 2.5 mM EGTA, 1 mM EDTA, 0.1% Tween 20, 100 µM PMSF, 20 U/ml aprotinin, 10 mM β-glycerophosphate, 0.1 mM Na₃VO₄, 1 mM NaF, 1 mM DTT, 53 U/ml benzoyl-DL-tyrosyl-L-glutamate (Sigma-Aldrich), using a volume of 3 ml buffer per gram tissue [120]. After tissue homogenization, the reactions were sonicated 4 times for 15 sec each on ice and then incubated on ice for 30 min. Homogenates were centrifuged at 12,000 xg for 10 min at 4°C and the collected supernatant was stored at -70°C. The homogenate concentration was determined using the Bio-Rad Protein Assay (Bio-Rad).

2.6 Preparation of RNA.

Total RNA was isolated from RNAlater preserved *Rana catesbeiana* tadpole tail tips using TRIzol reagent as described by the manufacturer (Invitrogen Canada Inc., Burlington, ON). The procedure was adapted from procedures described previously [72, 82, 121]. Individual tail tips were homogenized in 1 ml TRIzol per 100 mg tail tissue using a MM 300 Mixer Mill (Retsch GmbH & Co.KG, Haan, Germany) at 20 Hz for 6 min. After tissue homogenization, chloroform (200 µl chloroform /1 ml TRIzol) was

added for phase separation. RNA was precipitated using isopropyl alcohol and washed with 75% ethanol. The isolated RNA was resuspended in RNase-free water and stored at -70°C until cDNA or amplified RNA (aRNA) was prepared. The concentration of total RNA for each sample was determined by spectrophotometry at 260 nm.

2.7 Preparation of amplified RNA (aRNA).

Amplified RNA (aRNA) was made using a MessageAmp aRNA kit (Ambion Inc., Austin, Texas, USA) according to the manufacturer. Briefly, first-strand cDNA was generated using 1 μg total RNA annealed with 1 μl (100 ng/ μl) T7 Oligo (dT)₂₄ primer and 200 U of Reverse Transcriptase. The 20 μl reaction was incubated at 42°C for 2 h. Second-strand cDNA was synthesized using 2 μl (5 U/ μl) DNA polymerase (supplied by the kit) and incubated at 16°C for 2 h. cDNA purification was performed as described by the manufacturer (reagents supplied by kit). *In vitro* transcription to synthesize aRNA was conducted by using double-stranded cDNA, 7.5 mM dNTPs, and 4 μl (20 U/ μl) T7 RNA polymerase mix at 37°C for 14 h. Two microlitres (2U/ μl) of DNase I was applied to digest any remaining cDNA following the *in vitro* transcription. aRNA purification was performed as described by the manufacturer (reagents supplied by kit). aRNA was stored at -70°C until cDNA array analysis. The concentration of aRNA for each sample was determined by spectrophotometry at 260 nm. The typical yield is ~ 20 μg .

2.8 Target preparation and labeling for cDNA array analysis.

Five hundred nanograms tadpole tail aRNA was annealed with 500 ng random hexamer oligonucleotide (Amersham Biosciences Inc., Montreal, QC), and cDNA targets were generated in a 20 μl reaction using 200 U Superscript II RNase H⁻ reverse

transcriptase (Invitrogen Canada Inc., Burlington, ON) incubated for 2 h at 42°C with 500 µM dGTP, dTTP, and dCTP, and 4 µM dATP, and 50 µCi [α -³²P] dATP (PerkinElmer Life Sciences Inc., Boston, MA) as described previously [72, 82, 121]. RNA was removed from the cDNA probe by adding 10 µl of 1 M NaOH and incubated at 70°C for 10 min. The cDNA probes were neutralized by adding 10 µl of 1 M HCl and then purified using QIAquick PCR purification column (Qiagen Inc., Mississauga, ON) with the following modification: wash cDNA with 600 µl PE buffer instead of 700 µl to avoid overflow. The specific activity of the cDNA target was measured by taking 1 µl target in 10 ml scintillation fluid (Fisher Scientific) using Beckman LS8000 series liquid scintillation systems (Beckman Instruments Inc., Irvine, CA). Various amounts of cDNA targets were used for following hybridization to reach a final concentration of 5×10^5 counts per minute (cpm)/ml.

2.9 Multi-species analysis of gene expression cDNA hybridization.

The frog MAGEX (multi-species analysis of gene expression) cDNA array membranes (ViagenX Biotech. Inc., Victoria, BC) were used to examine the gene expression profiles in the genistein inhibition study (see **Figure 2.1** for experimental design). This frog MAGEX cDNA array consists of a total of 420 gene sequences spotted in duplicate at adjacent grid positions on a nylon membrane. About 90% of the genes are *Xenopus laevis* and 10% are *Rana catesbeiana* in origin. The abundance of *Xenopus* cDNA compared to *Rana* sequences on the array is proportional to their relative abundance in GenBank (2001) [121]. The cDNA sequences represented on the array mainly consisted of cDNA fragments (~450-550 bp) encoding structurally and functionally important products involved in the regulation of amphibian development

(embryogenesis and metamorphosis) and basal cell metabolism. Two intron controls were also present to assess if there was any genomic DNA contamination. Radiolabeled cDNA from 3 individual animals of each treatment from the genistein inhibition study were independently examined. Before hybridization, the membranes were overlaid on two 3MM filter papers (Rose Scientific Ltd., Edmonton, AB) for 5 min each with the following solutions: 0.5 M NaOH (for denaturation of cDNA on the membrane), 1 M Tris pH 7.5, and 0.5 M Tris pH 7.5/1.25 M NaCl. To block nonspecific hybridization, the membranes were prehybridized with pre-warmed (58°C) hybridization solution at 58°C in a siliconized glass hybridization tube of 35 mm inner diameter x 150 mm length (Amersham Biosciences Inc., Montreal, QC) for 2 h. The 20 ml hybridization solution contained 4 x SSC [0.6M NaCl and 0.06M NaCitrate, pH 7.0, (both chemicals supplied by EMD Chemicals Inc., Gibbstown, NJ)], 1% SDS (Fisher Scientific), 0.5% skim milk powder (Fraser Valley Milk Producers' Cooperative Association, Vancouver, BC) and 10% dextran sulfate (Sigma-Aldrich, Oakville, ON). Before hybridization, the cDNA targets were heat denatured for 5 min at 95°C and then quickly cooled on ice for 5 min to prevent renaturation. To prevent direct exposure of the membrane to concentrated target, I transferred 13 ml of the prehybridization solution to a 15 ml Falcon tube and added the target. The hybridization solution was then reapplied to the membrane at a final concentration of 5×10^5 cpm/ml and incubated at 58°C for 18 h.

After hybridization, membranes were rinsed with 50 ml 2 x SSC at room temperature and then washed twice with 50 ml 2 x SSC/0.1% SDS at 58°C for 15 min, once with 50 ml 0.1 x SSC/1.0% SDS at 58°C for 30 min, and finally rinsed with 50 ml 0.1 x SSC at room temperature. The arrays were placed on two 3MM filter papers soaked

with ddH₂O and wrapped with plastic wrap (SC Johnson & Son, Inc., ON). The membranes were exposed to phosphor screens (Molecular Dynamics Inc., Sunnyvale, CA) for 5 days. The hybridization signals were collected using a Storm 840 optical scanner phosphor-imaging system at 50 μ m resolution (Molecular Dynamics, Inc. Piscataway, NJ). The resulting image data were converted to a standard 16-bit TIFF file using Photoshop version 7.0 software (Adobe Systems Inc., San Jose, CA). Both nonauto- and auto-level images were prepared for analysis to account for signal saturation.

2.10 Array data analysis.

Array image data collection was performed using ImaGene version 5.6.1 software (BioDiscovery Inc., El Segundo, CA). Signal intensities for each gene and blank position were determined from the median spot pixel intensities subtracted by the local background by ImaGene. Non-specific hybridization on the arrays was checked manually and excluded for further analysis. Multiple transcripts were used for inter-array normalization. These transcripts were chosen after analysis for stable expression using Bestkeeper [122] (results section **table 2.1**) and Spearman's correlation analysis using SPSS version 11.0 software (Chicago, IL) (results section **table 2.2**) followed by an estimation of inter-array variance analysis (**Appendix 2.1**). Then the variance of individual genes was determined as follows: the mean of duplicate spots per array was determined for each gene. Then the minimum value was subtracted from the maximum and the difference was divided by the median for that gene. If the value was greater than 1.50 on any array for a gene, then that gene was not considered further for gene analysis. Using this method, ribosomal protein L8 (L8), protein S10 (S10), glyceraldehyde-3-

phosphate dehydrogenase (GAPDH), elongation factor-1 α chain (EF-1), NM23/nucleoside diphosphate kinase (NM23), and ubiquitin were chosen as normalization genes. The geometric mean of these six genes were used to calculate the normalization factor (NF) for each array in Excel (Microsoft) (**Appendix 2.2**). The geometric mean was chosen rather than the arithmetic mean in order to equalize the relative contributions of the individual gene median values in the overall mean calculation.

After normalization, the no-signal (“floor”) value was determined for each array by using all of the blank positions on the array (**Appendix 2.3**). The floor value for each array was determined by the following formula: Median + (3rd quartile-1st quartile)/2 [as a robust standard deviation (SD)]. The highest value across the all arrays were chosen as the final floor value, and signal intensities for gene positions below this value were adjusted to the floor.

Normalized, floor adjusted and non-blank data were subjected to intraclass correlation coefficient (ICC) analysis to examine the quality of the array replicates using SPSS version 12.0 software (Chicago, IL) (**Appendix 2.4**). One sample was removed from the 48 h T₃-D set (tadpole sacrificed 48 h after T₃ injection and tail subsequently incubated in DMSO for 48 h) for further data analysis due to its high background, some non-specific hybridization spots, and not passing ICC analysis for examining sample integrity. After removing this sample, the intraclass correlation range is 0.51 to 0.94.

For the cDNA probe spots, saturated gene positions identified in auto-leveled data were replaced across all data sets by the corresponding values obtained in the non auto-level data. Both non-auto- and autolevel data for each array were normalized using the

same normalization factors derived from the geometric means of the six genes mentioned above. The relative expression values for each gene were determined from the median intensities across at least 4 replicate spots of array membranes for each treatment. For the normalized and floor adjusted final data applied for the determination relative gene expression see **Appendix 2.5.1** for the 24 h injection sets and **Appendix 2.5.2** for the 48 h injection set.

The overall signal intensities from the tadpole T_3 injection and tail tips incubated in the presence of genistein (T_3 -G) for both 24 h and 48 h sets were lower than other 3 treatments which can be observed from NF (**Appendix 2.2**). However, the auto-level procedure (Photoshop) enhanced the overall signal intensities for T_3 -G treatment artificially. This was determined to be the case by comparison of QPCR to cDNA array data. Therefore, the median intensities for T_3 -G treatment were subjected to correction factors of 13.5 for 24 h injection set or 10 for 48 h injection set respectively (non-autolevel data were not subjected to the adjustment). These two correction factors were derived from QPCR data versus cDNA array data for $TR\alpha$ and $TR\beta$. Because QPCR is a much more accurate method to measure gene expression levels than cDNA array. After correction, the signal intensities for gene positions below floor value were adjusted to the floor value. Fold change for all available genes and correction procedures for T_3 -G treatment see **Appendix 2.6.1** for the 24 h injection set and **Appendix 2.6.2** for the 48 h injection set.

Gene transcripts that met an arbitrary 2-fold cut-off were further examined by variance analysis as described above. The variance analysis cut-off was less than or equal to 1.50. If the gene did not pass variance analysis, the gene was removed from 2-fold

change gene list. Cluster analysis were done as follows: the fold change ratios were imported into Cluster [123] and log-transformed before being filtered to values greater than or equal to 1.0 in at least one observation (corresponds to 2.0-fold change). The un-centered data were then subjected to average linkage clustering to produce a hierarchical cluster tree in Treeview [123].

2.11 Statistical analysis.

Statistical analysis was conducted using SPSS version 11.0 software (Chicago, IL). Shapiro-Wilk test and Levene's test was used for examination of normality of data distribution and homogeneity of variances respectively. Parametric One-Way ANOVA test followed by Post Hoc Tukey test were applied for the examination of expression *rING1_{brain}* transcript during natural and T₃-precocious metamorphosis in the *Rana catesbeiana* tail. The rest of the data analyses used non-parametric Kruskal-Wallis test (for K-independent samples) followed by Mann-Whitney U two-tailed test (for two-independent samples). We consider it statistically significant if P value is less than 0.05 or 0.001.

2.12 Preparation of cDNA.

One microgram total RNA was annealed with 500 ng random hexamer oligonucleotides and cDNA was generated using 200 units (U) Superscript II Rnase H⁻ reverse transcriptase as described by the manufacturer (Invitrogen Canada Inc., Burlington, ON). The 20- μ l reaction was incubated at 42°C for 2 h to generate cDNA and then diluted 20-fold for real-time quantitative polymerase chain reaction (QPCR) examination.

2.13 Real-time quantitative polymerase chain reaction (QPCR).

A MX4000 real-time quantitative polymerase chain reaction system (Stratagene, La Jolla, CA) was used to examine the expression of several gene transcripts. Each 15- μ l DNA amplification reaction contained 5 mM Tris HCl, 5 mM Tris Base, 50 mM KCl, 3 mM MgCl₂, 0.01% Tween 20, 0.8% glycerol, 40,000-fold dilution of SYBR Green I (Molecular Probes Inc., Eugene, OR), 200 μ M dNTPs, 83.3 nM ROX reference dye (Stratagene), 10 pmol of each primer (except 5 pmol for HSP30 and alpha 1 collagen type I primers), 2 μ l of 20-fold diluted cDNA, and 1.0 U platinum Taq DNA polymerase (Invitrogen). The primers used were: TR α -forward 5'-GGACCAGAATCTTAGCGG-3', TR α -reverse 5'-CATTGGTGCTTCGGTGAG-3'; TR β -forward 5'-CAGGGGACAGAGAAAAGGTG-3', TR β -reverse 5'-TGAGCTTTCTTGCCACAG-3'; L8-forward 5'-AGCAGCATGTCAGGGTAC-3', L8-reverse 5'-TGAAGGCTTCTAAGTCCA-3'; HSP30-forward 5'-GCCTCCACCAGACTTACCA-3', HSP30-reverse 5'-CAGAGGAAGGAAGGCAGGAG-3'. α 1 collagen type I-forward 5'-CCCAGGTGGCGGATTTGA-3', α 1 collagen type I-reverse 5'-AGGCGGAGGAAGGTGAGT-3'; α 2 collagen type I-forward 5'-TGGCAACACTGGACCCTC-3', α 2 collagen type I-reverse 5'-GTGGCATCAACTTCATAATCCT-3'; cytoplasmic β actin-forward 5'-TCACCACCACAGCCGAAAG-3', cytoplasmic β actin-reverse 5'-GGGCCAGACTCATCATACTCCT-3'. For each set of QPCRs, I included two controls which do not have cDNA template or Taq DNA polymerase to determine the specificity of target cDNA amplification. The specificity of the appropriate products were verified by electrophoresis on 2% agarose gels. Standard plots for each target sequence were

generated using known amounts of plasmid containing the amplicon of interest. The thermocycle started at 95°C (9 min) and then 40 cycles of 95°C (15 sec), 55°C (30 sec) annealing (except for HSP30 primers at 61°C, α 1 collagen type I at 63°C, and α 2 collagen type I at 58°C), and 72°C (45 sec) extension (except for HSP30 30 sec). Cycle threshold (C_t) values obtained were converted into copy numbers. The copy numbers were determined using standard plots of C_t versus log copy number. Quadruplicate data for each target cDNA amplification were averaged and normalized to the invariant ribosomal L8 control to get relative copy numbers.

2.14 Cloning and sequence analysis of *rING1* (Rana inhibitor of growth 1) from *Rana catesbeiana* brain and tail.

rING1_{tail} and *rING1_{brain}* were cloned using forward primer 5'-TGGTGGAGTTGGTTGAGAAC-3' and reverse primer 5'-CCTGGATCTTTTATTGCTGG-3' provided by Mary Wagner in our lab from *Xenopus laevis* *ING1* for cross-species cloning. The RT-PCR products were cloned into a pCR II-TOPO vector and TOP10 cells using a TOPO TA Cloning Kit (Invitrogen). The potentially positive clones were confirmed by colony RT-PCR using M13 forward primer and reverse primer provided by TOPO TA Cloning Kit. The confirmed clones were picked for the creation of liquid stocks in LB broth containing 100 μ g/ml ampicillin (Sigma-Aldrich, Oakville, ON) overnight at 37°C with shaking. Plasmids were isolated with a Qiaprep Spin Miniprep kit (Qiagen, Mississauga, ON,) and sequenced in the DNA Sequencing Facility, Centre for Biomedical Research, University of Victoria. The DNA and predicted amino acid sequence alignment was conducted using CLUSTALW version 1.8 software (<http://clustalw.genome.ad.jp>)

2.15 RT-PCR and densitometry analysis for *rING1_{brain}* transcripts expression in *Rana catesbeiana* tail.

To examine the expression level of *rING1_{brain}* and *rING1_{tail}*, two primer sets which are specific for these two isoforms were designed manually (the product is only 145 and 150 bp, which are not long enough for using the software to design). The primer sets were: *rING1_{brain}*-forward 5'-TGGTGGAGTTGGTTGAGAACAG-3', *rING1_{brain}*-reverse 5'-TCAGTCTGAGAGATTGTTTCAC-3'; *rING1_{tail}*-forward 5'-TGGTGGAGTTGGTTGAGAACAA-3', *rING1_{tail}*-reverse 5'-TCTTTTCAGTCTGGGCAATGGC-3'. *rING1_{brain}* is expressed in *Rana catesbeiana* brain and tail. To determine the relative expression level of *rING1_{brain}* transcripts in *Rana catesbeiana* tail, RT-PCR followed by densitometry analysis was performed. The reason QPCR is not applied is that the *Ct* value difference between no cDNA template control (NTC) and the target is ~2 cycles, which is not good enough for distinguishing signal between the targets and primer dimers. QPCR is based on the detection and quantitation of the fluorescent dye of SYBR Green [binds to any double strand DNA (dsDNA)] emitted during the reaction as an indicator of amplicon production during each PCR cycle. RT-PCR for each 15- μ l DNA amplification reaction contained 5 mM Tris HCl, 5 mM Tris Base, 50 mM KCl, 3 mM MgCl₂, 0.01% Tween 20, 0.8% glycerol, 40,000-fold dilution of SYBR Green I (which can be monitored by MX4000 QPCR system for the reaction cycles), 200 μ M dNTPs, 83.3 nM ROX reference dye, 2.5 pmol of each primer, 2 μ l of 20-fold diluted *Rana catesbeiana* tail cDNA, and 1.0 U platinum Taq DNA polymerase. The PCR reaction conditions were 95°C (9 min); 30 to 32 cycles of 95°C (15 sec), 63°C (30 sec), and 72°C (30 sec). The PCR reaction was stopped at 30 to 32 cycles

in the linear range of amplification, which was monitored by the MX4000 QPCR system. The amplified products were separated on 2% agarose gels and visualized by ethidium bromide staining. Densitometry of the bands was done using Northern Eclipse version 5.0 software. Relative band densitometry was determined by band intensity subtracted by local background, then normalized by the expression of the invariant ribosomal L8 determined by QPCR.

2.16 Immunoprecipitation (IP).

Tissue homogenates (500 μ g) were diluted to a 1 ml volume in IP buffer containing 25 mM Tris-HCl (pH 8.0), 400 mM KCl, 10 mM EDTA, 0.1% Triton X-100, 1 mM dithiothreitol, 1 mM β -glycerophosphate, 2.5 mM sodium pyrophosphate, 1 mM Na_3VO_4 , 1 μ g/ml leupeptin, and 1 mM phenylmethylsulfonyl fluoride. Homogenates were precleared by rotation with 20 μ l/ml of protein G-sepharose beads (Amersham) for 20 minutes at 4°C. Following preclearing, the mixture was centrifuged at 3,000 \times g for 10 min at 4°C and the supernatant transferred to microfuge tubes containing 20 μ l of fresh beads and 5 μ l of TR α rabbit polyclonal antibodies (gifts from D. Brown, Carnegie Institute). The antibody-bead-homogenate mixture was mixed by rotation at 4°C for 3 h and the beads were washed 3 times with 1 ml IP buffer. The proteins on the beads were boiled for 3 minutes in 30 μ l 3 x sodium dodecyl sulfate (SDS) (187.5 mM Tris-HCl, 6% SDS, 30% glycerol, 150 mM DTT, 0.03% bromophenol blue, pH 6.8) and then resolved by 10% SDS-polyacrylamide gel electrophoresis (SDS-PAGE).

2.17 Immunoblotting.

Equal quantities of tail tissue homogenates [64 μ g (30 μ l) /lane] or 30 μ l IP proteins in SDS sample buffer were electrophoresed through either 8% or 10% SDS-

PAGE respectively. The proteins were transferred to 0.2 μ m nitrocellulose membrane (Bio-Rad) [124]. Protein loading and transfer quality were verified by membrane staining with 0.1% Ponceau S (Sigma) in 5% acetic acid. Membranes were blocked with 5% nonfat milk in 140 mM NaCl, 20 mM Tris-base (TBS), pH 7.6, at 4°C overnight and probed with a primary antibody solution diluted in 5% nonfat milk/TBS and 0.1% Tween (TBST) with gentle agitation for 1 h at room temperature. The primary antibodies are mouse monoclonal anti-phospho-tyrosine antibody (1:2000 dilution, Cell Signaling technology, Inc., MA), a rabbit polyclonal anti-phospho-serine antibody (1:125 dilution, Stressgen Bioreagents, BC), or a mouse monoclonal anti-human TR α whose epitope has 60% amino acid sequence identity to *Rana catesbeiana* TR α (1:1000 dilution, LabVision, Corp., CA). The blots were washed with TBST for 1 h. The membranes were incubated with secondary antibody solution diluted (1:2000) in 5% nonfat milk/TBST for 1 h at room temperature. The secondary antibody is a IRDye 800CW conjugated anti-mouse IgM or anti-rabbit IgG antibody depending upon the primary antibody used, which has a emission wavelength at 800 nm (Rockland Inc., Gilbertsville, PA) The blots were washed with TBST for 1 h. The prepared blots were scanned by Odyssey infrared imaging system (LI-COR Biosciences, Lincoln, NE) at 42 μ m resolution. The bands intensities were measured using Northern Eclipse version 5.0 software.

3. Results

3.1 Induction of T₃-dependent tadpole tail regression in serum-free organ culture.

Previous studies showed that tadpole tail regression can be induced by administration of exogenous 100 nM T₃ in serum-free organ culture *in vitro* [73, 109]. However, the physiological range of T₃ is ~8 nM [67]. To determine whether T₃ can

induce tadpole tail regression at a more physiological concentration, 2 cm tail tips from premetamorphic (TK stage VI to X) *Rana catesbeiana* tadpoles were removed and cultured *in vitro* over 96 h in the presence of vehicle control (DMSO), 100 nM T₃, 10 nM T₃, or 1 nM T₃ (n=4 for each treatment group). At 100 nM T₃ (**Figure 2.2**), tail tips showed a significant regression at 48 h, 72 h, 96 h time points in comparison to control (P<0.05). At 10 nM T₃, tail tips showed a significant regression at 72 h and 96 h in comparison to control (P<0.05). However, 1 nM T₃ has no effect on tail regression during the time points tested. T₃ at 10 nM (close to physiological concentration) has very similar effects as 100 nM T₃, except for at 96 h in which 100 nM T₃ showed a statistical difference compared to 10 nM T₃ (P<0.05).

3.2 Genistein inhibits T₃-induced tadpole tail regression.

Previous work indicates that genistein affects TH action, but no information exists as to its possible cellular effects on TH signaling. Genistein (G), an analog of estrogen at low concentrations (10 nM-10 μM), can exert either estrogenic or anti-estrogenic effects [11]. This effect of G is through binding to estrogen receptor and sex hormone binding proteins [86]. At higher concentrations (≥30 μM), G is a specific tyrosine kinase inhibitor [18]. To determine whether genistein affects TH-dependent tail regression, 2 cm tail tips from premetamorphic stage tadpoles were removed and cultured in serum-free medium over 96 h and treated with vehicle control (DMSO), 100 nM T₃, 100 μM G, 1 μM G, 0.1 μM G, 100 nM T₃ + 100 μM G, 100 nM T₃ + 1 μM G, or 100 nM T₃ + 0.1 μM G (n=4 for each treatment group). Tails treated with 100 nM T₃ showed a 83% reduction in tail area over 96 h in organ culture media (**Figure 2.3B**). This regression is completely inhibited by the addition of 100 μM G (P<0.001). However, tails cultured in the presence

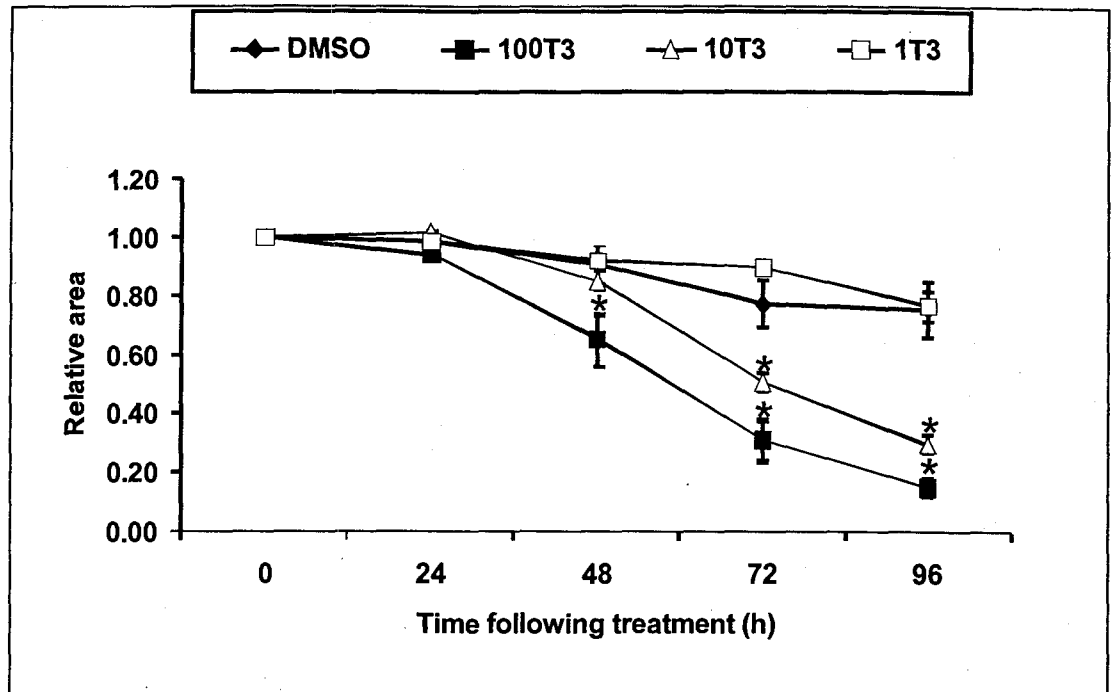


Figure 2.2. 100 nM T₃ and 10 nM T₃ induce T₃-dependent tadpole tail regression in serum-free organ culture.

Two centimetre tail tips were aseptically removed from premetamorphic tadpoles (TK stage VI to X) and cultured in serum-free organ culture medium, TMEM, over 96 h. Tail tips were treated with either vehicle (DMSO), 100 nM T₃, 10 nM T₃, 1 nM T₃. The tail tip area was measured at each time point and plotted relative to the 0 h time point of its treatment. N/treatment = 4. * P<0.05 relative to DMSO. The error bars represent standard error of the mean (SEM).

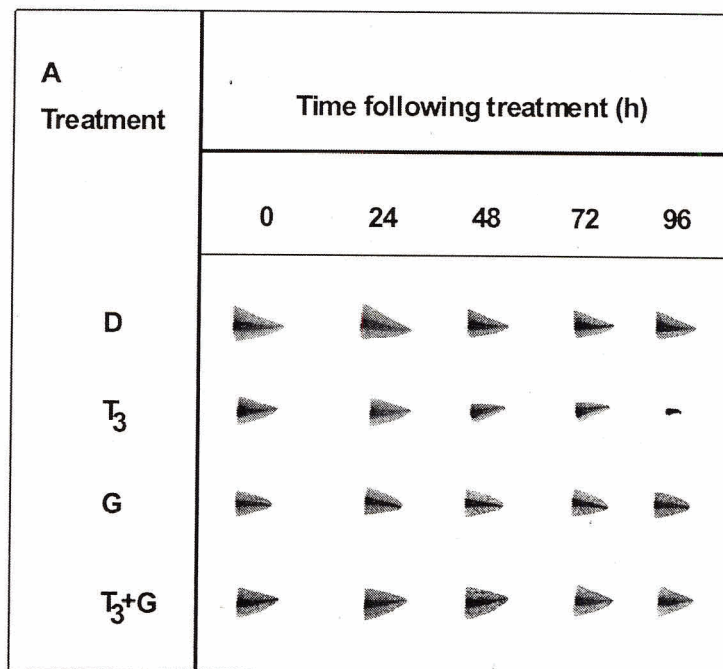


Figure 2.3. 100 μ M genistein inhibits T₃-induced tadpole tail regression.

Two centimeter tail tips were aseptically removed from premetamorphic tadpoles and cultured over 96 h. (A) Shown is representative pictures of tail tip regression inhibited by addition 100 μ M Genistein. Abbreviation: DMSO, D; 100 nM T₃, T₃; 100 μ M genistein, G.

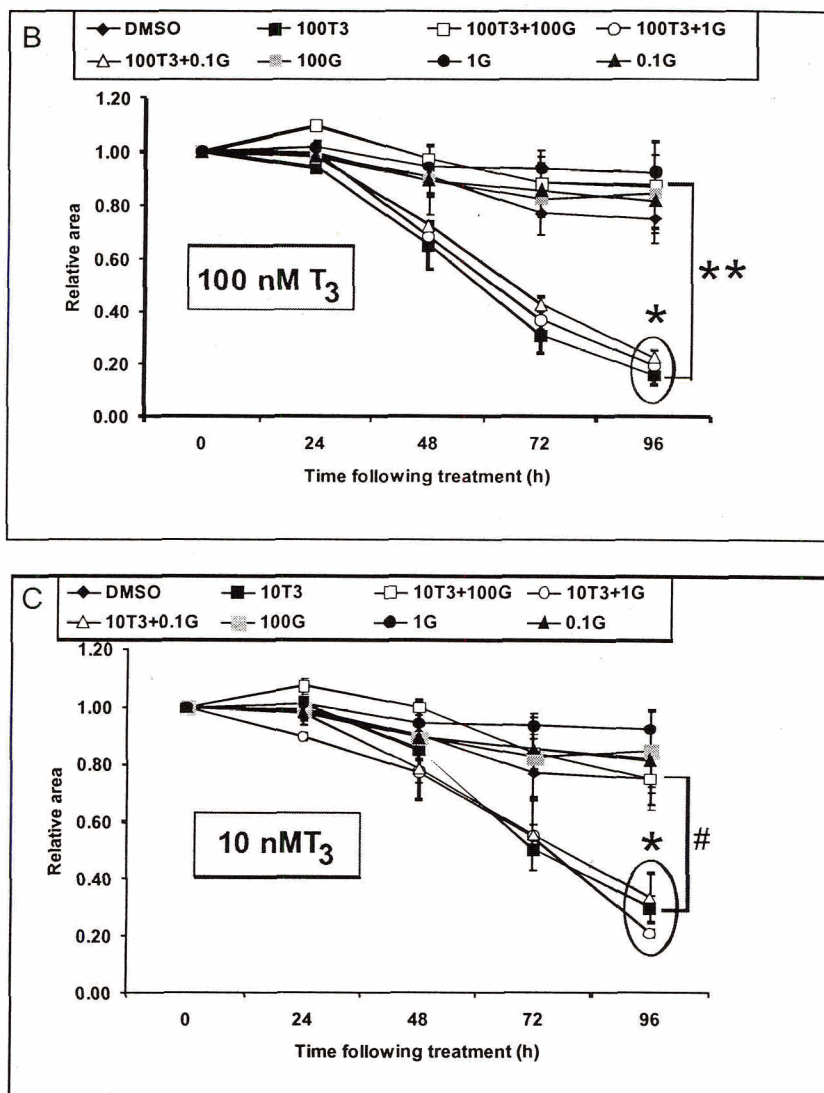


Figure 2.3. 100 μ M genistein inhibits 100 nM T₃- (B) or 10 nM T₃-induced (C) tadpole tail regression.

(B) Tail tips were treated with either vehicle (DMSO), 100 nM T₃, 100 μ M genistein (G), 1 μ M G, 0.1 μ M G, or a combination 100 nM T₃ and G. The tail tip area was measured at each time point and plotted relative to the 0 h time point of its treatment. (C) Tail tips were treated with 10 nM T₃ instead of 100 nM T₃. * P<0.05 relative to DMSO.

****P<0.001 in comparison 100 nM T₃ with 100 nM T₃ + 100 μM G. # P<0.05 in comparison 10 nM T₃ with 10 nM T₃ + 100 μM G. (n=4 for each group of treatment).**

of 100 nM T_3 + 1 μ M G or 100 nM T_3 + 0.1 μ M G still underwent significant regression over 96 h in comparison to DMSO ($P < 0.05$) (the experiment has been repeated four times). There is no statistical difference among 100 nM T_3 + 1 μ M G, 100 nM T_3 + 0.1 μ M G, and 100 nM T_3 . I also applied 10 nM T_3 and got very similar results as with 100 nM T_3 (Figure 2.3C).

3.3 Genistein reduces steady state levels of a 75 kDa protein phosphorylation during T_3 -induced tail regression.

Genistein inhibits the EGF-stimulated increase in phosphotyrosine level in mammalian cells [18]. To further confirm that genistein inhibition of T_3 -induced tail regression is *via* inhibition of protein phosphotyrosine levels, TK stage VI to XV tadpoles were injected with T_3 or DMSO vehicle control for 24 h and then the tail tips were removed and incubated in serum-free medium in the presence of 100 μ M G or vehicle control for a further 24 h. The tail tip protein homogenates were collected and separated by SDS-PAGE. The protein phosphotyrosine levels were assessed by immunoblot analysis. A 75 kDa protein phosphotyrosine level up-regulated by 60% upon T_3 treatment in comparison to the control (Figure 2.4). In contrast, the 75 kDa protein phosphotyrosine level is attenuated by 20% when tail tips were cultured in the medium in the presence of 100 μ M G after tadpole T_3 injection. This result was reproducible in another independent set of pooled tail tip protein homogenates. This indicates T_3 treatment is associated with an elevation in tyrosine phosphorylation and that genistein inhibits that phosphorylation. This method is limited in that the entire cell homogenate was examined for rare phosphorylation events. It is therefore not very sensitive.

3.4 Genistein blocks tail regression up to hours to days after T_3 -treatment.

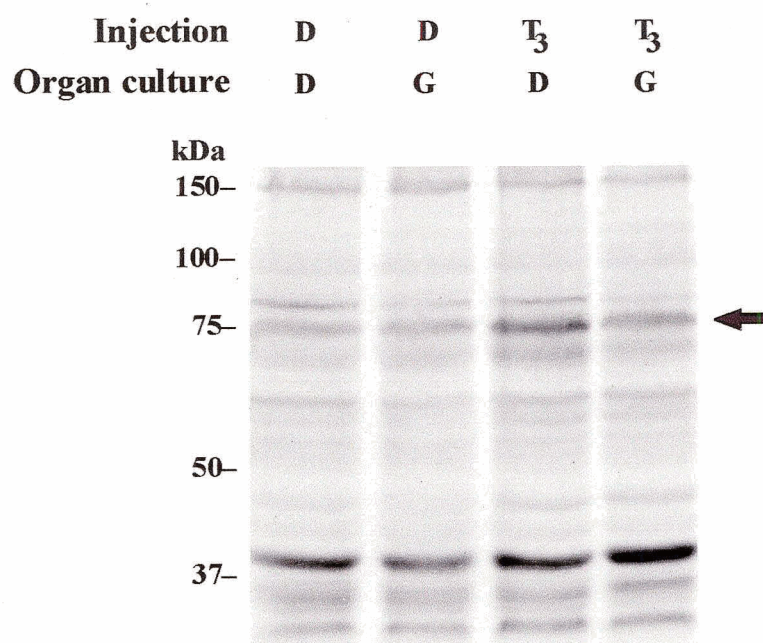


Figure 2.4. Genistein inhibits protein phosphotyrosine level during T₃-induced tail regression.

TK stage VI to XV tadpoles were injected with 3×10^{-10} moles/body weight vehicle (DMSO, D) or T₃ and maintained for 24 h. At this time point, tail tips were removed and cultured in serum-free medium in the presence of DMSO or 100 μ M genistein (G) for 24 h. Tail tip protein homogenates [64 μ g (30 μ l)/lane] were separated by 8% SDS-PAGE and immunoblotted with mouse monoclonal anti-phospho-tyrosine antibodies. This blot is representative of two independent experiments.

Previous studies showed that there is a critical time for the establishment of the genetic program for tail regression [73]. Up until about 24 h, inhibition of transcription and translation can prevent tail regression. However, after 48 h, these inhibitors are not effective at inhibiting tail regression. This important transition phase was referred to as the “commitment point” [73]. To determine when genistein inhibits T₃-induced tadpole tail regression, tadpoles (TK stage VI to X) were injected with 3×10^{-10} moles/body weight T₃ or vehicle alone (DMSO) and maintained in 25°C dechlorinated water for either 24 h or 48 h (see **Figure 2.1** for experimental design). At this time, 2 cm tail tips were aseptically removed and placed in serum-free organ culture medium in the presence of vehicle (DMSO, D) or 100 μM G and incubated at 25°C for 24 h, 48 h, or 72 h. Tail tips from tadpoles injected with T₃ and subsequently cultured in DMSO-containing serum-free medium showed at least 80 % regression by day 2 (**Figure 2.5A**). This is statistically significant compared to animals that were injected with DMSO and their tail tips subsequently cultured in DMSO ($P < 0.001$). Tail tips collected from animals injected with T₃ after 24 h and incubated in the presence of 100 μM G showed a complete inhibition of tail regression (**Figure 2.5B**). Tail tips collected from tadpoles sacrificed 48 h after T₃ injection and then cultured in 100 μM G did not show a complete inhibition (68% inhibition). This release from inhibition is statistically significant ($P < 0.05$) (**Figure 2.5B**). This suggests that the target(s) for genistein action are available up to 24 h with more limited availability after 48 h.

3.5 cDNA array analysis to examine the effects of genistein on T₃-induced gene expression profiles.

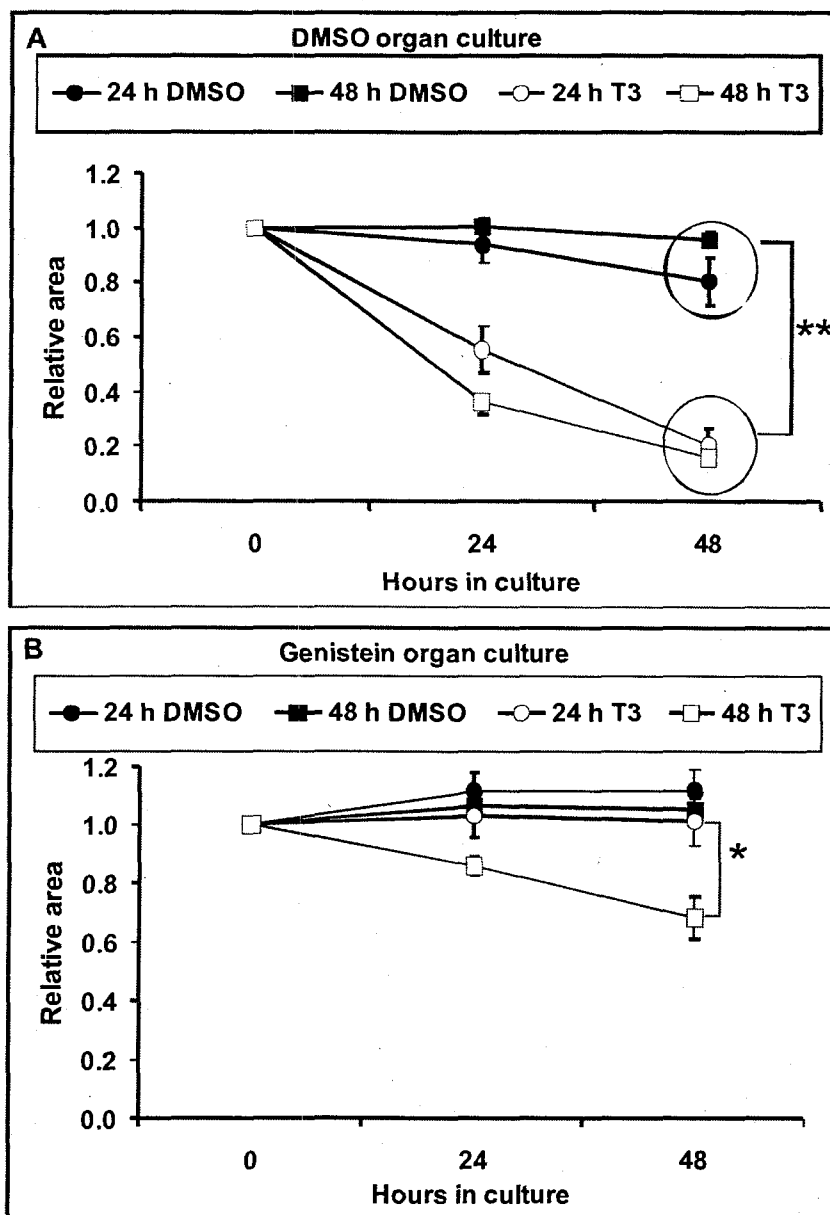


Figure 2.5. Genistein inhibits T₃-induced tail regression in serum-free organ culture within 24h.

Premetamorphic stage tadpoles (TK stage VI to X) were injected with 3×10^{-10} moles/body weight vehicle (DMSO) or T₃ and maintained for 24 h or 48 h, then tail tips were removed and cultured in the presence of DMSO or 100 μ M genistein (G) for a further 48 h. The tail tip area was measured at each time point and plotted relative to the

0 h time point of its treatment. (A) Tail tips that were collected from tadpoles that were DMSO or T₃ injected and cultured in DMSO containing medium. ** P<0.001 in comparison to animals that were injected with DMSO and their tail tips subsequently cultured in DMSO. (B) After tadpole injection, tail tips removed and cultured in 100 μM G. * P<0.05 in comparison to 24 h T₃-injected then cultured in 100 μM G. (n=4 for 24 h group, n=8 for 48 h group).

24 h/48 h denotes: tail tips collected from animals were injected with DMSO or T₃ after 24 h/48 h.

A primary factor controlling tail regression is through the modulation of gene expression [73, 80]. Evidence from my organ culture experiments suggests that the critical tyrosine signaling is coincident with the establishment of the genetic program. To begin to identify genes that may be targets for tyrosine kinase signaling in T_3 -induced tail regression in *Rana catesbeiana*, I employed the frog multispecies analysis of gene expression (MAGEX) cDNA array [72] as a “gene expression screen” tool. This array is comprised of 420 genes with a variety of origins (90% of *Xenopus* and 10% of *Rana*) and is a powerful tool for simultaneously examining hundreds of coordinated gene expression profiles. Tail tips from tadpoles injected with T_3 or DMSO only and subsequently cultured with G or DMSO alone were used for array hybridization analysis (see **Figure 2.1** for experimental design). Three individual animals were subject to array analysis separately for each treatment condition.

3.5.1 Determining stable normalizer genes for array data analysis.

Although I attempted to ensure that equal amount of input target was used for each array hybridization (such as equal amounts of total RNA to make aRNA, equal amount of aRNA to make radiolabeled cDNA, and equal amount of radiolabeled cDNA for hybridization), experimental errors during hybridization itself are not easy to control. These errors include different hybridization efficiency between individual samples, different background from exposure within or between experiments. Therefore, determination of stable normalization genes for accounting for differences only due to hybridization efficiency and exposure is necessary. A number of normalizer genes, such as tubulins, actins, GAPDH, 18S or 28S rRNA, and ubiquitin, have been described in the literature [125, 126]. To determine stable normalizer genes in my experimental system, I

applied the BestKeeper method [122] and Spearman correlation analysis. First, 12 potential normalizer genes were selected. Descriptive statistics of the derived crossing points (CP) for each potential normalizer gene are shown in **Table 2.1**. Based on the calculation of variation [coefficient of variance (CV)], the first estimation of the stability of the potential normalizer genes was done. The lower the coefficient of variation (CV) of the gene is, the more stably the gene is expressed across all arrays. Therefore, α skeletal actin, C/EBP-2, and HSP30, whose CV value was greater than 1.00, were excluded for further pair-wise correlation analysis. To determine inter-gene relations of those 9 potential normalizer genes, pair-wise correlation analyses were performed. Within each such correlations the Spearman correlation coefficient (r) and the probability p value are calculated. All those highly correlated genes (**Table 2.2**), L8, S10, GAPDH, elongation EF-1, NM23, and ubiquitin were considered as normalizer genes in my experimental system for further normalization factor (NF) calculation. An estimation of inter-array variance analysis were further performed (**Appendix 2.1**) to examine expressional stability of those 12 potential normalizer genes. All those 6 genes chosen as normalizer genes described above passed the 1.50 cut-off variance analysis.

The NF value for each array was determined using the highest geometric mean (GM) derived from those six normalizer genes for each array among all 24 arrays as a divisor for each individual GM (**Appendix 2.2**). **Figure 2.6** shows the expression profiles of the six normalizer genes (median pixel values for each gene in each array) and GM for each array across all 24 arrays. These six housekeeping genes showed tight correlation with their GM.

Table 2.1. Descriptive statistics of twelve candidate normalizer genes based on their crossing point (CP) values.

Factors	Number (N)	Mean (CP)	Min (CP)	Max (CP)	GM (CP)	SD of CP	CV (SD/Mean)
-Ribosomal protein L8	24	415	97	891	341	332	0.80
-Ribosomal protein S 10	24	535	101	1251	427	485	0.91
-GAPDH	24	348	85	757	295	281	0.81
-Elongation factor-1 α chain	24	663	89	1388	554	537	0.81
-Cytosolic β actin	24	1365	507	2709	1280	915	0.67
-Repressor brain factor 2	24	421	153	825	384	279	0.66
-Brain factor 2	24	332	130	693	302	237	0.71
-NM23/nucleoside diphosphate kinase	24	833	298	1672	744	573	0.69
- α skeletal actin	24	513	67	1388	388	565	1.10
-Ubiquitin	24	493	136	1095	410	404	0.82
-C/EBP-2	24	296	11	752	240	311	1.05
-HSP30	24	155	1	854	57	396	2.56

- Non-auto-leveled data from “Median Intensity” of each gene across all 24 arrays were collected, then their Mean, Minimum, Maximum, and Geometric Mean were calculated.
- Standard deviation (SD) of the CP is based on Mean, Minimum, Maximum, and Geometric Mean (GM).
- Coefficient of variance (CV) is SD divided by mean.
- The smaller the CV of the genes is, the more stably the gene is expressed. Therefore, α skeletal actin, C/EBP-2, and HSP30 were excluded for further pairwise correlation analysis.

Table 2.2. Pair-wise correlation analysis of candidate normalizer genes. Target genes are pair-wise correlated among each other. Non-parametric Spearman correlation coefficient (r) and the value of probability p are shown.

vs.	L8	S10	GAPDH	EF-1	β -actin	RBF-2	BF2	NM23
S10	0.884							
<i>p</i> -value	0.000							
GAPDH	0.831	0.617						
<i>p</i> -value	0.000	0.001						
EF-1	0.915	0.747	0.823					
<i>p</i> -value	0.000	0.000	0.000					
*β-actin	0.573	0.337	0.787	0.657				
<i>p</i> -value	0.003	0.107	0.000	0.000				
*RBF-2	0.472	0.446	0.293	0.293	0.324			
<i>p</i> -value	0.020	0.029	0.157	0.165	0.122			
*BF2	0.612	0.640	0.395	0.439	0.308	0.900		
<i>p</i> -value	0.001	0.001	0.056	0.032	0.143	0.000		
NM23	0.931	0.773	0.726	0.888	0.536	0.434	0.563	
<i>p</i> -value	0.000	0.000	0.000	0.000	0.007	0.034	0.004	
Ubiquitin	0.925	0.862	0.749	0.835	0.456	0.414	0.610	0.890
<i>p</i> -value	0.000	0.000	0.000	0.000	0.025	0.044	0.002	0.000

• Gray highlighted is the p -value greater than 0.05 and does not show significant correlation.

• Abbreviations: β -actin (cytoplasmic β actin), RBF-2 (repressor brain factor 2), BF-2 (brain factor 2).

* Gene is excluded as normalizer gene for array data analysis.

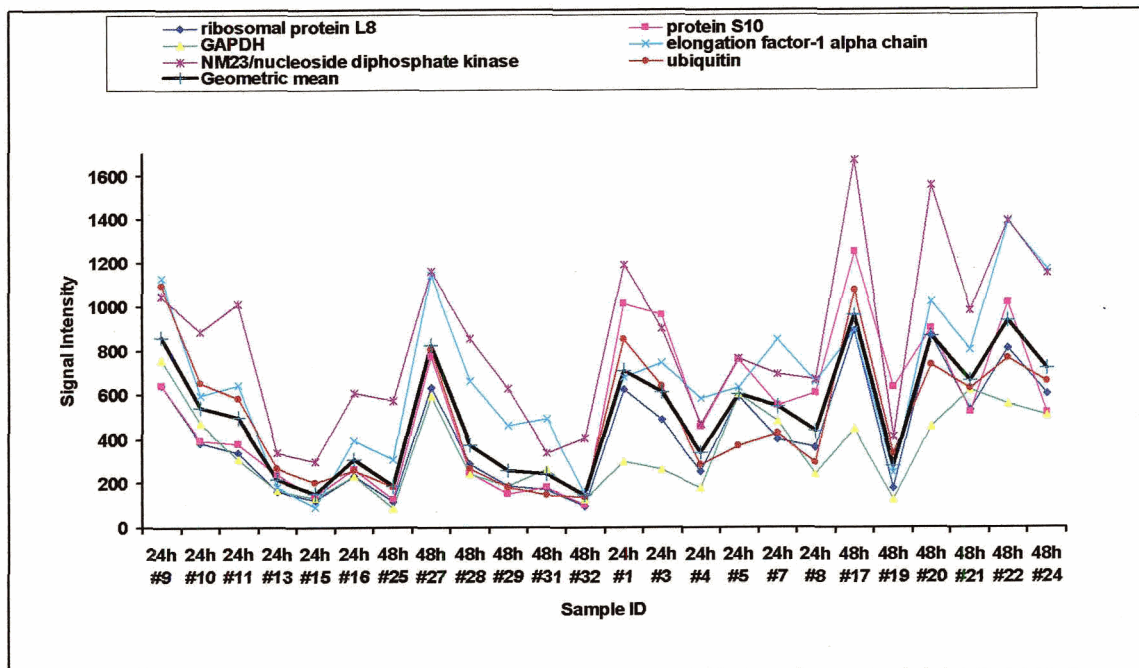


Figure 2.6. Expression of six normalizer genes and their geometric mean across all 24 arrays.

Signal intensities for each gene are represented median intensities. The signal intensities of Geometric Mean (GM) is derived from median intensities of these six normalizer genes for each array.

3.5.2 Identification of T₃-responsive genes.

TH is responsible for a change in the expression of many target genes during tadpole tail regression [72, 73, 80, 121]. To identify T₃-responsive genes, normalized and floor adjusted densitometric values obtained from MAGEX array analysis of the T₃-D tail samples (T₃ injection and tail subsequently incubated in DMSO in culture) were expressed as fold change relative to the D-D tails (DMSO injection and DMSO in culture). In the 24 h injection set, six genes were up-regulated and five genes were down-regulated (**Table 2.3**). Nine genes were previously identified as T₃-responsive, or up-regulated or down-regulated in anuran natural metamorphosis or mammals (81.82%). The relative expression levels of α 1 collagen type I and α 2 collagen type I were confirmed by QPCR respectively (**Table 2.3**). Five genes (myosin heavy chain 3, mitochondrial cytochrome c oxidase subunit 1, arginase, proteasome subunit Y, and hsp30) did not pass variance analysis (**Appendix 2.7**) and are therefore not presented in **Table 2.3**.

In the 48 h injection set, twenty genes were up-regulated and one gene was down-regulated (**Table 2.4**). Seventeen of these genes were previously identified as T₃-responsive, or up-regulated or down-regulated in anuran natural metamorphosis or mammals (80.95%). The relative expression levels of cytoplasmic β actin and α 2 collagen type I were confirmed by QPCR (**Table 2.4**). Nine of these genes (mitochondrial cytochrome c oxidase subunit 1, hsp30, proteasome subunit XC3, C/EBP, brain factor 1, NK-2 homolog, POU2, zic2, and frizzled 7) did not pass variance analysis (**Appendix 2.8**) and do not appear in the final **Table 2.4**.

A total of twenty-six genes displayed a 2 fold-change in relative gene expression in at least one time point. Five genes were up-regulated at both time points. These include

Table 2.3. T₃-induced gene expression profiles in the tail of *Rana catesbeiana* tadpoles in the 24 h injection set.

Gene Name	GenBank Accession No.	Functional Code ^a	T ₃ -D vs. D-D	
			Array	QPCR
•• cyclin D2 ^d	X89476	1	-3.33	
activated protein kinase C	AF105259	3	-2.20	
• MAP kinase phosphatase	X83742	3	-2.13	
•• lactate dehydrogenase B	U07176	6	-2.12	
•• proteasome subunit XC3	S51111	8	-2.15	
•• GSK-3 binding protein	AF062738	3	2.12	
Δ •• α 1 collagen type I ^c	AB015440	9	2.17	1.98
α skeletal actin ^c	X03470	9	2.27	
Δ •• α 2 collagen type I ^c	D88764	9	2.45	2.62
•• SPARC ^c	X62483	1	3.10	
•• gelatinase B (MMP-9) ^c	AF072455	8	3.52	

•• Genes previously identified as T₃-responsive in *Xenopus laevis*, *Rana catesbeiana* or mammals.

• Genes previously identified up- or down-regulated during natural metamorphosis in *Xenopus laevis* or *Rana catesbeiana*.

Δ Gene relative expression level was confirmed by QPCR.

^a Functional codes: 1, cell growth control; 2, chromatin structure; 3, signal transduction; 4, transcription; 5, hormonal regulation; 6, metabolism/biosynthesis; 7, transport/binding; 8, apoptosis/protein processing; 9, structural; 10, unknown function.

^b Fold change T₃-D vs. D-D is that tadpoles were injected with T₃ and at 24 h time point tail tips were removed and subsequently incubated in serum-free medium containing DMSO versus DMSO injection followed by incubation in medium containing DMSO. The positive ratio denotes up-regulation, the negative ratio is down-regulation.

^cGene that was up-regulated at both time points.

^dGene that was down-regulated at both time points.

Table 2.4. T₃-induced gene expression profiles in the tail of *Rana catesbeiana* tadpoles in the 48 h injection set.

Gene Name	GenBank Accession No.	Functional Code ^a	Fold Change ^b	
			T ₃ -D vs. D-D Array	QPCR
•• cyclin D2 ^d	X89476	1	-2.78	
Δ • cytoplasmic β actin	AF079161	9	2.24	3.71
Δ •• α 2 collagen type I ^c	D88764	9	2.27	3.75
retinoic acid converting enzyme	AF057566	5	2.55	
aldolase B	AB030822	6	2.56	
DLL4	L09728	4	2.57	
•• DAD-1	D15059	8	2.59	
•• α 1 collagen type I ^c	AB015440	9	2.64	
•• RNA pol I transcription factor UBF	X57561	4	2.64	
•• arginase	D38303	6	2.64	
•• nuclear factor I-C1	L43149	4	2.65	
•• mitotic phosphoprotein 90	U95102	2	2.67	
• caspase-6	AB038169	8	3.10	
α skeletal actin ^c	X03470	9	3.68	
•• thyroid hormone binding protein	U03878	5	3.73	
•• raf ser/thr kinase	X12948	3	3.75	
•• SERCa1 fast skeletal muscle	X63009	3	4.01	
•• SPARC ^c	X62483	1	4.47	
•• gelatinase B (MMP-9) ^c	AF072455	8	5.13	
• iodothyronine deiodinase type II	L42815	5	5.49	
•• myosin heavy chain 3	AF097906	9	10.77	

•• Genes previously identified as T₃-responsive in *Xenopus laevis*, *Rana catesbeiana* or mammals.

• Genes previously identified up- or down-regulated during natural metamorphosis in *Xenopus laevis* or *Rana catesbeiana*.

Δ Gene relative expression level was confirmed by QPCR.

^a Functional codes: 1, cell growth control; 2, chromatin structure; 3, signal transduction; 4, transcription; 5, hormonal regulation; 6, metabolism/biosynthesis; 7, transport/binding; 8, apoptosis/protein processing; 9, structural; 10, unknown function.

^b Fold change T₃-D vs. D-D is that tadpoles were injected with T₃ and at 48 h time point tail tips were removed and subsequently incubated in serum-free medium containing DMSO versus DMSO injection followed by incubation in medium containing DMSO. The positive ratio denotes up-regulation, the negative ratio is down-regulation.

^c Gene that was up-regulated at both time points.

^d Gene that was down-regulated at both time points.

α 2 collagen type I, α 1 collagen type I, gelatinase B, SPARC, α skeletal actin. Cyclin D2 was down-regulated at both time-points. Thirteen out of those twenty-six genes (50.00%) encode protein products important in transcription, signal transduction and cell structure. Activated protein kinase C, α skeletal actin, retinoic acid converting enzyme, aldolase B, and DLL4 are newly identified as T₃-response genes.

To identify the expression pattern of T₃-response genes at both time points, a hierarchical tree cluster was generated for those 18 genes having a 2 fold-change in at least one time point and with values that passed all of the quality control measures for both time points (**Figure 2.7**) (Among those 26 genes, 8 genes had data for only one time point due to replicate spots being less than 4 or not passing variance analysis). Three clusters were identified with correlation coefficients ranging 0.97 to 0.99. Gene cluster 1 is characterized by down-regulation in only the 24 h injection set. These include activated protein kinase C and lactate dehydrogenase B. Cluster 2 is characterized by up-regulation in both injection sets. These include α 2 collagen type I, α 1 collagen type I, gelatinase B (MMP-9), SPARC, and α skeletal actin. Cluster 3 is characterized by up-regulation in only the 48 h injection set. These include cytoplasmic β actin, nuclear factor I-C1, iodothyronine deiodinase type II, raf ser/thr kinase, aldolase B, caspase-6, mitotic phosphoprotein 90, retinoic acid converting enzyme, thyroid hormone binding protein, and SERCa1 fast skeletal muscle. Cyclin D2 did not fall into the three clusters. Cyclin D2 was down-regulated in both injection sets.

3.5.3 T₃-responsive transcripts modulated by genistein during T₃-induced tail regression.

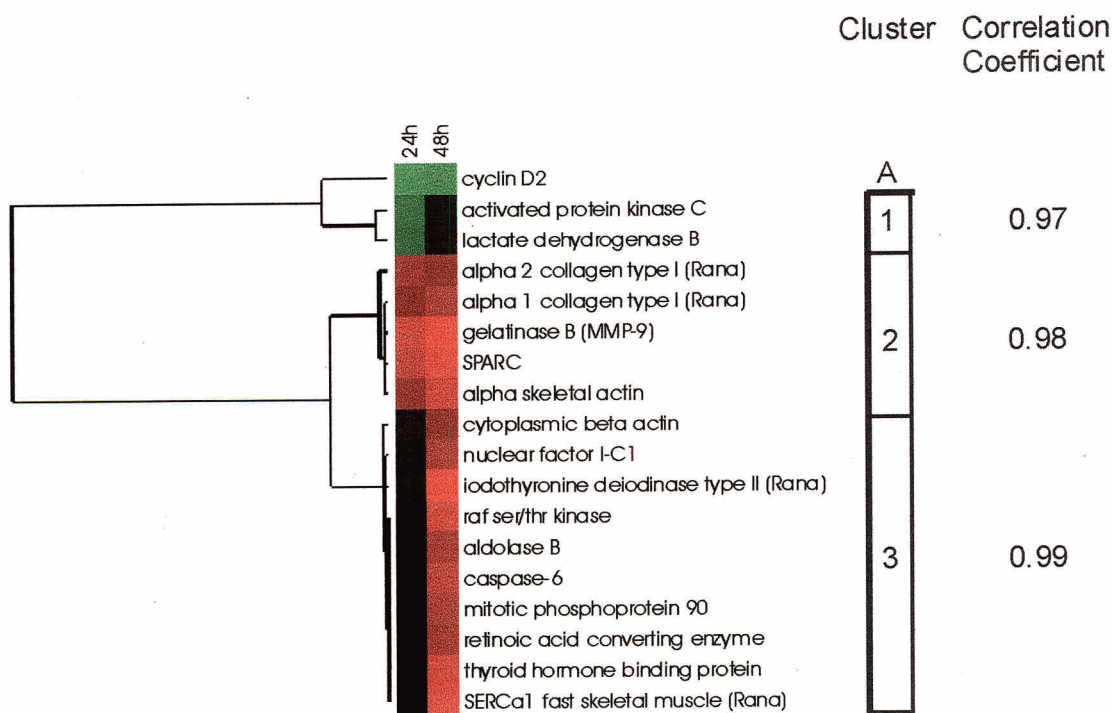


Figure 2.7. Cluster analysis of transcripts responsive to T_3 in the tadpole tail tissue of *Rana catesbeiana*.

Gene transcripts that met an arbitrary 2-fold change in at least one observation and with values for both time points (in the 24 h injection set and in the 48 h injection set), were subjected to agglomerative hierarchical clustering analysis. Shown is a hierarchical tree. All gene expression data were normalized to NF before clustering. An increase of gene expression is red, a decrease is green, and no change is black. The right of the diagram shows three gene clusters and their correlation coefficient. A is an unclustered gene.

Since the change in the gene expression program appears to be affected by genistein, possible gene targets should be uncovered by identifying genes that are T₃-responsive that are affected by genistein treatment after T₃ exposure, but not DMSO injection after 24 h injection, but not after the 48 h injection.

To identify transcripts potentially affected by genistein during T₃-induced tail regression program, I examined the fold changes of genes that were affected by T₃ identified above and compared their T₃-induced levels with those from T₃-injected animals whose tails were incubated in genistein. If the values differed by less than a factor of two, the gene was removed from the list. I then compared the remaining genes to DMSO injected and genistein organ cultured (D-G) tails. If the gene was affected by genistein regardless of whether the animals were injected with DMSO or T₃, this gene was removed from the list since unlikely that a change in its expression contributed to the biological outcome.

For the 24 h injection set, genistein treatment with T₃ injection results in arrays with a high intraclass correlation coefficient similar to the T₃-D tails (**Appendix 2.4**). This correlation coefficient decreases substantially in the 48 h injection set suggesting that the tail tissue responses are becoming more divergent. Only three gene transcripts are substantially affected by genistein after T₃ injection in the 24 h injection set. Of these, two that are down-regulated by T₃ are further depressed (**Table 2.5**). The remaining gene, gelatinase B, shows that its T₃-induced up-regulation is strongly attenuated. This is maintained in the 48 h injection set (**Table 2.6**) suggesting that its T₃-induced up-regulation may require a constant input of a tyrosine kinase mediated signal. In 48 h injection set, four other genes showed marked down-regulation by genistein in the

Table 2.5. Transcripts modulated by genistein during T₃-induced tail regression in *Rana catesbeiana* in the 24 h injection set.

Gene Name	GenBank Accession No.	Functional Code ^a	Fold Change ^b	
			T ₃ -D vs. D-D	T ₃ -G vs. D-D
activated protein kinase C	AF105259	3	-2.20	-9.64
•• lactate dehydrogenase B	U07176	6	-2.12	-6.30
•• gelatinase B (MMP-9) ^d	AF072455	8	3.52	1.00

•• Genes previously identified as T₃-responsive in *Xenopus laevis* or *Rana catesbeiana*.

^a Functional codes: 1, cell growth control; 2, chromatin structure; 3, signal transduction; 4, transcription; 5, hormonal regulation; 6, metabolism/biosynthesis; 7, transport/binding; 8, apoptosis/protein processing; 9, structural; 10, unknown function.

^b Fold change: T₃-D/T₃-G vs. D-D, is that tadpoles were injected with T₃ and at 24 h time point and whose tail tips were removed and subsequently incubated in serum-free medium containing DMSO/100 μM genistein (G) versus animals injected with DMSO and tail tips incubated in medium containing DMSO.

The positive ratio denotes up-regulation, the negative ratio is down-regulation.

^dGene that was down-regulated by genistein at both time points.

Table 2.6. Transcripts modulated by genistein during T₃-induced tail regression in *Rana catesbeiana* in the 48 h injection set.

Gene Name	GenBank Accession No.	Functional Code ^a	Fold Change ^b	
			T ₃ -D vs. D-D	T ₃ -G vs. D-D
•• raf ser/thr kinase	X12948	3	3.75	1.00
• caspase-6	AB038169	8	3.10	1.00
••gelatinase B (MMP-9) ^d	AF072455	8	5.13	1.00
iodothyronine deiodinase type II	L42815	5	5.49	0.99
aldolase B	AB030822	6	2.56	1.00

•• Genes previously identified as TH-responsive in *Xenopus laevis* or *Rana catesbeiana*.

• Genes previously identified up- or down-regulated during natural metamorphosis in *Xenopus laevis* or *Rana catesbeiana*.

^a Functional codes: 1, cell growth control; 2, chromatin structure; 3, signal transduction; 4, transcription; 5, hormonal regulation; 6, metabolism/biosynthesis; 7, transport/binding; 8, apoptosis/protein processing; 9, structural; 10, unknown function.

^b Fold change: T₃-D/T₃-G vs. D-D, is that tadpoles were injected with T₃ and at 48 h time point and whose tail tips were removed and subsequently incubated in serum-free medium containing DMSO/100 μM genistein (G) versus animals injected with DMSO and tail tips incubated in medium containing DMSO.

The positive ratio denotes up-regulation, the negative ratio is down-regulation.

^dGene that was down-regulated by genistein at both time points.

presence of T₃ treatment but not DMSO injected animals (**Table 2.6**). None of the other genes that were identified to be affected by T₃ showed any alteration in the T₃-induced response by genistein in either injection set.

The arrays were able to identify strongly expressed genes, but due to their limit of sensitivity, key regulators of the T₃-induced program such as transcription factors, were not detected. This includes TR α and TR β transcripts.

3.6 Using reverse transcriptase quantitative real-time PCR (RT-QPCR) to examine effects of genistein on T₃-induced TR α , TR β , and HSP30 gene expression profiles.

Total RNA was isolated from the tail tips of tadpoles that were cultured in the presence or absence of genistein for 24 h, 48 h or 72 h after the tadpoles were injected with T₃ or vehicle control (see **Figure 2.1** for experimental design). Ribosomal L8 protein mRNA, which remains relatively constant throughout different treatments, was used as an internal control [127] (see **Appendix 2.2**)

3.6.1 T₃-induced TR α transcript levels are not affected by genistein.

Tail tips from animals sacrificed 24 h after T₃ injection and subsequently incubated in serum-free medium (T₃-D) showed a significant increase in TR α mRNA levels at 24–72 h in organ culture compared to tail tips from DMSO only injected tadpoles (D-D) (P<0.05) (**Figure 2.8A**). However, when T₃-induced tail regression was completely blocked by 100 μ M G (**Figure 2.5B**), TR α transcript levels were still significantly up-regulated in comparison to DMSO injected followed by DMSO cultured (D-D) (P<0.05). Furthermore, there was no statistical difference between T₃ injection followed by DMSO culture (T₃-D) and T₃ injection followed by 100 μ M G culture (T₃-

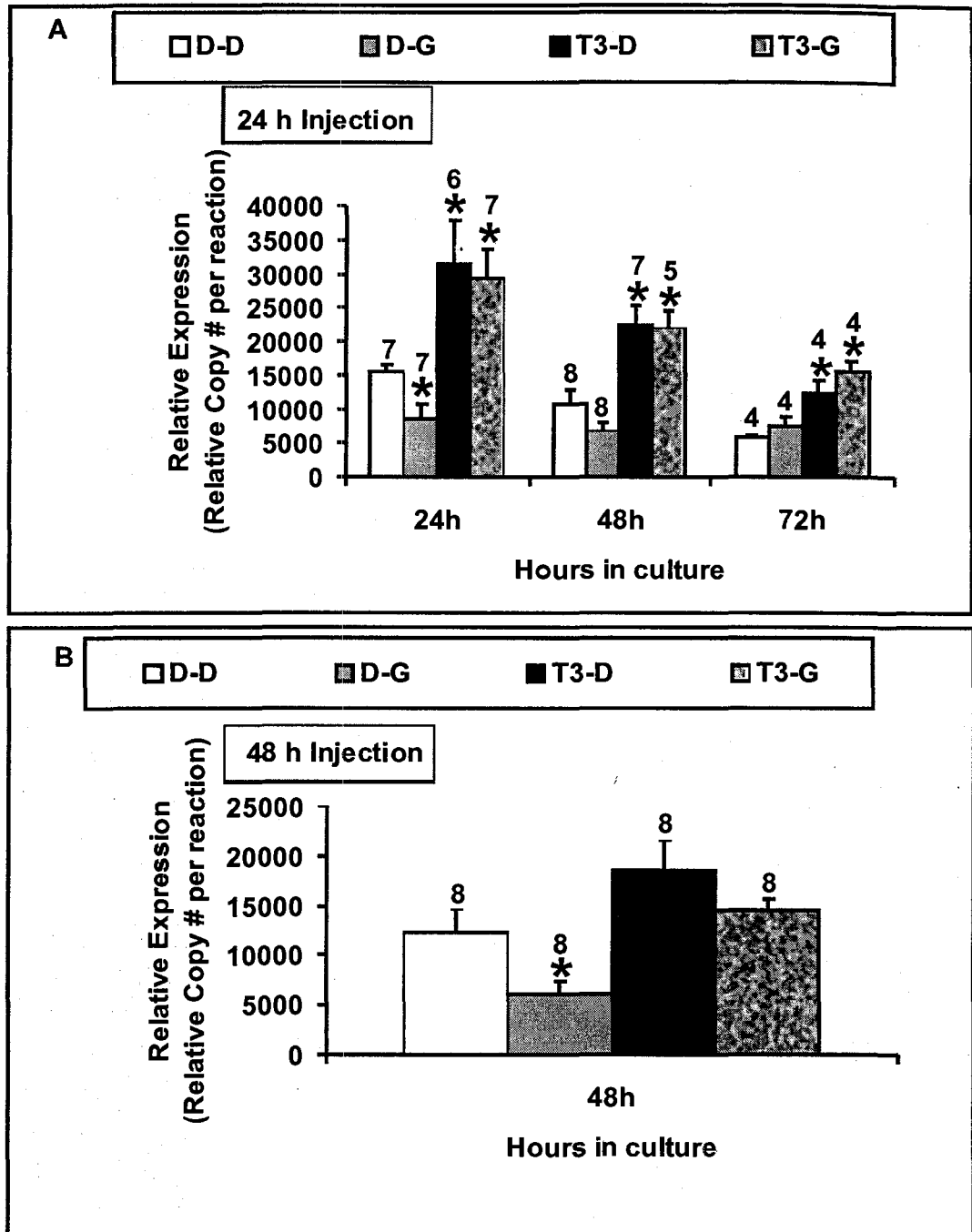


Figure 2.8. T₃-dependent TR α expression is not affected by genistein.

Relative expression levels of TR α (A) After 24 h DMSO (D) or T₃ injection *in vivo*,

tadpole tail tips were removed and cultured in medium in the presence of D or 100 μ M G

for 24 h, 48 h, or 72 h. (B) After 48 h D or T₃ injection *in vivo*, tadpole tail tips were removed and cultured in medium in the presence of D or 100 μM G for 48 h. * P<0.05 relative to D injection followed by D culture (D-D). N number for each treatment group is shown above the error bar.

G). This suggests that TR α up-regulation is not affected by genistein. Tail tips from animals sacrificed 48 h after T₃ injection and subsequently incubated in serum-free medium for 48 h (T₃-D) showed that TR α expression was not significantly up-regulated (**Figure 2.8B**). This may be due to the examining time after 96 h T₃ administration, which is consistent with the observation from Zhang *et al.* (Helbing lab unpublished data) that TR α goes down at 96 h. However, genistein culture alone [24 h after DMSO injection of tadpoles and tail tips culturing for 24 h (**Figure 2.8A**) and 48 h after DMSO injection of tadpoles and tail tips culturing for 48 h (**Figure 2.8B**)] did show a significant decrease in TR α levels in comparison to control.

3.6.2 Genistein affects T₃-induced up-regulation of TR β .

Tail tips from animals sacrificed 24 h after T₃ injection and subsequently incubated in serum-free medium (T₃-D) showed a significant increase in TR β mRNA levels at 24-72 h in organ culture compared to tail tips from DMSO only injected tadpoles (D-D) (P<0.05) (**Figure 2.9A**). This increase was significantly attenuated (P<0.05) (T₃-D vs. T₃-G) (**Figure 2.9A**) when tail regression was completely blocked by 100 μ M G (**Figure 2.5B**). Tail tips from animals sacrificed 48 h after T₃ injection and subsequently incubated in DMSO containing medium for 48 h showed a significant increase in TR β mRNA levels compared to DMSO only injected tadpoles (T₃-D vs. D-D) (**Figure 2.9B**). This T₃-induced increase in TR β transcript levels was significantly attenuated in the presence of G (T₃-D vs. T₃-G) (P<0.05). This effect was to a lesser extent than that observed in the tail tips taken from after 24 h tadpoles injected with T₃ and incubated in G containing culture (**Figure 2.9A**) and is in keeping with the partial inhibition of G on tail regression (**Figure 2.5B**).

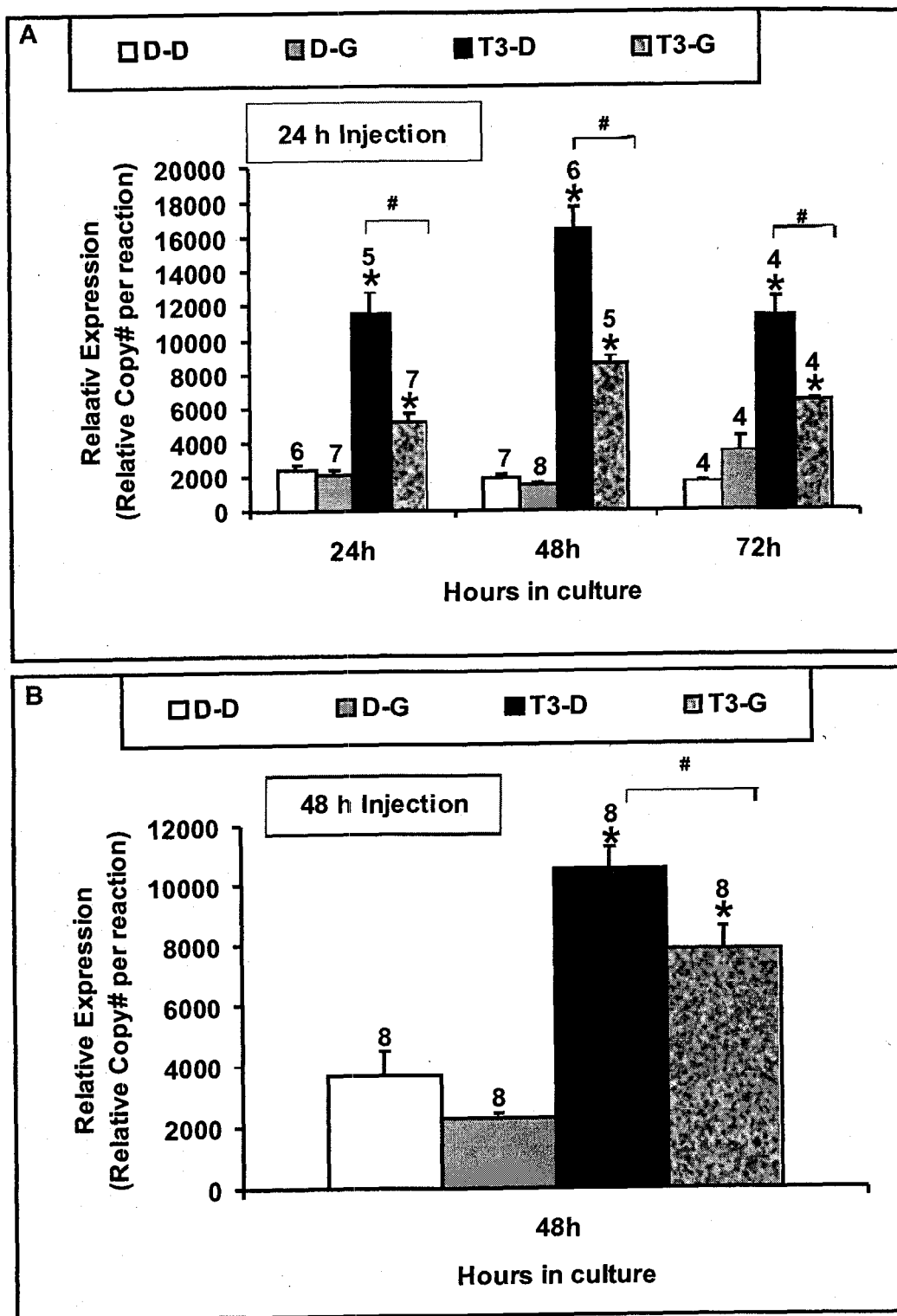


Figure 2.9. Genistein affects T₃-induced up-regulation of TR β .

A) After 24 h DMSO (D) or T₃ injection *in vivo*, tadpole tail tips were removed and cultured in medium in the presence of D or 100 μM G for 24 h to 72 h. (B) After 48 h D or T₃ injection *in vivo*, tadpole tail tips were removed and cultured in medium in the presence of D or 100 μM G for 48 h. * P<0.05 relative to D injection followed by D culture (D-D). # P<0.05 in comparison to T₃ injection followed by D culture (T₃-D). N number for each treatment group is shown above the error bar.

To determine whether there is any correlation between TR α , TR β expression levels and tail regression, I applied non-parametric Spearman correlation analysis. After 24 h tadpole injection with DMSO or T₃ followed by culturing of the tail tip in serum-free medium in the presence of DMSO or 100 μ M G, TR β relative expression levels correlate with tail regression ($r=0.368$, $P<0.01$). In contrast, no correlation was found between TR α relative expression levels and tail regression ($r=0.086$, $P=0.487$). These data suggest that TR β up-regulation is crucial for tail regression and that this up-regulation may, in part, require tyrosine kinase signaling.

3.6.3 T₃ up-regulated HSP30 expression is not affected by genistein.

It is possible that more T₃-responsive genes may be affected by genistein in the same way as TR β . HSP30 has been previously shown to be T₃-responsive [79] and is also an indicator of cellular stress [128]. To determine whether HSP30 expression is affected when tail regression is blocked by 100 μ M G, RT-QPCR was performed to examine HSP30 expression levels. Tail tips from animals sacrificed 24 h after T₃ injection and subsequently incubated in serum-free medium showed that HSP30 was significantly up-regulated at 24-72 h in comparison to D-D control ($P<0.05$) (**Figure 2.10A**). This is consistent with previous work that HSP30 is a T₃-responsive gene [79]. This response was not affected when tail regression was completely inhibited by 100 μ M G (**Figure 2.10A**). Tail tips from animals sacrificed 48 h after T₃ injection and subsequently incubated in serum-free organ culture for 48 h also showed a significant increase of HSP30 mRNA levels compared to controls (**Figure 2.10B**). Like the response for the 24 h T₃ injected animals, G had no effect on this response. However, genistein alone (DMSO injected tadpoles) did show a significant increase in HSP30 levels which

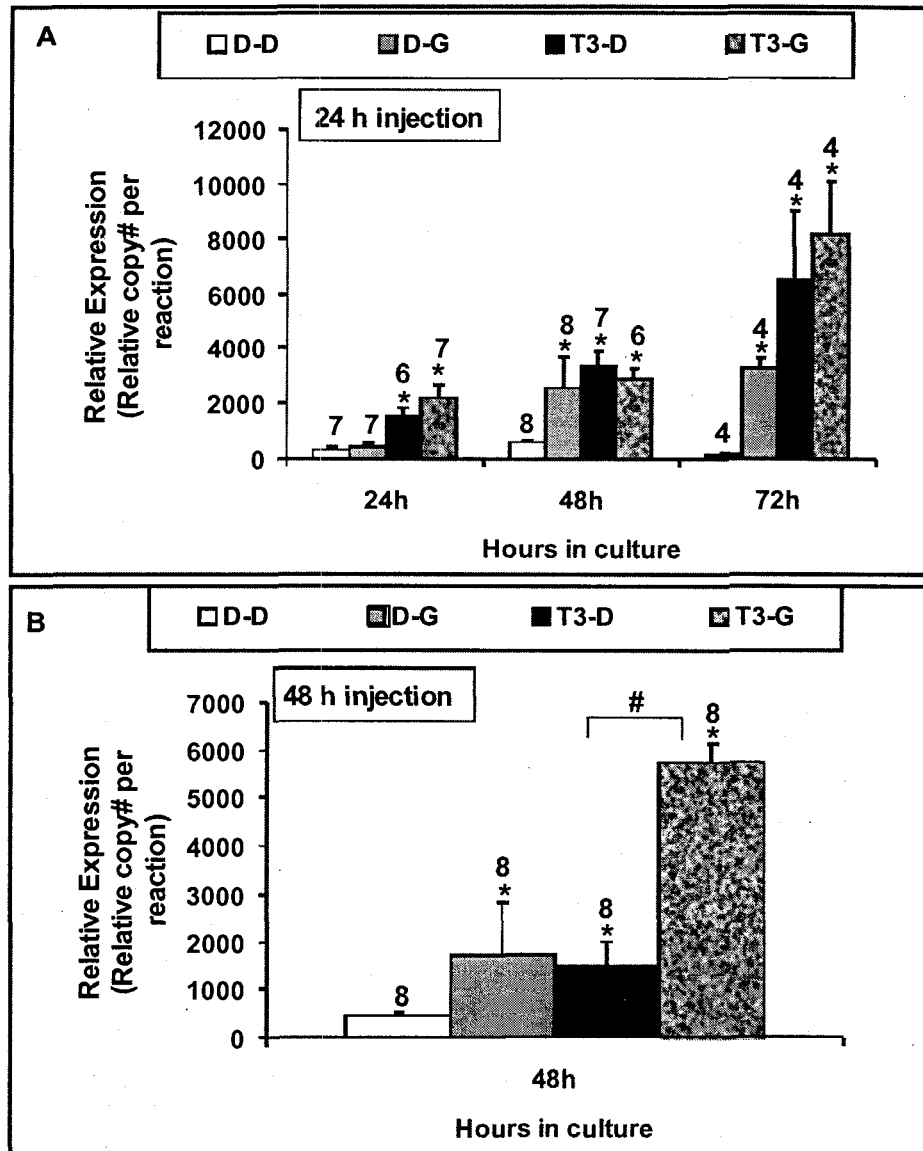


Figure 2.10. T₃-dependent increase in HSP30 expression is not affected by genistein. Relative expression levels of HSP30 after 24 h (A) and 48 h (B) DMSO (D) or T₃ injection *in vivo*, then tail tips were removed and incubated in the presence of D or 100 μM G. * P<0.05 relative to D injection followed by D culture (D-D). # P<0.05 in comparison to T₃ injection followed by D (T₃-D) culture. N number for each treatment group is shown above the error bar.

indicates that prolonged G treatment may be perceived as a stress in the tail tips. Overall, these data show that T₃-induced HSP30 expression is not affected by genistein.

3.7 Isolation and determination of T₃- and genistein sensitivity of two *Rana catesbeiana* ING1 (inhibitor of growth) genes.

To determine ING1 cellular function, we use amphibian metamorphosis as an experimental model in which TH acts to orchestrate tissue-specific proliferation, differentiation and apoptosis. I isolated the partial sequences of two *ING1* variants from the tail (*rING1_{tail}*) and brain (*rING1_{brain}*) tissue of the North American bullfrog, *Rana catesbeiana*. Multiple CLUSTALW alignments comparison *rING1_{brain}* and *rING1_{tail}* with isoforms of *Xenopus laevis* *ING1* (*xING1*) [118] show that they are most identical to *xING1b* exon 2 and share 85% DNA sequence identity to *xING1b*. CLUSTALW alignment shows that *rING1_{tail}* and *rING1_{brain}* share 85% sequence identity (**Figure 2.11A**). The predicted polypeptide is translated from the third reading frame for *rING1_{tail}* and *rING1_{brain}*. The putative *rING1_{tail}* and *rING1_{brain}* share 78% amino acid sequence identity to the putative *xING1b* protein [118] (**Figure 2.11B**); and they are located after the conserved exon 1 and 2 boundary and before the highly conserved C terminus of the ING proteins containing a PHD finger domain, which is common to a family of proteins known to be associated with chromatin remodeling [129] (**Figure 2.11C**).

The *rING1_{tail}* transcripts is only expressed in the *Rana catesbeiana* tail but not the brain. The *rING1_{brain}* is expressed in the *Rana catesbeiana* brain and tail (**Figure 2.12A**). However, *rING1_{tail}* mRNA expression levels are too low making it impossible to

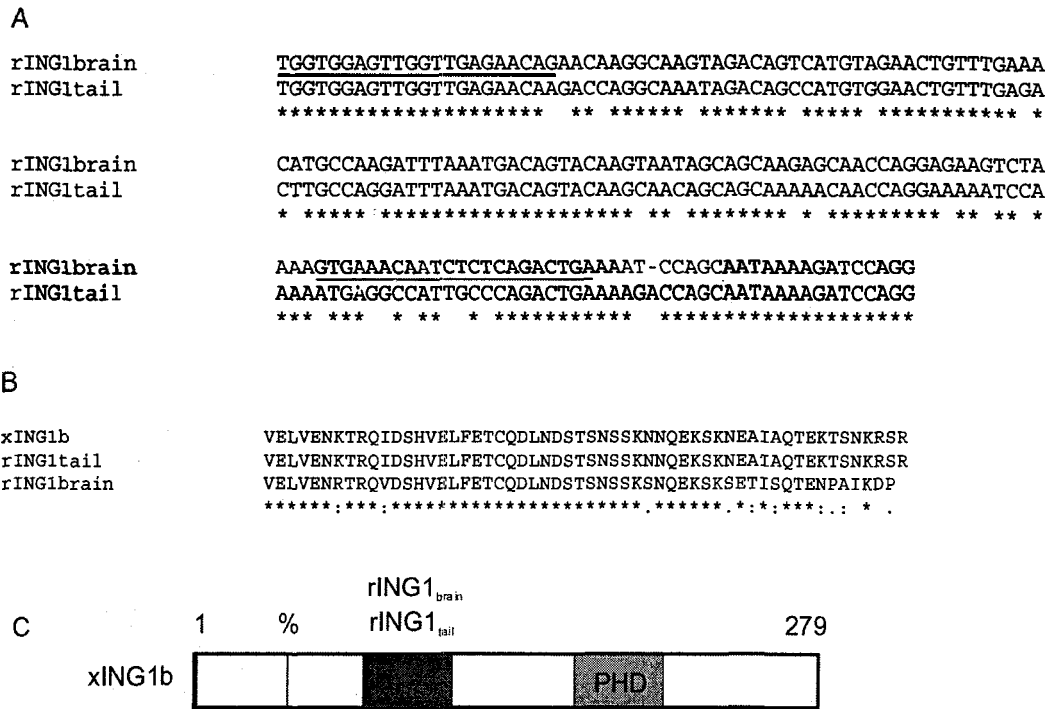


Figure 2.11. Sequence alignments of transcript variants for *rING1_{brain}* and *rING1_{tail}* and their putative encoded proteins.

(A) CLUSTALW alignment shows that *rING1_{brain}* and *rING1_{tail}* share 85% sequence identity. The locations of forward and reverse primer pair used for *rING1_{brain}* RT-PCR analyses are underlined. (B) CLUSTALW Multiple alignments of putative *rING1_{brain}* and *rING1_{tail}* amino acid sequences with putative xING1b protein. The predicted proteins, *rING1_{tail}* and *rING1_{brain}*, share 78% amino acid identity to the putative xING1b protein. (C) Schematic diagram shows the location of *rING1_{brain}* and *rING1_{tail}* in putative xING1b. The % symbol indicates the boundary between exon 1 and exon 2 as determined from the *Xenopus laevis* [117, 118].

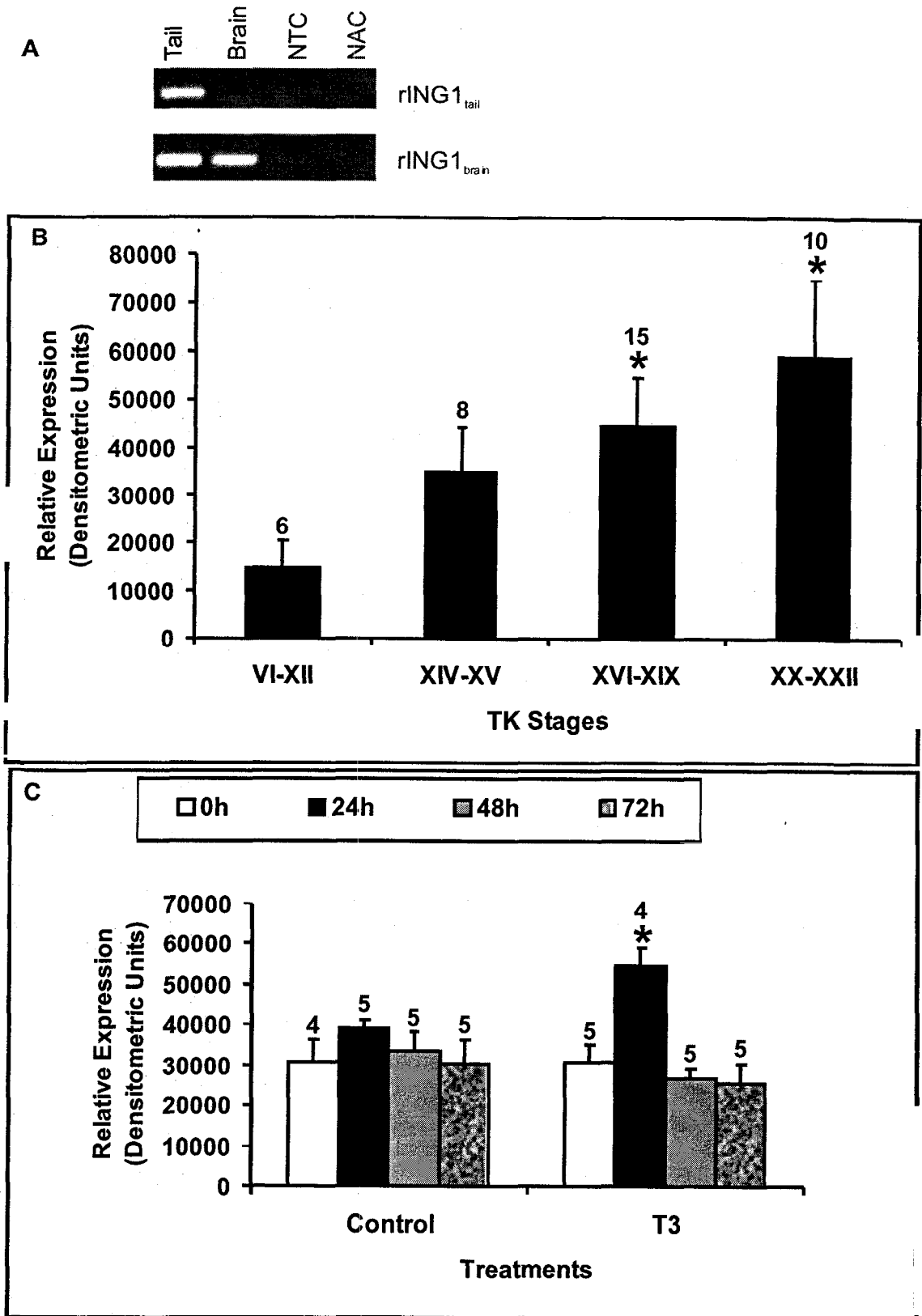


Figure 2.12. Expression of the *rING1_{brain}* transcript during natural and T₃-

precocious metamorphosis in the *Rana catesbeiana* tail.

(A) Shown here are the representative 2% agarose gels of RT-PCR products of *rING1_{tail}* and *rING1_{brain}*. NTC denotes no template control; NAC denotes no enzyme control. (B) *rING1_{brain}* expression during natural metamorphosis in tail tips. * P<0.05 comparison to TK stages VI to XII. (C) *rING1_{brain}* expression during T₃-precocious metamorphosis in tail. Tail biopsy was taken at each time point for each animal. * P<0.05 comparison to 0 h. N number for each treatment time points is shown above the error bar. Parametric One-Way ANOVA test followed by Post Hoc Tukey test were applied.

determine its expression level within all samples. I therefore focused on *rING1_{brain}* for expression analysis. To determine *rING1_{brain}* expression at the mRNA level in the tail during natural and T₃-induced precocious metamorphosis (both natural and T₃-precocious metamorphosis tail cDNA were kindly provided by Dr. Nik Veldhoen), I performed a modified RT-QPCR in which PCR reaction was stopped at 30 to 32 cycles in the linear range of amplification, followed by densitometry analysis. The *rING1_{brain}* transcript is significantly up-regulated during tadpole natural metamorphosis in comparison to TK stages VI to XII (P<0.05) (**Figure 2.12B**). During T₃-induced metamorphosis (**Figure 2.12C**), *rING1_{brain}* transcript is transiently up-regulated at 24 h in comparison to 0 h control (P<0.05). This indicates that *rING1_{brain}* expression is T₃-responsive.

To address whether *rING1_{brain}* expression is affected by genistein, I examined the effect of G on T₃-induced *rING1_{brain}* expression. Tail tips from animals sacrificed 24 h after T₃ injection and cultured in serum-free medium showed that *rING1_{brain}* maintained a significant up-regulation throughout tail tip culture compared to the D-D control (P<0.05) (**Figure 2.13A**). When tail regression was completely suppressed by addition of 100 μM G, the increase of *rING1_{brain}* levels remained high until 72 h in culture where the increase was no longer evident. Tail tips from animals sacrificed 48 h after T₃ injection and cultured in serum-free medium for 48 h showed a significant increase of *rING1_{brain}* in comparison to the D-D control (**Figure 2.13B**) (P<0.05). However, when tail regression was partially blocked by 100 μM G (**Figure 2.5B**), the T₃-induced increase of *rING1_{brain}* was not evident. This suggests that *rING1_{brain}* may be a later contributor for T₃-induced tail regression program and its expression is dependent, in part, on tyrosine kinase signaling.

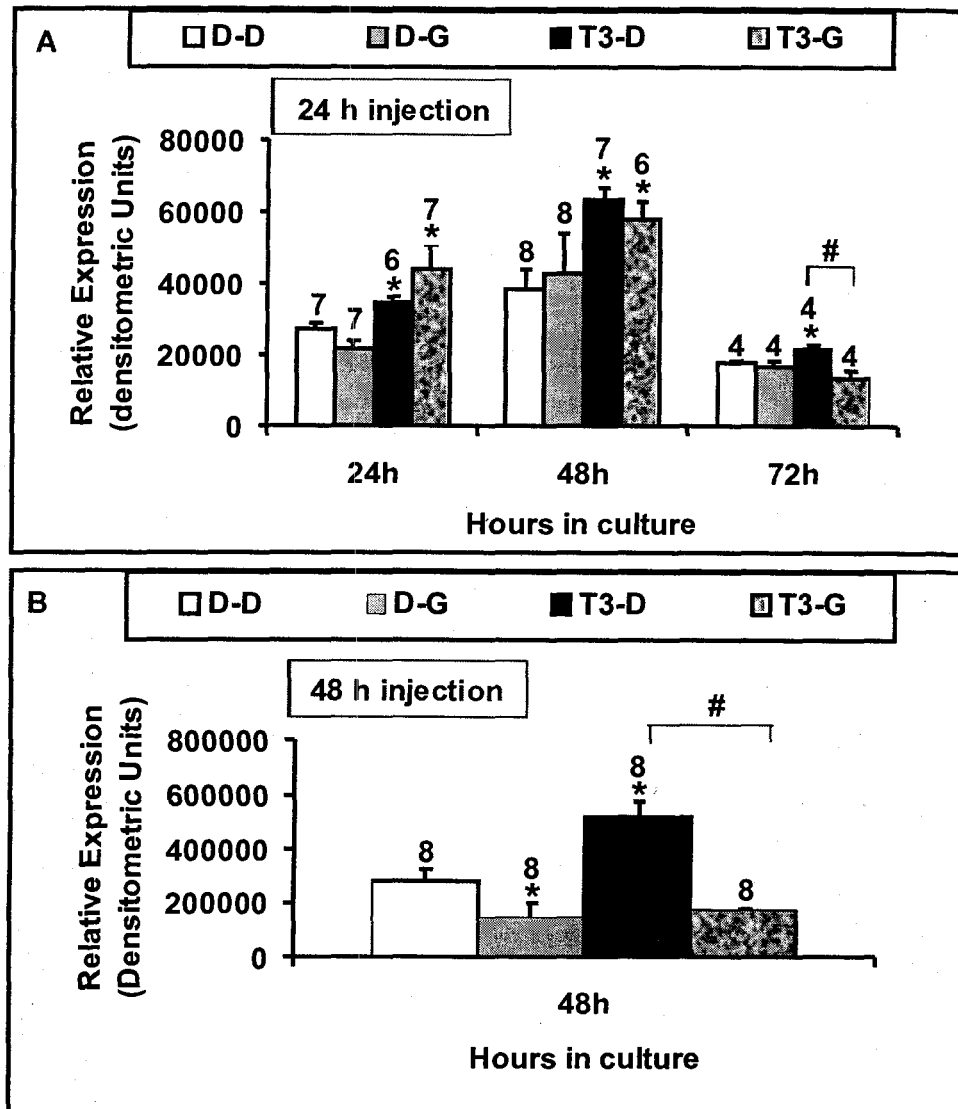


Figure 2.13. Relative expression levels of *rING1_{brain}* in the tadpole injection followed by genistein inhibition study.

RT-QPCR followed by densitometry analysis was used to determine the relative expression level of *rING1_{brain}* at (A) 24 h injection (B) 48 h injection. * $P < 0.05$ comparison to DMSO (D) injection followed by D culture (D-D). # $P < 0.05$ comparison to T_3 injection followed by D (T_3 -D) culture. N number for each treatment time point is shown above the error bar.

3.8 TR α steady state level of phosphorylation is reduced by genistein during T₃-induced tail regression.

My data showed that TR β mRNA (**Figure 2.9**), but not TR α mRNA (**Figure 2.8**), is significantly attenuated by genistein. My data also showed that genistein inhibition of T₃-induced tail regression is through alteration of protein phosphorylation level (**Figure 2.4**). *In vitro* and mammalian cell studies showed that phosphorylation of TRs modulates TR-mediated regulation of target gene expression [45, 46]. But there is no information about the functional role of TR phosphorylation *in vivo*.

To further understand the molecular mechanism underlying TR α transcriptional regulation of TR β and determine whether this regulation is *via* alteration of TR α steady state level of phosphorylation, tadpoles (TK stage VI to XV) were injected with T₃ or vehicle control (DMSO) for 24 h and then the tail tips were removed and incubated in serum-free medium in the presence of 100 μ M G or DMSO for a further 24 h. The tail tip protein homogenates were subjected to IP with anti-TR α and immunoblotted with anti-human TR α (hTR α) or anti-phospho-serine antibodies (**Figure 2.14**). T₃ induces TR α phosphorylation, this T₃-induced phosphorylation is attenuated by genistein by 24.23%. This result is re-reproducible in another pooled tail tip protein homogenate. This suggests that genistein inhibition of T₃-induced tail regression is *via* inhibition TR α phosphorylation, which regulates TR β mRNA expression.

4. Discussion

Recent studies at the molecular level have demonstrated that TH regulates target gene expression through genomic effects by binding TRs [1]. Although there is increasing evidence of TH-induced signaling transduction affecting TH genomic action

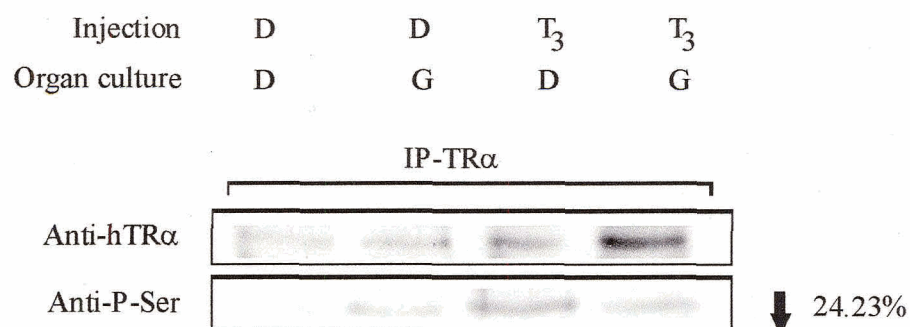


Figure 2.14. Genistein inhibition T₃-induced TR α phosphorylation.

TK stage VI to XV tadpoles were injected with 3×10^{-10} moles/body weight vehicle (DMSO, D) or T₃ and maintained for 24 h then the tail tips were removed and incubated in serum-free medium in the presence of 100 μ M G or D for a further 24 h. The tail tip protein homogenates were subjected to immunoprecipitation (IP) with anti-TR α . The IP-proteins were resolved on 10% SDS-PAGE and immunoblotted with anti-human TR α (hTR α) or anti-phospho-serine antibodies.

[6-10] *in vitro*, few studies have addressed their relevance at cellular level *in vivo*. In this study, by using a tadpole tail organ culture system as an experiment model, I demonstrate the possible involvement of TH-induced tyrosine kinase signaling regulating TR classical/genomic action both at mRNA and protein phosphorylation levels.

Anuran metamorphosis is a complex process, which is absolutely dependent upon the TH controlling of gene expression as its basis. Tadpole tail regression is one of the most conspicuous events at the climax of metamorphosis. It requires a series of very complex changes of biochemical and gene expression [67, 72, 73, 80, 81]. We chose this system because it has distinct advantages for study. The tail can be cultured in a serum free medium for many days, and it responds to exogenously administrated T₃ in a fashion similar to the normal process of tail resorption that occurs at the climax of metamorphosis when endogenous TH is at its highest level. More importantly, it allows us to use specific inhibitors which would otherwise be toxic to the intact tadpoles and determining the involvement of a particular signaling pathway.

In tadpole tail organ culture experiment, it is shown that 100 μ M genistein inhibits T₃-induced tail resorption (**Figure 2.3**). Although genistein shares structural similarity with E₂ and Sone *et al.* [130] showed that 10 μ M E₂ alters *Xenopus laevis* embryonic development, genistein is ~1000 times less potent than E₂ [87, 91]. Genistein at high concentrations (30 μ M to 100 μ M) acts as a tyrosine kinase inhibitor, this suggests that the inhibition of T₃-induced tail regression most likely is through alteration of tyrosine kinase signaling rather than through TR/estrogen pathway crosstalk. Protein analysis show that this effect is *via* genistein inhibition of protein phosphotyrosine level of a 75 kDa protein (**Figure 2.4**).

In the tadpole injection experiment, it is shown that 24 h to 48 h is a critical window for this signaling to occur (**Figure 2.5**). This is coincident with the time required for the establishment genetic program for tail resorption [73]. The timing of these effects suggests that tyrosine kinase signaling may be important in the genetic program transition. This would be consistent with genistein's action as a tyrosine kinase inhibitor. This may also suggest that tyrosine kinase activity is required within 24 h during T_3 -induced tail regression, while after 48 h its activity is not so crucial (G partially inhibited tail regression). Furthermore, it was shown that the inhibitor of Cdks, roscovitine, also completely inhibited tail regression in organ culture after 24 h exogenous T_3 administration [109]. This suggests that non-classical effects persist at least 24 h after TH treatment and stands in contrast to the concept that non-classical effects act within minutes up to 30 min [48]. Therefore, non-classical effects can be important not only minutes but also hours to days after TH treatment.

Induction of metamorphosis is dependent upon the TH-responsive nuclear receptors, $TR\alpha$ and $TR\beta$. Previous studies showed that the steady-state levels of $TR\alpha$ mRNA and protein remained relatively constant during both natural and T_3 -precocious metamorphosis, whereas the expression of $TR\beta$ was increased [72, 76, 82]. $TR\alpha$ levels were present in the premetamorphic tadpole whereas $TR\beta$ levels were extremely low until TH induction [76, 82] suggesting that $TR\alpha$ is critical for competence to respond to TH, $TR\beta$ is required for establishment the genetic programs during metamorphosis. Using QPCR analysis, an induction of mRNA $TR\alpha$ and $TR\beta$ was observed upon T_3 treatment (**Figure 2.15**, **Figure 2.8**, and **Figure 2.9**) as was expected from previous studies. T_3 -induced up-regulation of $TR\beta$ transcripts levels, but not $TR\alpha$, and the $TR\beta$ response was

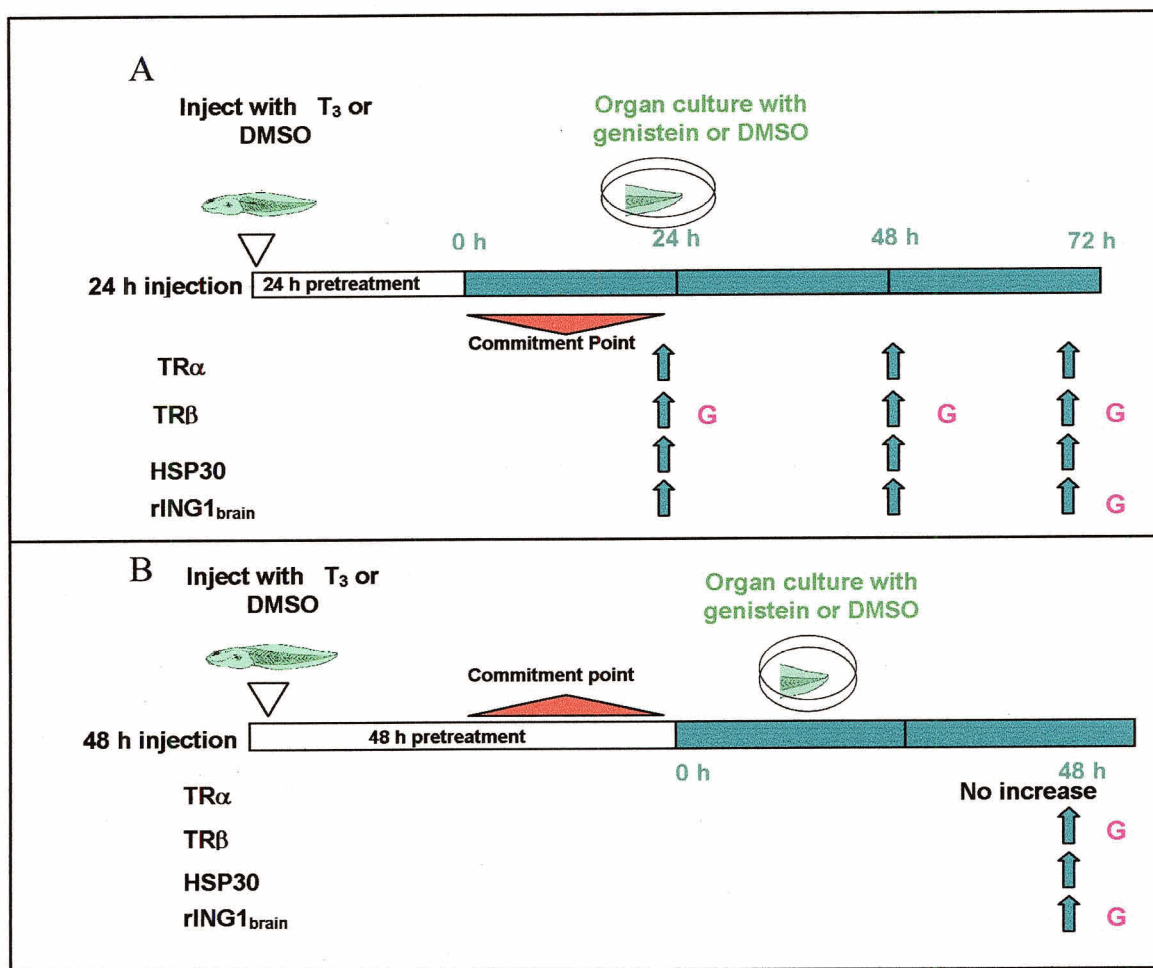


Figure 2.15. Summary of effects of genistein on T_3 -induced TR α , TR β , HSP30, and rING1_{brain} mRNA expression levels in the 24 h injection set (A) and in the 48 h injection set (B).

The green arrows show the measured effect of T_3 treatment at the indicated time points. In those instances where genistein affects the T_3 induction, these effects are indicated by the pink "G".

attenuated by genistein in a time course that strongly correlated with the biological effects of this chemical on the inhibition T_3 -induced tail regression (**Figure 2.3** and **Figure 2.5**). Moreover, genistein inhibition of $TR\beta$ mRNA in the tail tips taken from tadpoles injected with T_3 and incubated in culture 48 h after injection showed a lesser inhibition than that observed at 24 h (**Figure 2.9**), and this coincided with the partial inhibition by genistein on tail regression (**Figure 2.5**). These data are consistent with the previous studies that THs regulate the target gene expression at the transcriptional level and also suggest that tyrosine kinase signaling may play a role in the regulation of this process.

Although the TRs are ligand-activated receptors, they are also phosphoproteins and their functions can be regulated by phosphorylation [45, 46]. The phosphorylation and dephosphorylation reactions are accomplished by multiple enzymes, indicating cell alteration of protein activity in response to different signaling pathways. In eukaryotes, protein phosphorylation is the most important regulatory event. Since most signaling pathways contain tyrosine phosphorylation steps early on in the pathway that are amplified by subsequent serine/threonine phosphorylation events and since TRs have many more serine/threonine phosphorylation sites with regulatory consequences [131, 132], I examined the steady state level of $TR\alpha$ phosphorylation to investigate a possible molecular mechanism of genistein down-regulation of the $TR\beta$ gene. I showed that T_3 -induced phosphorylation of $TR\alpha$ is reduced by genistein (**Figure 2.14**). This suggests that T_3 induces $TR\alpha$ phosphorylation, which regulates T_3 -response gene, $TR\beta$ mRNA. This observation agrees with a previous study [32] that showed using dominant-negative $TR\alpha$ not only blocks transgenic tadpole metamorphosis, but also inhibits the expression of

known T_3 response genes, such as TR β , TH/bZIP, and ST3 at transcriptional level in tail. More importantly, it provides the first direct biologically relevant *in vivo* evidence suggesting TR phosphorylation may be one of the mechanisms by which TRs achieve their diverse biological functions. Previous work from D. Brown's laboratory suggested that TR phosphorylation is not important during metamorphosis [76]. However, they only examined stage 59 tadpoles (*Xenopus laevis*) in which most TRs have already been phosphorylated and will not be able to further phosphorylated by [32 P]orthophosphate. Protein phosphorylation targets the protein for degradation by the ubiquitin-proteasome pathway [133]. I also observed that the increase of steady state levels TR α upon genistein treatment (**Figure 2.14**). This suggests that genistein inhibits TR α phosphorylation, which make this protein less likely to be degraded. It is also important to note that the T_3 -dependent induction of TR β transcripts, although greatly attenuated, is not completely blocked even when tail regression is (**Figure 2.9**). This suggests that part of the induction of the TR β gene does not require phosphorylation with further enhancement requiring it. How this translates to the production TR β protein is currently being investigated.

ING protein acts as a class II tumor suppressor [111]. ING proteins contain a plant homeodomain (PHD) finger, a motif common to many chromatin-regulatory proteins. Recent studies suggested that the ING family of protein contribute to chromatin remodeling, and bind to and affect the activity of HATs, HDACs, and factor acetyltransferase protein complexes [134-137]. It is also shown that ING2 PHD finger interacts with phosphoinositides *in vivo*, which play a critical role in cytoplasmic signal transduction pathways [138]. Despite reports linking ING to chromatin remodeling and signal transduction, the molecular basis of how ING is involved in regulation of gene

expression has not been fully elucidated. There is evidence showing that down-regulation or mislocalization of ING1 protein, particularly the p33^{ING1b} isoforms are common events in gliomas, glioblastomas [115], and human brain tumors [116]. Little is known how ING1 affects the phenotype by expression changes. To address the functional significance of ING1, we used anuran metamorphosis as an experimental model. In this study, *rING1_{brain}* was cloned from *Rana catesbeiana* brain. *rING1_{brain}* expression at transcript level is significantly up-regulated in natural and T₃-precocious tail resorption respectively (**Figure 2.12**), a finding that is consistent with previous studies in *Xenopus laevis* [117, 118]. Evidence also shows when tail regression is blocked by genistein, *rING1_{brain}* expression is significantly down-regulated (**Figure 2.13**). This suggests that *rING1_{brain}* may be a later contributor during TH-dependent tail regression. The mechanism of how *ING1_{brain}* is involved in tyrosine kinase signaling during this process remains to be elucidated.

cDNA array hybridization experiments were designed to identify the potential genes affected by genistein during T₃-induced tail resorption. Across species cDNA hybridization and stringent step by step analysis were performed. The Excel (Microsoft) and SPSS based normalizer genes selection, SPSS based ICC analysis examining the quality of replicates, and Excel (Microsoft) based variance analysis of expressional stability of target genes serve as a good example for how to analyze complicated cDNA array data.

By comparison of fold change of transcript expression levels of T₃-G to T₃-D tail data, I showed that very few gene transcripts were affected by G in the presence of T₃. This suggests that tyrosine kinase signaling may be important in the regulation of only a

specific subset of T_3 -responsive genes. It is important to note that the cNDA arrays may have missed important factors due to sensitivity and/or absence of the probes on the array. More work needs to be done to look at more candidates. Nevertheless, gelatinase B, a matrix metalloproteinase, is down-regulated by genistein at 24 h (Table 2.5) and 48 h (Table 2.6) sets, which supports a role for gelatinase B in T_3 -induced tail regression. However, the relationship of this down-regulation of gelatinase B transcript by genistein and the inhibition of tail regression do not coincide, it is unlikely that the modulation of this gene is a key factor in this process. The observation of gelatinase B in cDNA arrays needs to be further confirmed by QPCR. The mechanism of how gelatinase B is linked to tyrosine kinase signaling transduction during T_3 -dependent tail regression remain to be investigated. Recently, MAPK [139-142] and PI3K [141] pathways involving transcriptional regulation of gelatinase B has been demonstrated in mammals. It may be possible that PI3K and/or MAPK pathways are involved in the regulation of the gelatinase B in tadpole tail regression.

In summary, this study demonstrates phosphorylation is an important factor in establishing TH-dependent gene expression programs and suggests that TH classical/genomic and non-classical actions are interwoven to elicit a cellular response important in development. These data strongly implicate $TR\alpha$ as a target for phosphorylation which may selectively change the induction of specific target genes. However, it is possible that the major mechanism involving tyrosine kinase signaling may target additional cellular components that are important in the induction of tail regression. They may not be directly involved with gene expression changes such as caspases for example. Nevertheless, the findings presented in this thesis help decipher

non-classical and classical mechanisms behind T_3 -dependent tail regression in the *Rana catesbeiana* tadpole. This work also contributes insight into our understanding the mechanism of TH-induced apoptosis.

5. Conclusions and Future Directions

The objective of this study was to determine whether tyrosine kinase signaling transduction affects TH classical/genomic action at cellular level *in vivo*. Genistein (one of major components in soy formula), which acts as tyrosine kinase inhibitor *in vitro* as well as shares similar structural features with E_2 , was applied as a tool to investigate this hypothesis. Results show that genistein inhibits T_3 -dependent tadpole tail regression and this effect is most likely through its tyrosine kinase inhibition action. QPCR data suggest a possible involvement of TR β as a tyrosine signaling target during T_3 -dependent tadpole tail resorption, which could reflect a novel mechanism interweaving of TH classical/genomic and non-classical actions. It is also shown that genistein affects T_3 -induced phosphorylation of TR α , which indicates that phosphorylation is an important factor in establishing aspects of the T_3 -dependent gene expression program.

TRs regulate target gene expression by recruiting TR-interacting cofactors [143-146], which are tissue dependent. Future work needs to investigate whether genistein affects TR β phosphorylation level as well the interaction of TRs with their cofactors in the context of T_3 -induced tail regression program. The steady state level of phosphorylation of TR cofactors will be investigated as it is well known that their activities can modulated by changes in phosphorylation. The well-characterized cofactors are SMRT, NCoR, and SRC. Of particular interest are the cofactors that inhibit TR-mediated gene activation [31, 147-149]. IP and immunoblotting using specific

antibodies can be performed. Both cell homogenates and fractionate protein homogenates into nuclear and cytoplasmic proteins can be examined. Fractionating cells into cellular compartments can enrich low abundance proteins and give us information about the function of the proteins whose expression profile can differ between cell compartments. SMRT for example has been shown to be a target for phosphorylation which results in the translocation of the protein from nucleus (active) to the cytoplasm (inactive) [149, 150]. Future work will focus on identifying possible targets for tyrosine kinase to begin to identify which signaling pathways are important for TH-dependent tail regression. Pro-Q Diamond stain (stains only phosphoproteins) for 1D and 2D gels can be performed to examine the change of overall phosphoproteins affected by genistein. The potential spots identified on 2D gel can be isolated for MS analysis to characterize the proteins.

My cDNA array data suggest that gelatinase B requires ongoing tyrosine kinase signaling during TH-dependent tadpole tail regression and might be important early on in tail regression. To further confirm the involvement of gelatinase B, QPCR analysis at its transcript level and gelatin zymography analysis [151] at the protein level can be performed. Cloning the gelatinase B gene is being conducted in our lab. Once the gene has been cloned, specific primers will be designed for QPCR analysis. Genes identified as affected by genistein in the **Table 2.5** and **Table 2.6** can be confirmed by QPCR when those genes have been cloned. The known T_3 -response genes, such as TH/bZIP and ST3 which are undetectable on cDNA array, will also be examined by QPCR.

This work has and will contribute to the understanding of the connection between TH classical and non-classical effects, which helps to establish a new model for TH-induced apoptosis.

Literature cited

1. Yen, P.M., *Physiological and molecular basis of thyroid hormone action*. *Physiol Rev*, 2001. **81**(3): p. 1097-142.
2. Bergh, J.J., et al., *Integrin $\alpha V\beta 3$ contains a cell surface receptor site for thyroid hormone that is linked to activation of mitogen-activated protein kinase and induction of angiogenesis*. *Endocrinology*, 2005. **146**(7): p. 2864-71.
3. Ritchie, J.W., et al., *A role for thyroid hormone transporters in transcriptional regulation by thyroid hormone receptors*. *Mol Endocrinol*, 2003. **17**(4): p. 653-61.
4. Friesema, E.C., et al., *Identification of monocarboxylate transporter 8 as a specific thyroid hormone transporter*. *J Biol Chem*, 2003. **278**(41): p. 40128-35.
5. Dumitrescu, A.M., et al., *A novel syndrome combining thyroid and neurological abnormalities is associated with mutations in a monocarboxylate transporter gene*. *Am J Hum Genet*, 2004. **74**(1): p. 168-75.
6. Lin, H.Y., et al., *Thyroid hormone promotes the phosphorylation of STAT3 and potentiates the action of epidermal growth factor in cultured cells*. *Biochem J*, 1999. **338** (Pt 2): p. 427-32.
7. Lin, H.Y., et al., *Potentialiation by thyroid hormone of human IFN-gamma-induced HLA-DR expression*. *J Immunol*, 1998. **161**(2): p. 843-9.
8. Lin, H.Y., et al., *Protein synthesis-dependent potentiation by thyroxine of antiviral activity of interferon-gamma*. *Am J Physiol*, 1997. **273**(4 Pt 1): p. C1225-32.
9. Schmidt, B.M., et al., *Nongenomic cardiovascular effects of triiodothyronine in euthyroid male volunteers*. *J Clin Endocrinol Metab*, 2002. **87**(4): p. 1681-6.
10. Wang, Y.G., et al., *Acute exposure to thyroid hormone increases Na^+ current and intracellular Ca^{2+} in cat atrial myocytes*. *J Physiol*, 2003. **546**(Pt 2): p. 491-9.
11. Dixon, R.A. and D. Ferreira, *Genistein*. *Phytochemistry*, 2002. **60**(3): p. 205-11.
12. Lee, H.P., et al., *Dietary effects on breast-cancer risk in Singapore*. *Lancet*, 1991. **337**(8751): p. 1197-200.
13. Lamartiniere, C.A., *Protection against breast cancer with genistein: a component of soy*. *Am J Clin Nutr*, 2000. **71**(6 Suppl): p. 1705S-7S; discussion 1708S-9S.

14. Marks, L.S., et al., *Prostate cancer in native Japanese and Japanese-American men: effects of dietary differences on prostatic tissue*. *Urology*, 2004. **64**(4): p. 765-71.
15. Hwang, J., H.N. Hodis, and A. Sevanian, *Soy and alfalfa phytoestrogen extracts become potent low-density lipoprotein antioxidants in the presence of acerola cherry extract*. *J Agric Food Chem*, 2001. **49**(1): p. 308-14.
16. Alekel, D.L., et al., *Isoflavone-rich soy protein isolate attenuates bone loss in the lumbar spine of perimenopausal women*. *Am J Clin Nutr*, 2000. **72**(3): p. 844-52.
17. File, S.E., et al., *Eating soya improves human memory*. *Psychopharmacology (Berl)*, 2001. **157**(4): p. 430-6.
18. Akiyama, T., et al., *Genistein, a specific inhibitor of tyrosine-specific protein kinases*. *J Biol Chem*, 1987. **262**(12): p. 5592-5.
19. Kim, H., T.G. Peterson, and S. Barnes, *Mechanisms of action of the soy isoflavone genistein: emerging role for its effects via transforming growth factor beta signaling pathways*. *Am J Clin Nutr*, 1998. **68**(6 Suppl): p. 1418S-1425S.
20. Utoh, R., et al., *Platelet-derived growth factor signaling as a cue of the epithelial-mesenchymal interaction required for anuran skin metamorphosis*. *Dev Dyn*, 2003. **227**(2): p. 157-69.
21. Doerge, D.R. and D.M. Sheehan, *Goitrogenic and estrogenic activity of soy isoflavones*. *Environ Health Perspect*, 2002. **110 Suppl 3**: p. 349-53.
22. Divi, R.L., H.C. Chang, and D.R. Doerge, *Anti-thyroid isoflavones from soybean: isolation, characterization, and mechanisms of action*. *Biochem Pharmacol*, 1997. **54**(10): p. 1087-96.
23. Doerge, D.R. and H.C. Chang, *Inactivation of thyroid peroxidase by soy isoflavones, in vitro and in vivo*. *J Chromatogr B Analyt Technol Biomed Life Sci*, 2002. **777**(1-2): p. 269-79.
24. Chang, H.C. and D.R. Doerge, *Dietary genistein inactivates rat thyroid peroxidase in vivo without an apparent hypothyroid effect*. *Toxicol Appl Pharmacol*, 2000. **168**(3): p. 244-52.
25. Mori, K., et al., *Involvement of tyrosine phosphorylation in the regulation of 5'-deiodinases in FRTL-5 rat thyroid cells and rat astrocytes*. *Endocrinology*, 1996. **137**(4): p. 1313-8.
26. Gorbman, A., W. W. W. Dickhoff, S. R. Vigna, N. B. Clark, and C. L. Ralph, *Comparative Endocrinology*. 1983: A Wiley-interscience Publication.

27. Norris, D., O., *Vertebrate Endocrinology*. Third edition ed. 1996: Academic Press.
28. Denver, R.J., *Acceleration of anuran amphibian metamorphosis by corticotropin-releasing hormone-like peptides*. Gen Comp Endocrinol, 1993. **91**(1): p. 38-51.
29. Griffin, J., E., and S. R. Ojeda, *Textbook of endocrine physiology*. Fourth edition ed. 2000: Oxford University Press.
30. Bassett, J.H., C.B. Harvey, and G.R. Williams, *Mechanisms of thyroid hormone receptor-specific nuclear and extra nuclear actions*. Mol Cell Endocrinol, 2003. **213**(1): p. 1-11.
31. Tomita, A., D.R. Buchholz, and Y.B. Shi, *Recruitment of N-CoR/SMRT-TBLR1 corepressor complex by unliganded thyroid hormone receptor for gene repression during frog development*. Mol Cell Biol, 2004. **24**(8): p. 3337-46.
32. Buchholz, D.R., et al., *Transgenic analysis reveals that thyroid hormone receptor is sufficient to mediate the thyroid hormone signal in frog metamorphosis*. Mol Cell Biol, 2004. **24**(20): p. 9026-37.
33. Sap, J., et al., *The c-erb-A protein is a high-affinity receptor for thyroid hormone*. Nature, 1986. **324**(6098): p. 635-40.
34. Weinberger, C., et al., *The c-erb-A gene encodes a thyroid hormone receptor*. Nature, 1986. **324**(6098): p. 641-6.
35. Eckey, M., U. Moehren, and A. Baniahmad, *Gene silencing by the thyroid hormone receptor*. Mol Cell Endocrinol, 2003. **213**(1): p. 13-22.
36. Apriletti, J.W., et al., *Molecular and structural biology of thyroid hormone receptors*. Clin Exp Pharmacol Physiol Suppl, 1998. **25**: p. S2-11.
37. O'Shea, P.J. and G.R. Williams, *Insight into the physiological actions of thyroid hormone receptors from genetically modified mice*. J Endocrinol, 2002. **175**(3): p. 553-70.
38. Brent, G.A., *Tissue-specific actions of thyroid hormone: insights from animal models*. Rev Endocr Metab Disord, 2000. **1**(1-2): p. 27-33.
39. Aranda, A. and A. Pascual, *Nuclear hormone receptors and gene expression*. Physiol Rev, 2001. **81**(3): p. 1269-304.
40. Sachs, L.M., et al., *Nuclear receptor corepressor recruitment by unliganded thyroid hormone receptor in gene repression during Xenopus laevis development*. Mol Cell Biol, 2002. **22**(24): p. 8527-38.

41. Yen, P.M., *Molecular basis of resistance to thyroid hormone*. Trends Endocrinol Metab, 2003. **14**(7): p. 327-33.
42. Chen, J.D. and R.M. Evans, *A transcriptional co-repressor that interacts with nuclear hormone receptors*. Nature, 1995. **377**(6548): p. 454-7.
43. Lee, J.W., et al., *Two classes of proteins dependent on either the presence or absence of thyroid hormone for interaction with the thyroid hormone receptor*. Mol Endocrinol, 1995. **9**(2): p. 243-54.
44. Rosenfeld, M.G. and C.K. Glass, *Coregulator codes of transcriptional regulation by nuclear receptors*. J Biol Chem, 2001. **276**(40): p. 36865-8.
45. Sugawara, A., et al., *Phosphorylation selectively increases triiodothyronine receptor homodimer binding to DNA*. J Biol Chem, 1994. **269**(1): p. 433-7.
46. Bhat, M.K., K. Ashizawa, and S.Y. Cheng, *Phosphorylation enhances the target gene sequence-dependent dimerization of thyroid hormone receptor with retinoid X receptor*. Proc Natl Acad Sci U S A, 1994. **91**(17): p. 7927-31.
47. Nicoll, J.B., et al., *Compartment-specific phosphorylation of rat thyroid hormone receptor alpha 1 regulates nuclear localization and retention*. Mol Cell Endocrinol, 2003. **205**(1-2): p. 65-77.
48. Schmidt, B.M., et al., *Rapid, nongenomic steroid actions: A new age?* Front Neuroendocrinol, 2000. **21**(1): p. 57-94.
49. Li, L., M.P. Haynes, and J.R. Bender, *Plasma membrane localization and function of the estrogen receptor alpha variant (ER46) in human endothelial cells*. Proc Natl Acad Sci U S A, 2003. **100**(8): p. 4807-12.
50. Zhu, Y., et al., *Cloning, expression, and characterization of a membrane progesterin receptor and evidence it is an intermediary in meiotic maturation of fish oocytes*. Proc Natl Acad Sci U S A, 2003. **100**(5): p. 2231-6.
51. Zhu, Y., J. Bond, and P. Thomas, *Identification, classification, and partial characterization of genes in humans and other vertebrates homologous to a fish membrane progesterin receptor*. Proc Natl Acad Sci U S A, 2003. **100**(5): p. 2237-42.
52. Moggs, J.G. and G. Orphanides, *Estrogen receptors: orchestrators of pleiotropic cellular responses*. EMBO Rep, 2001. **2**(9): p. 775-81.
53. Davis, P.J., et al., *Thyroxine promotes association of mitogen-activated protein kinase and nuclear thyroid hormone receptor (TR) and causes serine phosphorylation of TR*. J Biol Chem, 2000. **275**(48): p. 38032-9.

54. Lin, H.Y., et al., *Thyroid hormone induces activation of mitogen-activated protein kinase in cultured cells*. Am J Physiol, 1999. **276**(5 Pt 1): p. C1014-24.
55. Shih, A., et al., *Thyroid hormone promotes serine phosphorylation of p53 by mitogen-activated protein kinase*. Biochemistry, 2001. **40**(9): p. 2870-8.
56. Gustafsson, J.A., *Estrogen receptor beta--a new dimension in estrogen mechanism of action*. J Endocrinol, 1999. **163**(3): p. 379-83.
57. Iafrati, M.D., et al., *Estrogen inhibits the vascular injury response in estrogen receptor alpha-deficient mice*. Nat Med, 1997. **3**(5): p. 545-8.
58. Osborne, C.K., H. Zhao, and S.A. Fuqua, *Selective estrogen receptor modulators: structure, function, and clinical use*. J Clin Oncol, 2000. **18**(17): p. 3172-86.
59. Vasudevan, N., S. Ogawa, and D. Pfaff, *Estrogen and thyroid hormone receptor interactions: physiological flexibility by molecular specificity*. Physiol Rev, 2002. **82**(4): p. 923-44.
60. Zhu, Y.S., et al., *Estrogen and thyroid hormone interaction on regulation of gene expression*. Proc Natl Acad Sci U S A, 1996. **93**(22): p. 12587-92.
61. Zhu, Y.S., et al., *Molecular analysis of estrogen induction of preproenkephalin gene expression and its modulation by thyroid hormones*. Brain Res Mol Brain Res, 2001. **91**(1-2): p. 23-33.
62. Vasudevan, N., et al., *Crosstalk between oestrogen receptors and thyroid hormone receptor isoforms results in differential regulation of the preproenkephalin gene*. J Neuroendocrinol, 2001. **13**(9): p. 779-90.
63. Yarwood, N.J., et al., *Estradiol modulates thyroid hormone regulation of the human glycoprotein hormone alpha subunit gene*. J Biol Chem, 1993. **268**(29): p. 21984-9.
64. Yen, P.M., E.C. Wilcox, and W.W. Chin, *Steroid hormone receptors selectively affect transcriptional activation but not basal repression by thyroid hormone receptors*. Endocrinology, 1995. **136**(2): p. 440-5.
65. Gudernatsch, J.F., *Feed experiments on tadpoles. I. The influence of specific organs gives a food on frowth and differentiation. A contribution to the knowledge of organs with internal secretion*. Wilhelm Roux Arch. Entwicklungsmech. Org., 1912. **35**: p. 457-483.
66. Dodd, M.H., Dodd, J. M., *in physiology of the Amphibia*, ed. B. Lofts. 1976, New York: Academic Press.

67. Shi, Y.B., *Amphibian metamorphosis from morphology to molecular biology*. 2000, New York: A John Wiley & Sons, Inc., Publication.
68. Ishizuya-Oka, A. and A. Shimozawa, *Induction of metamorphosis by thyroid hormone in anuran small intestine cultured organotypically in vitro*. *In Vitro Cell Dev Biol*, 1991. **27A**(11): p. 853-7.
69. Shi, Y.B. and D.D. Brown, *The earliest changes in gene expression in tadpole intestine induced by thyroid hormone*. *J Biol Chem*, 1993. **268**(27): p. 20312-7.
70. Helbing, C., G. Gergely, and B.G. Atkinson, *Sequential up-regulation of thyroid hormone beta receptor, ornithine transcarbamylase, and carbamyl phosphate synthetase mRNAs in the liver of Rana catesbeiana tadpoles during spontaneous and thyroid hormone-induced metamorphosis*. *Dev Genet*, 1992. **13**(4): p. 289-301.
71. Helbing, C.C. and B.G. Atkinson, *3,5,3'-Triiodothyronine-induced carbamyl-phosphate synthetase gene expression is stabilized in the liver of Rana catesbeiana tadpoles during heat shock*. *J Biol Chem*, 1994. **269**(16): p. 11743-50.
72. Helbing, C.C., et al., *Expression profiles of novel thyroid hormone-responsive genes and proteins in the tail of Xenopus laevis tadpoles undergoing precocious metamorphosis*. *Mol Endocrinol*, 2003. **17**(7): p. 1395-409.
73. Wang, Z. and D.D. Brown, *Thyroid hormone-induced gene expression program for amphibian tail resorption*. *J Biol Chem*, 1993. **268**(22): p. 16270-8.
74. Kawahara, A., B.S. Baker, and J.R. Tata, *Developmental and regional expression of thyroid hormone receptor genes during Xenopus metamorphosis*. *Development*, 1991. **112**(4): p. 933-43.
75. Yaoita, Y. and D.D. Brown, *A correlation of thyroid hormone receptor gene expression with amphibian metamorphosis*. *Genes Dev*, 1990. **4**(11): p. 1917-24.
76. Eliceiri, B.P. and D.D. Brown, *Quantitation of endogenous thyroid hormone receptors alpha and beta during embryogenesis and metamorphosis in Xenopus laevis*. *J Biol Chem*, 1994. **269**(39): p. 24459-65.
77. Buckbinder, L. and D.D. Brown, *Thyroid hormone-induced gene expression changes in the developing frog limb*. *J Biol Chem*, 1992. **267**(36): p. 25786-91.
78. Shi, Y.B., et al., *Thyroid hormone regulation of apoptotic tissue remodeling during anuran metamorphosis*. *Cell Res*, 2001. **11**(4): p. 245-52.

79. Helbing, C., C. Gallimore, and B.G. Atkinson, *Characterization of a Rana catesbeiana hsp30 gene and its expression in the liver of this amphibian during both spontaneous and thyroid hormone-induced metamorphosis*. Dev Genet, 1996. **18**(3): p. 223-33.
80. Brown, D.D., et al., *The thyroid hormone-induced tail resorption program during Xenopus laevis metamorphosis*. Proc Natl Acad Sci U S A, 1996. **93**(5): p. 1924-9.
81. Brown, D.D., et al., *Amphibian metamorphosis: a complex program of gene expression changes controlled by the thyroid hormone*. Recent Prog Horm Res, 1995. **50**: p. 309-15.
82. Veldhoen, N., et al., *Distinctive gene profiles occur at key points during natural metamorphosis in the Xenopus laevis tadpole tail*. Dev Dyn, 2002. **225**(4): p. 457-68.
83. Gauthier, F.V., et al., *Postembryonic expression of the myosin heavy chain genes in the limb, tail, and heart muscles of metamorphosing amphibian tadpoles*. Microsc Res Tech, 2000. **50**(6): p. 458-72.
84. Suzuki, K., et al., *Novel Rana keratin genes and their expression during larval to adult epidermal conversion in bullfrog tadpoles*. Differentiation, 2001. **68**(1): p. 44-54.
85. Yamauchi, K., et al., *Structural characteristics of bullfrog (Rana catesbeiana) transthyretin and its cDNA--comparison of its pattern of expression during metamorphosis with that of lipocalin*. Eur J Biochem, 1998. **256**(2): p. 287-96.
86. Wang, T.T., N. Sathyamoorthy, and J.M. Phang, *Molecular effects of genistein on estrogen receptor mediated pathways*. Carcinogenesis, 1996. **17**(2): p. 271-5.
87. Zava, D.T. and G. Duwe, *Estrogenic and antiproliferative properties of genistein and other flavonoids in human breast cancer cells in vitro*. Nutr Cancer, 1997. **27**(1): p. 31-40.
88. Kuiper, G.G., et al., *Interaction of estrogenic chemicals and phytoestrogens with estrogen receptor beta*. Endocrinology, 1998. **139**(10): p. 4252-63.
89. Hill, L., W., and Stuart, H., C., *A soy bean food preparation for feeding infants with milk idiosyncrasy*. J. Am. Med. Assoc., 1929. **93**: p. 985-987.
90. *American Academy of Pediatrics. Committee on Nutrition. Soy protein-based formulas: recommendations for use in infant feeding*. Pediatrics, 1998. **101**(1 Pt 1): p. 148-53.

91. Badger, T.M., et al., *The health consequences of early soy consumption*. J Nutr, 2002. **132**(3): p. 559S-565S.
92. Setchell, K.D. and S.J. Cole, *Variations in isoflavone levels in soy foods and soy protein isolates and issues related to isoflavone databases and food labeling*. J Agric Food Chem, 2003. **51**(14): p. 4146-55.
93. Ishizuki, Y., et al., [*The effects on the thyroid gland of soybeans administered experimentally in healthy subjects*]. Nippon Naibunpi Gakkai Zasshi, 1991. **67**(5): p. 622-9.
94. Hunter, T. and J.A. Cooper, *Protein-tyrosine kinases*. Annu Rev Biochem, 1985. **54**: p. 897-930.
95. Ushiro, H. and S. Cohen, *Identification of phosphotyrosine as a product of epidermal growth factor-activated protein kinase in A-431 cell membranes*. J Biol Chem, 1980. **255**(18): p. 8363-5.
96. Ek, B., et al., *Stimulation of tyrosine-specific phosphorylation by platelet-derived growth factor*. Nature, 1982. **295**(5848): p. 419-20.
97. Jacobs, S., et al., *Somatomedin-C stimulates the phosphorylation of the beta-subunit of its own receptor*. J Biol Chem, 1983. **258**(16): p. 9581-4.
98. Uckun, F.M., et al., *Biotherapy of B-cell precursor leukemia by targeting genistein to CD19-associated tyrosine kinases*. Science, 1995. **267**(5199): p. 886-91.
99. Fritz, W.A., et al., *Dietary genistein: perinatal mammary cancer prevention, bioavailability and toxicity testing in the rat*. Carcinogenesis, 1998. **19**(12): p. 2151-8.
100. Hakkak, R., et al., *Diets containing whey proteins or soy protein isolate protect against 7,12-dimethylbenz(a)anthracene-induced mammary tumors in female rats*. Cancer Epidemiol Biomarkers Prev, 2000. **9**(1): p. 113-7.
101. Cotroneo, M.S., et al., *Genistein action in the prepubertal mammary gland in a chemoprevention model*. Carcinogenesis, 2002. **23**(9): p. 1467-74.
102. Brown, N.M., et al., *Prepubertal genistein treatment modulates TGF-alpha, EGF and EGF-receptor mRNAs and proteins in the rat mammary gland*. Mol Cell Endocrinol, 1998. **144**(1-2): p. 149-65.
103. Rowlands, J.C., et al., *Soy and whey proteins downregulate DMBA-induced liver and mammary gland CYP1 expression in female rats*. J Nutr, 2001. **131**(12): p. 3281-7.

104. Badger, T.M., M.J. Ronis, and R. Hakkak, *Developmental effects and health aspects of soy protein isolate, casein, and whey in male and female rats*. Int J Toxicol, 2001. **20**(3): p. 165-74.
105. Stroheker, T., et al., *Influence of dietary soy isoflavones on the accessory sex organs of the Wistar rat*. Food Chem Toxicol, 2003. **41**(8): p. 1175-83.
106. Adams, N.R., *Permanent infertility in ewes exposed to plant oestrogens*. Aust Vet J, 1990. **67**(6): p. 197-201.
107. Setchell, K.D., et al., *Exposure of infants to phyto-oestrogens from soy-based infant formula*. Lancet, 1997. **350**(9070): p. 23-7.
108. Zoeller, R.T. and J. Rovet, *Timing of thyroid hormone action in the developing brain: clinical observations and experimental findings*. J Neuroendocrinol, 2004. **16**(10): p. 809-18.
109. Skirrow, R.C., *Cyclin dependent kinase activity is necessary for thyroid hormone induced tail regression in the Rana catesbeiana tadpole (M.Sc. thesis)*. 2003, University of Victoria.
110. Lim, W., et al., *A thyroid hormone antagonist that inhibits thyroid hormone action in vivo*. J Biol Chem, 2002. **277**(38): p. 35664-70.
111. Sager, R., *Expression genetics in cancer: shifting the focus from DNA to RNA*. Proc Natl Acad Sci U S A, 1997. **94**(3): p. 952-5.
112. Helbing, C.C., et al., *A novel candidate tumor suppressor, ING1, is involved in the regulation of apoptosis*. Cancer Res, 1997. **57**(7): p. 1255-8.
113. Campos, E.I., et al., *Mutations of the ING1 tumor suppressor gene detected in human melanoma abrogate nucleotide excision repair*. Int J Oncol, 2004. **25**(1): p. 73-80.
114. Zhu, J.J., et al., *[p33(ING1b) enhances chemosensitivity of osteosarcoma cell U2OS to etoposide]*. Ai Zheng, 2004. **23**(6): p. 640-4.
115. Vieyra, D., et al., *Altered subcellular localization and low frequency of mutations of ING1 in human brain tumors*. Clin Cancer Res, 2003. **9**(16 Pt 1): p. 5952-61.
116. Tallen, G., et al., *No ING1 mutations in human brain tumours but reduced expression in high malignancy grades of astrocytoma*. Int J Cancer, 2004. **109**(3): p. 476-9.
117. Wagner, M.J., et al., *Expression of novel ING variants is regulated by thyroid hormone in the Xenopus laevis tadpole*. J Biol Chem, 2001. **276**(50): p. 47013-20.

118. Wagner, M.J., Helbing, C. C., *Multiple variants of the ING1 and ING2 tumor suppressors are differentially expressed and thyroid hormone-responsive in Xenopus laevis. (in press).* General and Comparative Endocrinology, 2005.
119. Taylor, A.C., J.J. Kollros, *Stages in the normal development of Rana pipiens larvae.* Anatomical Record, 1946. **94**: p. 7-24.
120. Minshull, J., et al., *A MAP kinase-dependent spindle assembly checkpoint in Xenopus egg extracts.* Cell, 1994. **79**(3): p. 475-86.
121. Crump, D., et al., *Exposure to the herbicide acetochlor alters thyroid hormone-dependent gene expression and metamorphosis in Xenopus Laevis.* Environ Health Perspect, 2002. **110**(12): p. 1199-205.
122. Pfaffl, M.W., et al., *Determination of stable housekeeping genes, differentially regulated target genes and sample integrity: BestKeeper--Excel-based tool using pair-wise correlations.* Biotechnol Lett, 2004. **26**(6): p. 509-15.
123. Eisen, M.B., et al., *Cluster analysis and display of genome-wide expression patterns.* Proc Natl Acad Sci U S A, 1998. **95**(25): p. 14863-8.
124. Helbing, C.C., et al., *Quiescence versus apoptosis: Myc abundance determines pathway of exit from the cell cycle.* Oncogene, 1998. **17**(12): p. 1491-501.
125. Foss, D.L., M.J. Baarsch, and M.P. Murtaugh, *Regulation of hypoxanthine phosphoribosyltransferase, glyceraldehyde-3-phosphate dehydrogenase and beta-actin mRNA expression in porcine immune cells and tissues.* Anim Biotechnol, 1998. **9**(1): p. 67-78.
126. Schmittgen, T.D. and B.A. Zakrajsek, *Effect of experimental treatment on housekeeping gene expression: validation by real-time, quantitative RT-PCR.* J Biochem Biophys Methods, 2000. **46**(1-2): p. 69-81.
127. Shi, Y.B. and V.C. Liang, *Cloning and characterization of the ribosomal protein L8 gene from Xenopus laevis.* Biochim Biophys Acta, 1994. **1217**(2): p. 227-8.
128. Piper, P.W., *The heat shock and ethanol stress responses of yeast exhibit extensive similarity and functional overlap.* FEMS Microbiol Lett, 1995. **134**(2-3): p. 121-7.
129. Aasland, R., T.J. Gibson, and A.F. Stewart, *The PHD finger: implications for chromatin-mediated transcriptional regulation.* Trends Biochem Sci, 1995. **20**(2): p. 56-9.

130. Sone, K., et al., *Effects of 17beta-estradiol, nonylphenol, and bisphenol-A on developing Xenopus laevis embryos*. Gen Comp Endocrinol, 2004. **138**(3): p. 228-36.
131. Goldberg, Y., et al., *Activation of protein kinase C or cAMP-dependent protein kinase increases phosphorylation of the c-erbA-encoded thyroid hormone receptor and of the v-erbA-encoded protein*. Embo J, 1988. **7**(8): p. 2425-33.
132. Glineur, C., M. Bailly, and J. Ghysdael, *The c-erbA alpha-encoded thyroid hormone receptor is phosphorylated in its amino terminal domain by casein kinase II*. Oncogene, 1989. **4**(10): p. 1247-54.
133. Poizat, C., et al., *Phosphorylation-dependent degradation of p300 by doxorubicin-activated p38 mitogen-activated protein kinase in cardiac cells*. Mol Cell Biol, 2005. **25**(7): p. 2673-87.
134. Loewith, R., et al., *Three yeast proteins related to the human candidate tumor suppressor p33(ING1) are associated with histone acetyltransferase activities*. Mol Cell Biol, 2000. **20**(11): p. 3807-16.
135. Skowyra, D., et al., *Differential association of products of alternative transcripts of the candidate tumor suppressor ING1 with the mSin3/HDAC1 transcriptional corepressor complex*. J Biol Chem, 2001. **276**(12): p. 8734-9.
136. Kuzmichev, A., et al., *Role of the Sin3-histone deacetylase complex in growth regulation by the candidate tumor suppressor p33(ING1)*. Mol Cell Biol, 2002. **22**(3): p. 835-48.
137. Vieyra, D., et al., *Human ING1 proteins differentially regulate histone acetylation*. J Biol Chem, 2002. **277**(33): p. 29832-9.
138. Gozani, O., et al., *The PHD finger of the chromatin-associated protein ING2 functions as a nuclear phosphoinositide receptor*. Cell, 2003. **114**(1): p. 99-111.
139. Cooper, K.L., et al., *Roles of mitogen activated protein kinases and EGF receptor in arsenite-stimulated matrix metalloproteinase-9 production*. Toxicol Appl Pharmacol, 2004. **200**(3): p. 177-85.
140. Ringshausen, I., et al., *Constitutive activation of the MAPkinase p38 is critical for MMP-9 production and survival of B-CLL cells on bone marrow stromal cells*. Leukemia, 2004. **18**(12): p. 1964-70.
141. Qiu, Q., et al., *EGF-induced trophoblast secretion of MMP-9 and TIMP-1 involves activation of both PI3K and MAPK signalling pathways*. Reproduction, 2004. **128**(3): p. 355-63.

142. Kang, J.L., et al., *Genistein prevents nuclear factor-kappa B activation and acute lung injury induced by lipopolysaccharide*. Am J Respir Crit Care Med, 2001. **164**(12): p. 2206-12.
143. Burke, L.J. and A. Baniahmad, *Co-repressors 2000*. Faseb J, 2000. **14**(13): p. 1876-88.
144. Chen, J.D. and H. Li, *Coactivation and corepression in transcriptional regulation by steroid/nuclear hormone receptors*. Crit Rev Eukaryot Gene Expr, 1998. **8**(2): p. 169-90.
145. Ito, M. and R.G. Roeder, *The TRAP/SMCC/Mediator complex and thyroid hormone receptor function*. Trends Endocrinol Metab, 2001. **12**(3): p. 127-34.
146. McKenna, N.J., R.B. Lanz, and B.W. O'Malley, *Nuclear receptor coregulators: cellular and molecular biology*. Endocr Rev, 1999. **20**(3): p. 321-44.
147. Jones, P.L., et al., *Multiple N-CoR complexes contain distinct histone deacetylases*. J Biol Chem, 2001. **276**(12): p. 8807-11.
148. Hong, S.H., C.W. Wong, and M.L. Privalsky, *Signaling by tyrosine kinases negatively regulates the interaction between transcription factors and SMRT (silencing mediator of retinoic acid and thyroid hormone receptor) corepressor*. Mol Endocrinol, 1998. **12**(8): p. 1161-71.
149. Hong, S.H. and M.L. Privalsky, *The SMRT corepressor is regulated by a MEK-1 kinase pathway: inhibition of corepressor function is associated with SMRT phosphorylation and nuclear export*. Mol Cell Biol, 2000. **20**(17): p. 6612-25.
150. Zhou, Y., et al., *The SMRT corepressor is a target of phosphorylation by protein kinase CK2 (casein kinase II)*. Mol Cell Biochem, 2001. **220**(1-2): p. 1-13.
151. Jung, J.C., et al., *Matrix metalloproteinases mediate the dismantling of mesenchymal structures in the tadpole tail during thyroid hormone-induced tail resorption*. Dev Dyn, 2002. **223**(3): p. 402-13.

Appendix 2.3. Floor determination.

		24h set										
GM	4.4	6.3	3.1	1.4	1.6	2.8	1.6	1.8	2.2	1.1	1.8	1.9
Sample ID	#13	#15	#16	#1	#3	#4	#5	#7	#8	#9	#10	#11
Median	0	-684	0	0	0	-421	-38	-99	0	0	0	0
Quartile SD	2247	2894	1338	694	716	1065	477	447	1231	121	353	711
Floor	2247	2210	1338	694	716	644	439	348	1231	121	353	711
Max	8210	9928	6446	9216	2624	5438	6363	1825	6703	2708	4300	6738
Min	-8713	-9231	-7123	-2816	-4576	-6629	-3311	-3311	-5712	-1948	-2105	-3330
Blank value used	346	405	407	461	480	342	431	458	423	457	475	407
		48h set										
GM	1.0	3.4	1.1	1.4	1.0	1.3	5.2	1.2	2.6	3.8	4.0	6.5
Sample ID	#17	#19	#20	#21	#22	#24	#25	#27	#28	#29	#31	#32
Median	0	0	0	0	0	0	0	-84	-186	0	0	417
Quartile SD	169	705	445	374	369	419	1821	337	833	1136	1980	2129
Floor	169	705	445	374	369	419	1821	253	647	1136	1980	2545
Max	3215	7136	6615	3721	3848	5245	9033	3812	9831	8756	9922	9647
Min	-1184	-3544	-3049	-1898	-2603	-2273	-7632	-2799	-6939	-6340	-9850	-9784
Blank value used	499	501	477	455	409	409	437	405	433	398	359	464

• The highest value across the all arrays "2545" were chosen as the final no-signal background (floor).

Appendix 2.4. Intraclass correlation coefficient analysis sample integrity.

Treatments	24 h				48 h			
	D-D	D-G	T ₃ -D	T ₃ -G	D-D	D-G	T ₃ -D	T ₃ -G
Intraclass Correlation (α)*								
1) Consistency	0.82	0.51	0.9	0.87	0.76	0.94	0.79**	0.66
2) Absolute agreement	0.82	0.51	0.9	0.85	0.75	0.94	0.77**	0.62

* Denotes average measures.

** After removing sample #25, if include #25, the α value will be 0.33 and 0.32 for consistency and absolute agreement. 24 h/48 h is the period of time after the tadpoles were injected with DMSO or T₃.

Appendix 2.5.2. The normalized and floor adjusted final data applied for determination relative gene expression for 48 h injection set.

*Highlighted in grey number (N) = 4 for the gene.
 N.F. from GMI expression factors.

Gene Name	GeneBank Accession #	Functional Code	1.00 FD	1.54 #17	1.11 #19	1.11 #21	Median	1.65 D.G	1.03 #21	1.54 #22	1.54 #24	Median	1.17 T3.1	2.58 #28	Median	3.75 #29	3.90 #31	6.51 #32	Median
c-mos	M23566		4	2545	2545			2545	2545	2545	2545	2545	2545	2545	2545	2545	2545	2545	2545
c-mos	M23566		4	2545	2545	2545	2545	2545	2545	2545	2545	2545	2545	2545	2545	2545	2545	2545	2545
N-ras	M97960		3	2545	2545	2545	2545	2545	2545	2545	2545	2545	2545	2545	2545	2545	2545	2545	2545
N-ras	M97960		3	2545	2545	2545	2545	2545	2545	2545	2545	2545	2545	2545	2545	2545	2545	2545	2545
R-ras	AF105280		3	2545	2545	2545	2545	2545	2545	2545	2545	2545	2545	2545	2545	2545	2545	2545	2545
R-ras	AF105280		3	2545	2545	2545	2545	2545	2545	2545	2545	2545	2545	2545	2545	2545	2545	2545	2545
yes	X14377		3	2545	2545	2545	2545	2545	2545	2545	2545	2545	2545	2545	2545	2545	2545	2545	2545
yes	X14377		3	2545	2545	2545	2545	2545	2545	2545	2545	2545	2545	2545	2545	2545	2545	2545	2545
c-fos	AJ224511		4	2545	2545	2545	2545	2545	2545	2545	2545	2545	2545	2545	2545	2545	2545	2545	2545
c-fos	AJ224511		4	2545	2545	2545	2545	2545	2545	2545	2545	2545	2545	2545	2545	2545	2545	2545	2545
raf ser the kinase	X12648		3	2545	2545			2545	2545	2545	2545	2545	2545	2545	2545	2545	2545	2545	2545
raf ser the kinase	X12648		3	2545	2545			2545	2545	2545	2545	2545	2545	2545	2545	2545	2545	2545	2545
c-ras1a	X32992		4	2545	2545	2545	2545	2545	2545	2545	2545	2545	2545	2545	2545	2545	2545	2545	2545
c-ras1a	X32992		4	2545	2545	2545	2545	2545	2545	2545	2545	2545	2545	2545	2545	2545	2545	2545	2545
c-ras1b	X32991		4	2545	2545	4020	2545	2545	3109	2545	2545	2545	2545	3419	20295	2545	2545	2545	2545
c-ras1b	X32991		4	2545	2545	2545	2545	2545	2545	2545	2545	2545	2545	4294	9489	3192	2545	2545	2545
c-ras2a	M81683		4	2545	2545	2545	2545	2545	2545	2545	2545	2545	2545	2545	2545	2545	2545	2545	2545
c-ras2a	M81683		4	2545	2545	2545	2545	2545	2545	2545	2545	2545	2545	2545	2545	2545	2545	2545	2545
c-myc-1	X14896		4	2545	2545	2545	2545	2545	2545	2545	2545	2545	2545	2545	2545	2545	2545	2545	2545
c-myc-1	X14896		4	2545	2545	2545	2545	2545	2545	2545	2545	2545	2545	2545	2545	2545	2545	2545	2545
c-myc-2	X14896		4	2545	2545	2545	2545	2545	2545	2545	2545	2545	2545	2545	2545	2545	2545	2545	2545
c-myc-2	X14896		4	2545	2545	2545	2545	2545	2545	2545	2545	2545	2545	2545	2545	2545	2545	2545	2545
pro-onc	M23704		3	2545	2545	2545	2545	2545	2545	2545	2545	2545	2545	2545	2545	2545	2545	2545	2545
pro-onc	M23704		3	2545	2545	2545	2545	2545	2545	2545	2545	2545	2545	2545	2545	2545	2545	2545	2545
ras2	ParMed ID: 915696		1	2545	2545	2545	2545	2545	2545	2545	2545	2545	2545	2545	2545	2545	2545	2545	2545
ras2	ParMed ID: 915696		1	2545	2545	2545	2545	2545	2545	2545	2545	2545	2545	2545	2545	2545	2545	2545	2545
fos2	AY014017		4	2545	2545	2545	2545	2545	2545	2545	2545	2545	2545	2545	2545	2545	2545	2545	2545
fos2	AY014017		4	2545	2545	2545	2545	2545	2545	2545	2545	2545	2545	2545	2545	2545	2545	2545	2545
fos2	AY014017		4	2545	2545	2545	2545	2545	2545	2545	2545	2545	2545	2545	2545	2545	2545	2545	2545
colocalized cancer tumor suppressor	U11988		3	2545	2545	2545	2545	2545	2545	2545	2545	2545	2545	2545	2545	2545	2545	2545	2545
colocalized cancer tumor suppressor	U11988		3	2545	2545	2545	2545	2545	2545	2545	2545	2545	2545	2545	2545	2545	2545	2545	2545
protein lipid phosphatase Pten	AF144732		3	2545	2545	2545	2545	2545	2545	2545	2545	2545	2545	2545	2545	2545	2545	2545	2545
protein lipid phosphatase Pten	AF144732		3	2545	2545	2545	2545	2545	2545	2545	2545	2545	2545	2545	2545	2545	2545	2545	2545
Wnt1	D92051		4	2545	2545	2545	2545	2545	2545	2545	2545	2545	2545	2545	2545	2545	2545	2545	2545
Wnt1	D92051		4	2545	2545	2545	2545	2545	2545	2545	2545	2545	2545	2545	2545	2545	2545	2545	2545
retinoblastoma 1	ParMed ID: 1516743		4	2545	2545	2545	2545	2545	2545	2545	2545	2545	2545	2545	2545	2545	2545	2545	2545
retinoblastoma 1	ParMed ID: 1516743		4	2545	2545	2545	2545	2545	2545	2545	2545	2545	2545	2545	2545	2545	2545	2545	2545
C-EBP-1	U78604		4	3905	2545	10144	3905	7075	5638	3879	7490	2545	2545	2545	117902	30603	196617	2545	115381
C-EBP-1	U78604		4	3905	2545	10144	3905	7075	5638	3879	7490	2545	2545	2545	117902	30603	196617	2545	115381
C-EBP-2	U78605		4	214	468	479	468	377	179	425	372	451	399	525	2138	638	3359	2047	
C-EBP-2	U78605		4	214	468	479	468	377	179	425	372	451	399	525	2138	638	3359	2047	
C-EBP-2	U78605		4	214	468	479	468	377	179	425	372	451	399	525	2138	638	3359	2047	
C-EBP-2	U78605		4	214	468	479	468	377	179	425	372	451	399	525	2138	638	3359	2047	
transcription co-repressor Smc3	AF151412		2	2545	2545	2545	2545	2545	2545	2545	2545	2545	2545	2545	2545	2545	2545	2545	2545
transcription co-repressor Smc3	AF151412		2	2545	2545	2545	2545	2545	2545	2545	2545	2545	2545	2545	2545	2545	2545	2545	2545
circadian C1 ORF	AF203107		4	2545	2545	2545	2545	2545	2545	2545	2545	2545	2545	2545	2545	2545	2545	2545	2545
circadian C1 ORF	AF203107		4	2545	2545	2545	2545	2545	2545	2545	2545	2545	2545	2545	2545	2545	2545	2545	2545
c-Myc	M690723		4	2545	2545	2545	2545	2545	2545	2545	2545	2545	2545	2545	2545	2545	2545	2545	2545
c-Myc	M690723		4	2545	2545	2545	2545	2545	2545	2545	2545	2545	2545	2545	2545	2545	2545	2545	2545
c-Myc	M690723		4	2545	2545	2545	2545	2545	2545	2545	2545	2545	2545	2545	2545	2545	2545	2545	2545
c-Myc	M690723		4	2545	2545	2545	2545	2545	2545	2545	2545	2545	2545	2545	2545	2545	2545	2545	2545
nuclear factor I.B1	L43146		4	2545	2545	2545	2545	2545	2545	2545	2545	2545	2545	2545	2545	2545	2545	2545	2545
nuclear factor I.B1	L43146		4	2545	2545	2545	2545	2545	2545	2545	2545	2545	2545	2545	2545	2545	2545	2545	2545
nuclear factor I.C1	L43149		4	2545	2545	2545	2545	2545	2545	2545	2545	2545	2545	2545	2545	2545	2545	2545	2545
nuclear factor I.C1	L43149		4	2545	2545	2545	2545	2545	2545	2545	2545	2545	2545	2545	2545	2545	2545	2545	2545
nuclear factor I.C1	L43149		4	2545	2545	2545	2545	2545	2545	2545	2545	2545	2545	2545	2545	2545	2545	2545	2545
nuclear factor I.C1	L43149		4	2545	2545	2545	2545	2545	2545	2545	2545	2545	2545	2545	2545	2545	2545	2545	2545
TFIIA	R02098		4	2545	2545	2545	2545	2545	2545	2545	2545	2545	2545	2545	2545	2545	2545	2545	2545
TFIIA	R02098		4	2545	2545	2545	2545	2545	2545	2545	2545	2545	2545	2545	2545	2545	2545	2545	2545
TFIIA	R02098		4	2545	2545	2545	2545	2545	2545	2545	2545	2545	2545	2545	2545	2545	2545	2545	2545
TFIIA	R02098		4	2545	2545	2545	2545	2545	2545	2545	2545	2545	2545	2545	2545	2545	2545	2545	2545
Ucn-1	X17190		4	2545	2545	2545	2545	2545	2545	2545	2545	2545	2545	2545	2545	2545	2545	2545	2545
Ucn-1	X17190		4	2545	2545	2545	2545	2545	2545	2545	2545	2545	2545	2545	2545	2545	2545	2545	2545
AP-2	M94455		4	2545	2545	2545	2545	2545	2545	2545	2545	2545	2545	2545	2545	2545	2545	2545	2545
AP-2	M94455		4	2545	2545	2545	2545	2545	2545	2545	2545	2545	2545	2545	2545	2545	2545	2545	2545
AP-2	M94455		4	2545	2545	2545	2545	2545	2545	2545	2545	2545	2545	2545	2545	2545	2545	2545	2545
AP-2	M94455		4	2545	2545	2545	2545	2545	2545	2545	2545	2545	2545	2545	2545	2545	2545	2545	2545
TBF-binding repressor Dst	AF005382		4	2545															

Appendix 2.6.1 Fold change for all good data in the 24 h injection set.

A) Ratios of adjustment T3-G treatment

	Fold Change T3-G vs. T3-D	Fold Change T3-G vs. T3-D	Ratio of array vs. QPCR
TRa	dRNA array	QPCR	
TRb	2.26	1.24	17.82
TRc	0.46	0.56	13.5
Average of TRa and TRb			

B) Highlighted in green = 4, black delete the value.

Gene Name	GeneBank	Functional Code	D/D	D/G	T3/D	T3/G	Adjust with 13.5	Floor adjustment	D-G vs. D-D	T3-D vs. D-D	T3-G vs. D-D	T3-G vs. T3-D
c-myc	M20596	4	2545	2545	2545	189	2545	2545	1.00	1.00	1.00	1.00
N-ras	M87890	3	2545	2545	2545	189	2545	2545	1.00	1.00	1.00	1.00
K-ras	AF085280	3	2545	2545	2545	2926	2545	2545	1.00	1.00	1.15	1.15
v-src	X14377	3	2545	2545	2545	189	2545	2545	1.00	1.00	1.00	1.00
c-fos	A_229411	4	2545	2545	2545	189	2545	2545	1.00	1.00	1.00	1.00
raf ser/thr kinase	X12948	3	2545	2545	2545	8302	2545	2545	1.00	1.00	1.00	1.00
c-erb-1a	X82682	4	2545	2545	2545	4103	304	2545	1.00	1.00	1.00	1.00
c-erb-1b	X82691	3	2545	2545	2545	26140	1981	2545	1.00	1.00	1.00	1.00
erb-2a	M81683	4	2545	2545	2545	4418	327	2545	1.00	1.00	1.00	1.00
c-myc 1	X14806	4	2545	2545	2545	14871	1102	2545	1.00	1.00	1.00	1.00
L-myc	L11383	4	2545	2545	2545	3647	433	2545	1.00	1.00	1.00	1.00
myb-c-myc	M87074	3	2545	2545	2545	26514	1871	2545	1.00	1.00	1.00	1.00
mdm2	U014017	4	2545	2545	2545	189	2545	2545	1.00	1.00	1.00	1.00
ING2	U014017	4	2545	2545	2545	6067	449	2545	1.00	1.00	1.00	1.00
colorectal cancer tumor suppressor protein/p53 phosphatase Pten	U10086	3	2545	2545	2545	26997	1033	2545	1.00	1.00	1.00	1.00
WT1	D62051	4	2545	2545	2545	44084	3265	2545	1.00	1.00	1.28	1.28
retinoblastoma 1	U014017	4	2545	2545	2545	189	2545	2545	1.00	1.00	1.00	1.00
CEBP-1	U08604	4	2574	2545	2545	147760	10945	2545	1.58	0.99	4.28	4.30
CEBP-2	U08605	4	243	295	364	2488	2488	2488	1.21	1.50	10.24	6.84
transcription co-repressor Sin3	CEBP	4	2661	2545	2545	3889	4738	3011	0.98	1.36	1.32	0.98
circadian CLOCK	AF203107	4	2545	2545	2545	25222	1883	2545	1.00	1.00	1.00	1.00
c-Jun	S86725	4	2545	2545	2545	3179	304	2545	1.00	1.00	1.00	1.00
c-Myc	L22741	4	2545	2545	2545	6173	457	2545	1.00	1.00	1.00	1.00
nuclear factor I B1	L43146	4	2545	2545	2545	13182	976	2545	1.00	1.00	1.00	1.00
nuclear factor I C1	L43149	4	2545	2545	2545	120998	8963	2545	1.53	1.00	3.52	3.40
TFIIA	K29289	4	2545	2545	2545	3449	266	2545	1.00	1.00	1.00	1.00
Otd-1	X11160	4	2545	2545	2545	17282	1280	2545	1.00	1.00	1.00	1.00
AP-2	M69455	4	2545	2545	2545	6825	500	2545	1.00	1.00	1.00	1.00
TBP-binding repressor Dr1	AB000582	4	2545	2545	2545	1810	1810	2545	1.00	1.00	1.00	1.00
TFIID subunit	D30054	4	2545	2545	2545	8735	5610	5010	1.00	1.32	1.87	1.49
transcription factor A	U07238	4	2545	2545	2545	7273	519	2545	1.00	1.00	1.00	1.00
RNA pol I transcription factor UBF	X57561	4	2582	2545	2545	189	2545	2545	0.99	0.99	0.99	1.00
oncoprotein factor-1 alpha chain repressD	M65504	11	1188	1321	1154	811	811	811	1.13	0.99	0.89	0.70
Tcf-3 co-repressor C/EBP repressor brain factor 2	U07289	4	2545	2545	2545	4672	346	2545	1.00	1.00	1.00	1.00
co-repressor MTR	Z97214	4	2545	2545	2545	245	189	2545	1.00	1.00	1.00	1.00
receptor regulator R2	AB018620	4	2545	2545	2545	11732	673	2545	1.00	1.00	1.00	1.00
XCOE2	AF041138	4	2545	2545	2545	189	2545	2545	1.00	1.00	1.00	1.00
MZF4	S34382	4	2545	2545	2545	189	2545	2545	1.00	1.00	1.00	1.00
Pax-2	AF179300	4	2545	2545	2545	2713	275	2545	1.00	1.00	1.00	1.00
Pax-8	AF179301	4	2545	2545	2545	59235	4388	4388	1.00	1.00	1.72	1.72
LFB1/ANF1	64988	4	2545	2545	2545	47151	3493	3493	1.00	1.00	1.37	1.37
LFB3/ANF1 beta	U79063	4	2545	2545	2545	40792	3015	3015	1.00	1.00	1.18	1.18
OSF2	AF199923	4	2545	2545	2545	5281	189	2545	1.00	1.00	1.00	1.00
brain factor 1	AF101387	4	2545	2545	2545	143451	10626	10626	1.00	1.00	4.17	4.17
brain factor 2	AJ011852	4	459	429	429	1560	1560	1560	0.82	0.80	3.47	3.71
GATA-5a	L13701	4	2545	2545	2545	84678	4813	4813	1.87	1.87	1.88	1.88
COCH zinc finger protein C3H-3 NK-2 homolog	AF081082	4	3873	2545	2545	87860	5034	5034	0.88	0.86	1.30	1.30
Hras3	S86507	4	2545	2545	2545	9778	602	2545	1.00	1.00	1.00	1.00
IRSp53	AF027175	4	2545	2545	2545	22684	1688	2545	1.00	1.00	1.00	1.00
myc-related protein 1 (mrb 1)	M79670	4	2545	2545	2545	9521	873	2545	1.00	1.00	2.88	2.88
Pbx-1	AF155208	4	2545	2545	2545	55812	4134	4134	1.00	1.00	1.62	1.62
MDX2	L26432	4	2545	2545	2545	8286	468	2545	1.00	1.00	1.00	1.00
Hes21	L26567	4	2545	2545	2545	8286	468	2545	1.00	1.00	1.00	1.00
co-receptor homolog protein isoform B	M61481	4	2545	2545	2545	40533	3003	3003	1.00	1.00	1.18	1.18
Xroc2.2	X62053	4	2545	2545	2545	2545	189	2545	1.00	1.00	1.00	1.00
DLA	L08728	4	3355	2545	2545	58871	4436	4436	0.78	0.78	1.32	1.74
DL3	L08729	4	2545	2545	2545	19877	1439	1439	1.00	1.00	2.88	2.88
DL2	L08730	4	2545	2545	2545	7923	587	2545	1.00	1.00	1.00	1.00
Fox	AF196221	4	2545	2545	2545	90659	3763	3763	1.00	1.00	1.47	1.47
enrA	AJ254125	4	2545	2545	2545	17725	1314	2545	1.00	1.00	1.00	1.00
actin-like protein homolog (ASH1)	M63272	4	2545	2545	2545	37770	2786	2786	1.00	1.00	1.10	1.10
DNA binding protein E12	X89859	4	2545	2545	2545	5053	378	2545	1.00	1.00	1.00	1.00
ionic homeobox	L38213	4	2545	2545	2545	25407	1802	2545	1.00	1.00	1.00	1.00
DLX1	U91801	4	2545	2545	2545	47910	3656	3656	1.00	1.00	1.40	1.40
POU2	U17854	4	3883	4011	3141	33684	2494	2545	1.19	0.81	0.88	0.81
Kat5/1	U87078	4	2545	2545	2545	2787	205	2545	1.00	1.00	1.00	1.00
Hes1	L46583	4	2545	2545	2545	2545	189	2545	1.00	1.00	1.00	1.00
pic2	U57453	4	3857	2545	2545	10884	6999	6999	0.43	0.57	1.01	1.75
TFIIA	X58389	4	2545	2545	2545	189	2545	2545	1.00	1.00	1.00	1.00
TFIIIB	X73775	4	2545	2545	2545	45537	3362	2545	1.00	1.00	1.33	1.33
glucocorticoid receptor	U73211	6	2545	2545	2545	5332	410	2545	1.00	1.00	1.00	1.00
estrogen receptor	L20736	5	2545	2545	2545	189	2545	2545	1.00	1.00	1.00	1.00
vitamin D receptor	U91846	5	2545	2545	2545	189	2545	2545	1.00	1.00	1.00	1.00
R2	AJ264119	4	1384	3865	4118	187289	12082	12082	0.85	1.21	3.85	2.81
TRP4	AW190313	5	2545	2545	2545	5116	379	2545	1.00	1.00	1.00	1.00
TRP7	AW200482	5	2545	2545	2545	7557	560	2545	1.00	1.00	1.00	1.00
thyroid hormone receptor alpha A	M35343	5	2545	2545	2545	189	2545	2545	1.00	1.00	1.00	1.00
thyroid hormone receptor beta A1	M35349	5	2545	2545	2545	2741	189	2545	1.00	1.00	1.00	1.00
androgen receptor alpha	U87129	6	2545	2545	2545	139231	10313	10313	1.00	1.00	4.05	4.05
mineralocorticoid receptor	U15134	6	2545	2545	2545	2545	189	2545	1.00	1.00	1.00	1.00
FOXO3/SRC-3	AF044980	5	2545	2545	2545	2545	189	2545	1.00	1.00	1.00	1.00
RAR beta	X67396	5	2545	2545	2545	3471	257	2545	1.00	1.00	1.00	1.00
RAR gamma B	X58306	5	2545	2545	2545	2862	197	2545	1.00	1.00	1.00	1.00
PPAR alpha	M61161	5	2545	2545	2545	19940	1477	2545	1.00	1.00	1.00	1.00
PPAR beta	M61162	5	2545	2545	2545	2555	211	2545	1.00	1.00	1.00	1.00
PPAR gamma	M61163	6	2545	2545	2545	189	2545	2545	1.00	1.00	1.00	1.00
NGF-B	X70700	4	2545	2545	2545	3646	270	2545	1.00	1.00	1.00	1.00
orphan nuclear receptor	X78163	4	2545	2545	2545	27711	2087	2545	1.00	1.00	1.00	1.00
COUP transcription factor 1	AF157568	4	2545	2545	2545	22182	1644	2545	1.00	1.00	1.00	1.00
thyroid hormone receptor alpha	L08084	5	2545	2545	2545	98138	4158	4158	1.00	1.00	1.63	1.63
thyroid hormone receptor beta	L27344	6	2545	2545	2545	13852	1029	2545	1.00	1.00	1.00	1.00
retinoblastoma associated 1 like protein	AF170344	4	2545	2545	2545	8429	478	2545	1.00	1.00	1.00	1.00
recombination activator (RAD-2)	L18326	2	2545	2545	2545	11622	861	2545	1.00	1.00	1.00	1.00
myb-Ca2+ binding protein	AF170347	2	2545	2545	2545	8431	478	2545	1.00	1.00	1.00	1.00
repression protein A	X67240	2	2545	2545	2545	189	2545	2545	1.00	1.00	1.00	1.00
Mt-2 histone deacetylase	AF171099	2	2545	2545	2545	16156	1167	2545	1.00	1.00	1.00	1.00
mitochondrial RNA polymerase	AF200706	2	2545	2545	2545	7940	622	2545	1.00	1.00	1.00	1.00</

ribosomal protein L32	X56030	11	1142	911	871	1091	1091	1091	0.00	0.76	0.96	1.26
serum retinol binding protein	J02718	5	2545	2545	2545	2545	189	2646	1.00	1.00	1.00	1.00
cellular retinoic acid binding protein	S74833	6	2545	2545	2545	189	2646	1.00	1.00	1.00	1.00	1.00
thyroid hormone binding protein	U03876	6	2545	2545	2039	210	2545	1.00	1.00	1.00	1.00	1.00
FABP	L19848	7	2545	2545	2545	189	2646	1.00	1.00	1.00	1.00	1.00
L-leucine acid transporter-1	Y12716	7	2545	2545	2545	21582	1599	2545	1.00	1.00	1.00	1.00
chloride channel ClC-3	Y09941	7	2545	2545	28183	1939	2545	1.00	1.00	1.00	1.00	1.00
chloride channel ClC-6	AF033304	7	2545	2545	38102	2545	2545	1.00	1.00	1.00	1.00	1.00
multidrug resistance gene	U17008	7	2545	2545	34839	2581	2581	1.00	1.00	1.00	1.00	1.00
inositol alpha 1b	L36339	7	2545	2545	3260	241	2545	1.00	1.00	1.00	1.01	1.01
Ca ²⁺ -binding protein leucosain	L27274	7	2545	2545	3448	1826	2545	1.00	1.00	1.00	1.00	1.00
calbindin D28k	U78636	7	2545	2545	3236	240	2545	1.00	1.00	1.00	1.00	1.00
adult beta-2-globin	J09778	7	2545	2545	3236	240	2545	1.00	1.00	1.00	1.00	1.00
level beta-2-globin	X02143	7	2545	2545	3236	240	2545	1.00	1.00	1.00	1.00	1.00
sodium phosphate cotransporter	L78935	7	2545	2545	3081	228	2545	1.00	1.00	1.00	1.00	1.00
Na/H ⁺ carboxyle cotransporter	U87318	7	2545	2545	28775	2132	2545	1.00	1.00	1.00	1.00	1.00
Na-glucose cotransporter type 1	A3308225	7	2545	2545	2545	189	2545	1.00	1.00	1.00	1.00	1.00
epithelial Na ⁺ channel alpha subunit	U23535	7	2545	2545	2545	189	2545	1.00	1.00	1.00	1.00	1.00
soy A-binding protein ABP-EF	M07072	4	2545	2545	2545	189	2545	1.00	1.00	1.00	1.00	1.00
neovous system-specific RNA binding dot	M04894	4	2545	2545	21600	1500	2545	1.00	1.00	1.00	1.00	1.00
rIn	X02021	4	2545	2545	32248	2389	2545	1.00	1.00	1.00	1.00	1.00
m5A mRNA binding protein	M00297	4	2545	2545	80261	4306	4928	1.00	1.00	1.00	1.00	1.00
74 kDa/80 kDa serum albumin	M21442	7	2545	2545	2545	189	2545	1.00	1.00	1.00	1.94	1.94
aldolase dehydrogenase class 1	A3018718	8	2545	2545	5397	400	2545	1.00	1.00	1.00	1.00	1.00
Wnt inhibitor factor-1	AF122924	3	2545	2545	5392	392	2545	1.00	1.00	1.00	1.00	1.00
transferrin	X54530	7	2545	2545	5392	392	2545	1.00	1.00	1.00	1.00	1.00
hsc70NF 1-related RNA transport protein	AF091970	4	2545	2545	8633	492	2545	1.00	1.00	1.00	1.00	1.00
urea transporter	Y12754	7	2545	2545	16226	1158	2545	1.00	1.00	1.00	1.00	1.00
SPARC	X02483	1	2545	2545	7829	812	554	2545	1.00	1.00	1.00	1.00
L-leucine transporter	U72877	7	2545	2545	3045	226	2545	1.00	1.00	1.00	0.32	0.32
TGF-beta 2	AF027944	6	2545	2545	28742	2129	2545	1.00	1.00	1.00	1.00	1.00
transferrin	A3308134	6	2545	2545	2821	194	2545	1.00	1.00	1.00	1.00	1.00
interleukin 1 beta	AJ101497	3	2545	2545	6209	458	2545	1.00	1.00	1.00	1.00	1.00
NEDD8	Not Submitted	8	2545	2545	32486	2406	2545	1.00	1.00	1.00	1.00	1.00
catecholamine-1 homolga precursor	X40754	1	2545	2545	5138	382	2545	1.00	1.00	1.00	1.00	1.00
connective tissue growth factor XCTGF	U43524	1	2545	2545	30718	2275	2545	1.00	1.00	1.00	1.00	1.00
nerve growth factor	X65716	1	2545	2545	2545	189	2545	1.00	1.00	1.00	1.00	1.00
proton-symmetric Y	S65577	3	2545	2545	2545	189	2545	1.00	1.00	1.00	1.00	1.00
neurexin	L016500	3	2545	2545	8896	506	2545	1.00	1.00	1.00	1.00	1.00
thyroid-stimulating hormone a	L07919	5	2545	2545	2545	189	2545	1.00	1.00	1.00	1.00	1.00
thyroid-stimulating hormone precursor	X04056	5	2545	2545	8731	647	2545	1.00	1.00	1.00	1.00	1.00
cardiotropin-releasing factor	S50096	6	2545	2545	8654	4883	4883	1.00	1.00	1.00	1.00	1.00
prolactin	L07920	6	2545	2545	8654	4883	4883	1.00	1.00	1.00	1.91	1.91
ubiquitin	M11512	8	1062	637	1188	1180	1180	1.00	1.00	1.00	1.18	1.18
X W4-2b	U98298	3	2545	2545	6673	509	2545	1.00	1.00	1.00	1.00	1.00
A2-protein	D119467	3	2545	2545	11396	1304	2545	1.00	1.00	1.00	1.00	1.00
oemarin H	AF087856	2	2545	2545	2545	191	2545	1.00	1.00	1.00	1.00	1.00
fibroblast growth factor receptor ligand	U40457	1	2545	2545	2545	189	2545	1.00	1.00	1.00	1.00	1.00
FGF-3	Z25539	1	2545	2545	51335	3804	3804	1.00	1.00	1.00	1.49	1.49
FGF-20	A012815	1	2545	2545	6794	504	2545	1.00	1.00	1.00	1.00	1.00
TGF-beta 2	X51817	1	2545	2545	2545	189	2545	1.00	1.00	1.00	1.00	1.00
TGF-beta 5	AF035497	1	2545	2545	2545	189	2545	1.00	1.00	1.00	1.00	1.00
MG6	X62670	1	2545	2545	3433	254	2545	1.00	1.00	1.00	1.00	1.00
c-Neu neturonic peptide 1	D17413	5	2545	2545	2822	209	2545	1.00	1.00	1.00	1.00	1.00
thyroid-stimulating hormone beta	L07618	5	2545	2545	2545	189	2545	1.00	1.00	1.00	1.00	1.00
growth hormone A	AF129327	2	2545	2545	2545	189	2545	1.00	1.00	1.00	1.00	1.00
RSK2	AF185162	3	2545	2545	191	185	2545	1.00	1.00	1.00	1.00	1.00
PCNA	M04080	2	2545	2545	4007	297	2545	1.00	1.00	1.00	1.00	1.00
RND linear subunit MAY	U83067	1	2545	2545	2545	189	2545	1.00	1.00	1.00	1.00	1.00
CHK1 checkpoint kinase	AF117816	1	2545	2545	2545	189	2545	1.00	1.00	1.00	1.00	1.00
fm	X52188	3	2545	2545	2596	190	2545	1.00	1.00	1.00	1.00	1.00
XDRP1	A030502	1	2545	2545	3826	291	2545	1.00	1.00	1.00	1.00	1.00
wave 1A kinase	U13862	1	2545	2545	3826	291	2545	1.00	1.00	1.00	1.00	1.00
Mau2/Mau1	L09738	4	2545	2545	3320	246	2545	1.00	1.00	1.00	1.00	1.00
Mau1	L77888	1	2545	2545	3216	246	2545	1.00	1.00	1.00	1.00	1.00
Mau2	L77888	1	2545	2545	3216	246	2545	1.00	1.00	1.00	1.00	1.00
MAP kinase 1 (MPK1)	X02813	1	2545	2545	2545	189	2545	1.00	1.00	1.00	1.00	1.00
MAP kinase 2 (MPK2)	X02751	3	2545	2545	2545	189	2545	1.00	1.00	1.00	1.00	1.00
MAP kinase activator 2 (JAK2)	Z22726	3	2545	2545	43867	3235	3235	1.00	1.00	1.00	1.27	1.27
MAP kinase activator (JAK1)	AF122848	3	2545	2545	3445	403	2545	1.00	1.00	1.00	1.00	1.00
MAP kinase phosphatase	X63742	3	18787	7838	4578	3388	3388	1.00	0.47	0.21	0.43	0.43
MAP kinase interacting kinase	A020307	3	2545	2545	63960	4708	4708	1.00	1.00	1.00	1.00	1.00
MAPKIK	D13746	3	2545	2545	41371	3085	3085	1.00	1.00	1.00	1.85	1.85
phosphoinositide 3 kinase catalytic subunit	AF120424	3	2545	2545	3289	264	2545	1.00	1.00	1.00	1.20	1.20
casein kinase 1-alpha	Y08817	3	2545	2545	2545	189	2545	1.00	1.00	1.00	1.00	1.00
casein kinase 1-epsilon	AF183394	3	2545	2545	17548	1300	2545	1.00	1.00	1.00	1.00	1.00
calmodulin-dependent protein kinase beta	AF183394	3	2545	2545	2545	189	2545	1.00	1.00	1.00	1.00	1.00
protein kinase PDK	D43680	3	2545	2545	2545	189	2545	1.00	1.00	1.00	1.00	1.00
PDK-related kinase 2	AF027183	3	2545	2545	3483	269	2545	1.00	1.00	1.00	1.00	1.00
CNA-M	AF101413	2	2545	2545	2545	189	2545	1.00	1.00	1.00	1.00	1.00
ATM	AF17446	2	2545	2545	15348	1137	2545	1.00	1.00	1.00	1.00	1.00
protein phosphatase 5	AF018283	3	2545	2545	3119	279	2545	1.00	1.00	1.00	1.00	1.00
quartern cyclase 1	A0205111	3	2545	2545	4228	313	2545	1.00	1.00	1.00	1.00	1.00
quartern cyclase 2	A0205112	3	2545	2545	3185	226	2545	1.00	1.00	1.00	1.00	1.00
cyclin A1	X53745	1	2545	2545	2545	189	2545	1.00	1.00	1.00	1.00	1.00
cyclin A2	X08746	1	2545	2545	6479	480	2545	1.00	1.00	1.00	1.00	1.00
cyclin B1	X03188	1	2545	2545	2545	189	2545	1.00	1.00	1.00	1.00	1.00
cyclin B2	X03187	1	2545	2545	3364	397	2545	1.00	1.00	1.00	1.00	1.00
cyclin D1	X08475	1	2545	2545	8769	501	2545	1.00	1.00	1.00	1.00	1.00
cyclin D2	X08476	1	2545	2545	2545	189	2545	1.00	0.30	0.30	1.00	1.0

recruiter	AB021737	8	2545	2545	2545	34317	2542	2545	1.00	1.00	1.00	1.00	
i21-acetylase kinase (PAK1)	AF000259	3	2545	2545	2545	13664	1012	2545	1.00	1.00	1.00	1.00	
DAD-1	AF05052	8	2545	2545	2545	189	189	2545	0.94	0.94	0.94	0.94	
casease-2	AB038169	8	2545	2545	2545	2545	2545	2545	1.00	1.00	1.00	1.00	
casease-0	AB038169	8	2545	2545	2545	4053	300	2545	1.00	1.00	1.00	1.00	
casease-7	AB038170	8	2545	2545	2545	7992	502	2545	1.00	1.00	1.00	1.00	
casease-8	AB038171	8	2545	2545	2545	2545	189	2545	1.00	1.00	1.00	1.00	
casease-9	AB038172	8	2545	2545	2545	27821	2081	2545	1.00	1.00	1.00	1.00	
casease-10	AB038173	8	2545	2545	2545	17351	1265	2545	1.00	1.00	1.00	1.00	
metalloproteinase-disintegrin (MDC11a)	AF022283	8	2545	2545	2545	14531	1003	2545	1.00	1.00	1.00	1.00	
metalloproteinase (MMP)	U82541	8	2545	2545	2545	2545	189	2545	1.00	1.00	1.00	1.00	
membrane anchored metalloproteinase	U78185	8	2545	2545	2545	2545	189	2545	1.00	1.00	1.00	1.00	
metalloproteinase-disintegrin (MDC11b)	AF022283	8	2545	2545	2545	7752	574	2545	1.00	1.00	1.00	1.00	
pancreatic trypsin	X53466	6	2545	2545	2545	2545	189	2545	1.00	1.00	1.00	1.00	
trypsinogen	U72330	6	2545	2545	2545	40107	2971	2971	1.00	1.00	1.00	1.00	
serine protease (Cao1)	AF022404	6	2545	2545	2545	2545	189	2545	1.00	1.00	1.00	1.00	
stromelysin-3	Z27063	8	2545	2545	2545	2090	159	2545	1.00	1.00	1.00	1.00	
alpha-esterif dipeptidase	U37377	8	2545	2545	2545	2545	189	2545	1.00	1.00	1.00	1.00	
stromin	AB018694	8	2545	2545	2545	23280	1724	2545	1.00	1.00	1.00	1.00	
alpha-1 antitrypsinase	AB014091	8	2545	2545	2545	2545	189	2545	1.00	1.00	1.00	1.00	
carbamyl phosphate synthetase	U06193	6	2545	2545	2545	2545	189	2545	1.00	1.00	1.00	1.00	
ornithine transcarbamylase	D38304	6	2545	2545	2545	5333	397	2545	1.00	1.00	1.00	1.00	
ornithine decarboxylase	X56516	6	2545	2545	2545	2545	189	2545	1.00	1.00	1.00	1.00	
lactate dehydrogenase B	U01178	6	2545	2545	2545	33298	2466	2545	1.00	1.00	1.00	1.00	
GAPDH	U41753	6	415	817	792	783	783	783	0.51	0.47	0.16	0.34	
cathepsin B (HAMP-3)	AF072455	6	2545	2545	8971	5131	380	2545	1.00	3.52	1.00	0.28	
Nucleoside diphosphate kinase	X97199	2	1428	1283	1376	1807	1807	1807	0.96	1.10	1.27	1.15	
Nhl1	D86491	6	2545	2545	2545	2545	2545	2545	1.00	1.00	1.00	1.00	
Ne-NK+ transcription ATPase beta subunit	M37788	7	2545	2545	2545	2547	189	2545	1.00	1.00	1.00	1.00	
SEC11 like skeletal muscle	X82059	6	2545	2545	2545	6643	482	2545	1.00	1.00	1.00	1.00	
E2 ubiquitin conjugating enzyme (Ubc9)	U88561	8	2545	2545	2545	2545	189	2545	1.00	1.00	1.00	1.00	
metallothionein	M82729	7	2545	2545	2545	7845	581	2545	1.00	1.00	1.00	1.00	
iodothyronine dioxygenase type II	L42816	5	2545	2545	2545	2545	189	2545	1.00	1.00	1.00	1.00	
iodothyronine 5'-deiodinase II	L28111	5	2545	2545	2545	2545	189	2545	1.00	1.00	1.00	1.00	
retinoic acid converting enzyme	AF067566	5	2545	2545	2545	8029	595	2545	1.00	2.04	2.04	2.04	
Fcγ1 serine phosphatase	AJ132385	4	2545	2545	2545	2545	189	2545	1.00	1.00	1.00	1.00	
protein phosphatase 1-gamma 1	L11322	6	2545	2545	2545	2545	189	2545	1.00	1.00	1.00	1.00	
convertase PC2	X66493	6	2545	2545	2545	2545	189	2545	1.00	1.00	1.00	1.00	
acetylase	AF184471	6	2545	2545	2545	12707	941	2545	1.00	1.54	1.00	0.86	
phosphatase C-gamma-1a	AF090111	3	2545	2545	2545	24482	1812	2545	1.00	1.00	1.00	1.00	
Cu,Zn SOD	X16645	3	3461	2545	2545	2545	373	2545	0.75	1.03	0.76	0.73	
collagenase-4 precursor	L76275	8	2545	2545	2545	2545	189	2545	1.00	1.00	1.00	1.00	
calreticulin P-450 (11 beta, aldo)	D10994	6	2545	2545	2545	2545	373	2545	1.00	1.00	1.00	1.00	
mitochondrial cytochrome c oxidase subunit IV	M40217	6	2545	2545	2545	2545	189	2545	1.00	1.00	1.00	1.00	
alcohol dehydrogenase class I (ADH1)	AF054255	6	2545	2545	4248	7235	2545	189	1.87	2.84	1.00	0.35	
alcohol dehydrogenase class I (ADH4)	AF062556	6	2545	2545	2545	2545	189	2545	1.00	1.00	1.00	1.00	
adenyl cyclase	Z46908	3	2545	2545	2545	2545	189	2545	1.00	1.00	1.00	1.00	
Ribosomal activation factor alpha	U41856	1	2545	2545	2545	2545	189	2545	1.00	1.00	1.00	1.00	
aldolase C	Z62810	6	2545	2545	2545	5398	400	2545	1.00	1.00	1.00	1.00	
Z,3'-cyclic-nucleotide 3'-phosphodiesterase	AB021415	9	2545	2545	2545	2545	189	2545	1.00	1.00	1.00	1.00	
amylase	D38303	6	8779	2545	2545	14447	8487	774	2545	0.38	2.13	0.38	
amylase 1	U06408	6	2545	2545	2545	2545	189	2545	1.00	1.00	1.00	1.00	
argininosuccinate lyase	D38302	8	2545	2545	2545	2545	189	2545	1.00	1.00	1.00	1.00	
ATPase Na+/K+ pump alpha 1 subunit	U49238	6	2545	2545	2545	2545	189	2545	1.00	1.00	1.00	1.00	
ADP-ribosylation factor (ARF1)	L31350	6	2545	2545	2545	2545	189	2545	1.00	1.00	1.00	1.00	
serine kinase	AF153230	6	2545	2545	2545	2545	189	2545	1.00	1.00	1.00	1.00	
monomelic Elastin	AF134570	2	2545	2545	2545	2545	189	2545	1.00	1.00	1.00	1.00	
deoxynucleotidyl transferase	AF068612	2	2545	2545	2545	2545	189	2545	1.00	1.00	1.00	1.00	
DNA polymerase beta	V16732	2	2545	2545	2545	2545	189	2545	1.00	1.00	1.00	1.00	
kinase I	L43496	2	2545	2545	2545	2545	189	2545	1.00	1.00	1.00	1.00	
ATP-dependent RNA helicase	X57326	4	2545	2545	2545	4474	331	2545	1.00	1.00	1.00	1.00	
ribonucleo-G-methyltransferase	U79838	2	2545	2545	2545	15805	1171	2545	1.00	1.00	1.00	1.00	
RNA endonuclease 1 (FEN1)	U84553	2	2545	2545	2545	2545	189	2545	1.00	1.00	1.00	1.00	
terminal deoxynucleotidyl transferase	U07693	2	2545	2545	2545	4781	354	2545	1.00	1.00	1.00	1.00	
caseinase A	XV07943	8	2545	2545	2545	2545	189	2545	1.00	1.00	1.00	1.00	
liver helicase	AF342423	4	2545	2545	2545	3604	267	2545	1.00	1.00	1.00	1.00	
aldolase B	AB030822	6	2545	2545	4138	3131	1778	428	2545	1.63	1.23	1.00	0.81
cytochrome b	M10217	8	2545	2545	2545	4793	365	2545	1.00	1.00	1.00	1.00	
reninase p450	AB031278	5	2545	2545	2545	2545	189	2545	1.00	1.00	1.00	1.00	
NECD4	AJ000085	8	2545	2545	2545	14436	1069	2545	1.00	1.00	1.00	1.00	
ring finger protein	U83417	1	2545	2545	2545	3444	189	2545	1.00	1.00	1.00	1.00	
RE5T	AF068201	4	2545	2545	2545	2545	189	2545	1.00	1.00	1.00	1.00	
MC3R	U44047	1	2545	2545	2545	2545	189	2545	1.00	1.00	1.00	1.00	
proteasome subunit V	D87688	8	22	196	167	1038	1038	1038	1.00	1.00	1.00	1.00	
transmembrane protein containing an EGI	X83962	10	2545	2545	2545	3520	261	2545	1.00	1.00	1.00	1.00	
OT256	U82646	4	2545	2545	2545	2545	189	2545	1.00	1.00	1.00	1.00	
13S condensin XCAP-D2	AF067869	2	2545	2545	2545	26101	1803	2545	1.00	1.00	1.00	1.00	
chaperonin subunit CCT gamma	U37062	7	2545	2545	2545	5151	169	2545	1.00	1.00	1.00	1.00	
HMG-X	D38785	2	2545	2545	2545	6366	486	2545	1.00	1.00	1.00	1.00	
GSK-3 binding protein	AF062738	3	2545	2545	2545	9148	678	2545	1.00	1.00	1.00	1.00	
caseinase homeorprotein 1	U15278	4	2545	2545	2545	43286	3000	3000	1.07	2.12	1.19	0.56	
beta-amyloid precursor protein	352417	8	2545	2545	2545	46869	3030	3030	1.00	1.00	1.00	1.26	
Itzhak7	AF191906	3	8078	3250	4630	5493	1060	2545	1.00	1.00	1.00	1.00	
calcineurin A	AF191909	3	8078	3250	4630	5493	1015	4015	0.37	0.51	0.46	0.91	
BMP1	L12249	8	2545	2545	2545	2545	189	2545	1.00	1.00	1.00	1.00	
BMP1b	Y09680	8	2545	2545	2545	2545	189	2545	1.00	1.00	1.00	1.00	
BMP4	AF058764	3	2545	2545	2545	4183	310	2545	1.00	1.00	1.00	1.00	
18S ribosomal	X04025	11	281	294	183	780	760	760	1.13	0.70	0.70	2.91	
18S ribosomal	X04025	11	2545	2545	2545	2545	189	2545	1.00	1.00	1.00	1.00	
MC3R	U82657	1	2545	2545	2545	2545	189	2545	1.00	1.00	1.00	1.00	
MAM domain protein	U37376	10	17719	9338	13127	25356	189	2545	1.00	1.00	1.00	1.00	
XPA/CI	D31894	2	2545	2545	2545	2545	189	2545	1.00	1.00	1.00	1.00	
nuclear factor 7	X54515	4	2545	2545	2545	2545	189	2545	1.00	1.00	1.00	1.00	
vitellin	85210	6	2545	2545	2545	5109	378	2545	1.00	0.78	1.07	1.36	
hsc70	X02512	7	2545	2545	2545	46802	3467	3467	1.00	1.00	1.00	1.00	
hsc30	U44894	7	17	88	865	499	489	489	5.68	50.00	26.28	0.57	
ribonin alpha-1	U44205	9	2545	2545	2545	2545	189	2545	1.00	1.00	1.00	1.00	
gene 5	U37373	10	2545	2545	2545	4222	313	2545	1.00	1.00	1.00	1.00	
fox-related protein-2	U37374	4	2545	2545	2545	5300	393	2545	1.00	1.00	1.00	1.00	
gene 12	U41854	10	2545	2545	2545	2545	189	2545	1.00	1.00	1.00	1.00	
gene 16	U41857	10	2545	2545	2545								

tryptophan	U72330	8	2545	2545	2545	24389	2435	2545	100	100	100	100
sarime protease (Cae 1)	AF102904	6	2545	2545	2545	2587	2587	2545	100	100	100	100
stomoxen-3	U73777	8	2545	2545	2545	2545	2545	2545	100	100	100	100
alpha-azobenzyl diisothioester	U73777	8	2545	2545	2545	2545	2545	2545	100	100	100	100
scap1	AB018284	8	2545	2545	2545	2545	2545	2545	100	100	100	100
alpha-1 antitrypsinase	AB014081	8	2545	2545	2545	2545	2545	2545	100	100	100	100
carbamoyl phosphate synthetase	U05103	8	2545	2545	2545	2545	2545	2545	100	100	100	100
carbamoyl phosphate synthetase	U05103	8	2545	2545	2545	2545	2545	2545	100	100	100	100
ornithine transcarbamoylase	U05103	8	2545	2545	2545	2545	2545	2545	100	100	100	100
ornithine decarboxylase	U05103	8	2545	2545	2545	2545	2545	2545	100	100	100	100
lactate dehydrogenase B	U07170	6	19692	11766	12624	13082	2686	2686	0.93	0.93	0.14	0.12
GAD6H	U07170	6	19692	863	866	811	2886	2886	1.11	1.43	1.75	1.42
actinase B (LAMP-2)	AF127455	8	2545	2545	2545	2545	2545	2545	100	5.13	100	0.19
NM23/nucleolin 2 dihydrophala lunax	X87809	2	15509	1491	1673	2356	2356	2356	0.98	1.07	1.51	1.41
Nr1	D48461	6	2545	2545	2545	2545	2545	2545	100	100	100	100
Na ⁺ K ⁺ translocin ATPase beta su	M37788	7	2545	2545	2545	2545	2545	2545	100	1.15	100	0.87
SERCA1 fast skeletal muscle	X83009	3	2545	5649	10214	8681	888	2545	2.22	4.01	100	0.25
EZ ubiquitin-conjugating enzyme (ub	U88501	8	2545	2365	3533	2345	255	2545	100	100	100	100
malothiolase	M91720	7	2545	2545	3365	4367	4367	2545	100	100	100	0.77
codon-thymine diacylase type II	L42815	5	2545	2545	14078	874	874	2545	0.99	5.40	0.99	0.78
codon-thymine 5'-diacylase III	L28111	5	4294	5697	7988	28251	2835	2835	1.34	1.89	0.67	0.35
rainic acid synthase enzyme	AF157466	5	2545	2545	6502	6010	601	2545	100	2.55	100	0.39
FCP1 serine phosphatase	AJ182385	4	2545	2545	2545	6205	620	2545	100	100	100	100
protein phosphatase 1-gamma 1	L17036	1	2545	2545	2545	2545	255	2545	100	100	100	100
convulsase PC2	X89193	5	2545	2545	3607	5631	563	2545	100	1.38	100	0.73
acortase	AF186471	8	2545	2545	2545	8088	607	2545	100	100	100	100
phospholipase C-alpha-1a	AF080111	3	2545	2545	3541	12645	1264	2545	100	1.27	100	0.79
CuZn-SOD	X18985	6	4968	6630	6932	4465	450	2545	1.37	1.45	0.54	0.37
collagenase-4 precursor	L78275	8	2545	2545	2545	2545	255	2545	100	100	100	100
cytochrome P-450 (11beta, aldo)	D10894	8	2545	2545	2545	18699	1807	2545	100	100	100	100
retinol dehydrogenase oxidase	U73777	8	2545	2545	2545	15868	2545	2545	3.42	4.73	0.68	0.14
alcohol dehydrogenase class 4 (ADP	AF159256	8	2545	2545	2545	2646	265	2545	100	100	100	100
aldol dehydrogenase	U05103	8	2545	2545	2545	2545	2545	2545	100	100	100	100
fibroblast activation factor alpha	U41856	1	2545	2545	2545	2545	2545	2545	100	100	100	100
alcohol C	X87810	6	2545	2545	2545	2545	2545	2545	100	100	100	100
2',3'-cyclic-nucleotide 3'-phosphodi	X18985	6	4968	6630	6932	4465	450	2545	1.37	1.45	0.54	0.37
acylase	D38303	8	2545	3215	6718	15088	1510	2545	1.28	2.84	100	0.98
arugase 1	U08406	8	2545	2545	2545	36267	3626	3626	100	100	1.42	1.42
argininosuccinate lyase	D38303	8	2545	2545	2545	36267	3626	3626	100	100	1.42	1.42
ATPase Na ⁺ /K ⁺ pump alpha 1 subu	U41856	8	2545	2545	2545	2545	2545	2545	100	100	100	100
ADP-ribosylation factor (ARF 1)	U1350	8	2545	2545	2545	2545	255	2545	100	100	100	100
aliphaticase	AF154570	2	2545	2545	2545	2545	255	2545	100	100	100	100
acetylcholinesterase Eoc 1	AF154570	2	2545	2545	2545	2545	255	2545	100	100	100	100
diacylglycerol kinase gamma	AF159912	2	2545	2545	2545	2545	255	2545	100	100	100	100
DNA polymerase beta	L43498	2	2545	2545	2545	2545	255	2545	100	100	100	100
lyase 1	L43498	2	2545	2545	2545	2545	255	2545	100	100	100	100
ATP-dependent RNA helicase	X57328	4	2545	2545	2545	2550	255	2545	100	100	100	100
cytochrome 5-methyltransferase	D38303	8	2545	2545	2545	36267	3626	3626	100	100	100	100
flavonolignane 1 (FEN1)	U41856	2	2545	2545	2545	11791	1179	2545	100	100	100	100
terminal deoxynucleotidyl transferase	U07803	2	2545	2545	2545	2879	288	2545	100	100	100	100
sigma-class A	AJ037643	6	2545	2545	2545	2545	255	2545	100	100	100	100
hsc70	AF152423	4	2545	9813	4810	2545	255	2545	3.88	7.81	100	0.55
alkaline B	AB030822	8	2545	2545	6571	22798	2280	2545	100	2.58	100	0.99
cytochrome B	U18217	6	2545	2545	2545	2545	255	2545	100	100	100	100
acetylcholinesterase A50	AB031278	5	2545	2545	2545	2545	255	2545	100	100	100	100
NECD 4	AJ030085	8	2545	2545	2545	9829	993	2545	100	100	100	100
mta fibrin protein	L43498	2	2545	2545	2545	2545	255	2545	100	100	100	100
RCS1	AF196301	4	2545	2545	2545	2545	255	2545	100	100	100	100
MGM2	U41847	1	3024	2545	2545	8959	896	2545	0.84	0.84	0.84	1.00
proteasome subunit Y	D38303	8	2545	2545	2545	36267	3626	3626	100	100	100	100
transmembrane protein containing a	X87810	10	2545	2545	2545	2545	255	2545	100	100	100	100
OTX5b	A251846	4	2545	2545	2545	21218	2122	2545	100	100	100	100
13S core protein X2AP-D2	AF167969	2	2545	2545	2545	2552	255	2545	100	100	100	100
chaperonin subunit CCT gamma	U10702	7	2545	2545	2545	3362	336	2545	100	100	100	100
HAG-X	D30785	2	2545	2545	2545	2848	285	2545	100	1.16	100	0.88
GSK-3 binding protein	AF062738	3	2602	2626	7502	7621	2526	2626	1.47	2.88	100	0.39
cardiac homeoprotein 1	L19578	4	2545	2545	2545	7961	794	2545	100	100	100	100
beta-amyloid precursor protein	SS2417	9	2545	2545	2545	8333	933	2545	100	3.27	100	0.31
frizzled 7	AF159108	3	2789	4853	7880	6402	6480	6480	1.73	2.81	2.32	0.82
caseinogen A	AF109199	3	2545	2545	2545	2545	255	2545	100	100	100	100
Bmp1	L12246	8	2545	2545	2545	2839	284	2545	100	100	100	100
Bmp1b	V08880	8	2545	2545	2545	2545	255	2545	100	100	100	100
BMP	AF109199	3	2545	2545	2545	2545	255	2545	100	100	100	100
18S ribosomal	X04025	11	236	218	317	873	873	873	0.82	1.34	2.85	2.13
MK3D	L05057	1	2545	2545	2545	2545	255	2545	100	100	100	100
MAM domain protein	U73776	10	12628	13262	21910	6051	605	2545	1.05	1.73	0.20	0.12
XPA2c1	D31894	2	2545	2545	2545	2739	274	2545	100	100	100	100
nuclear factor-7	X04025	4	2545	2545	2545	4362	435	2545	100	100	100	100
vitellin	85270	6	2825	4941	5428	6537	6554	6554	1.75	1.92	2.32	1.21
hsc308	X04025	7	2545	2545	2545	2961	296	2545	100	1.53	100	0.89
hsc 30	U41844	7	52	107	1106	3715	371	2545	2.37	21.44	7.20	0.34
actin alpha-1	U41825	9	2545	2545	2545	2545	255	2545	100	100	100	100
gene 5	U73773	10	2545	2545	2545	2545	255	2545	100	100	100	100
loc-related actin alpha-2	U73773	10	2545	2545	2545	2545	255	2545	100	100	100	100
gene 12	U41825	10	2545	2545	2545	2545	255	2545	100	100	100	100
gene 18	U41825	10	2545	2545	2545	2545	255	2545	100	100	100	100
gene 17	U41825	10	2545	2545	2545	2545	255	2545	100	100	100	100
gene 16	U41825	10	2545	2545	2545	2545	255	2545	100	100	100	100
gene 19	U41825	10	2545	2545	2545	2545	255	2545	100	100	100	100
gene 20	U41825	10	2545	2545	2545	2545	255	2545	100	100	100	100
regulator for chromosome condenses	D00879	2	2545	3858	2545	6351	5355	5355	1.52	100	2.10	2.10
proteasome subunit X23	SS1111	8	3337	4781	8005	5560	558	2545	1.43	2.58	0.78	0.30
B-SODAP43	X87810	1	2545	2545	2545	3677	4013	4013	1.41	1.37	1.58	1.15
fractin mental retardation protein 1	AF108404	4	2545	2545	2545	2545	255	2545	100	100	100	100
forkhead protein lens1	AF108404	4	2545	2545	2545	6132	613	2545	100	100	100	100
ER1	AF154570	4	2545	2545	2545	2724	272	2545	100	100	100	100
B-cell translocation protein 1 (bcl	AB028243	4	2545	2545	2545	3673	367	2545	100	100	100	100
SP-1	AF027151	4	2545	2907	3581	21585	2159	2545	1.14	1.40	100	0.71
beta-A1-1 crystalin	X87810	8	2545	2545	2545	2545	255	2545	100	100	100	100
gamma-M1-1 crystalin	X87810	8	2545	2545	2545	2545	255	2545	100	100	100	100
SP-1/AdBP	AB017352	4	2545	2545	2545	2545	255	2545	100	100	100	100
fibronectin inton 1	control	control	2545	2545	2545	60650	8005	8005	100	100	2.38	2.38
alpha tubulin inton 1	AF108404	4	2545	2545	2545	2545</						

Appendix 2.7. 24 h set T₃-responsive genes variance analysis (VA).

Gene Name	GeneBank Accession #	Functional Code	estimated SD		estimated SD		T3/D		T3/G		T3/G		T3/G		T3/G	
			D/D 24h	D/G 24h	#9 Mean	#3 Mean	#4 Mean	#5 Mean	#7 Mean	#8 Mean	#13 Mean	#15 Mean	#16 Mean	Median		
myosin heavy chain 3	AF097906	9	3.27	0.90	2545	10862	2545	2545	17903	18464	9219	72122	18464	17903		
alpha skeletal actin	X03470	9	0.95	0.62	274	810	567	1069	1416	1436	670	1227	1227	749	4814	4814
alpha 1 collagen Type I	AB015440	9	0.00	0.67	2545	2545	2545	2545	2545	2545	2545	2545	2545	2545	2545	2545
alpha 2 collagen Type I	DB8764	9	0.17	0.99	3008	2545	2545	2545	2545	2545	2545	2545	2545	2545	2545	2545
SPARC	X62483	1	0.00	0.00	2545	2545	2545	2545	2545	2545	2545	2545	2545	2545	2545	2545
MAP kinase phosphatase	X63742	3	0.55	3.50	16787	11447	20705	2545	16787	16787	2545	2545	2545	2545	2545	2545
MAP kinase phosphatase	X89476	1	1.40	0.00	14401	2545	2545	2545	8473	8473	2545	2545	2545	2545	2545	2545
cyclin D2	AF105259	3	0.29	2.62	30494	28081	36937	2545	30494	30494	2545	21359	58400	21359	21359	21359
activated protein kinase C	U07176	6	0.56	2.54	27935	27122	42873	2545	27935	27935	2545	14344	39033	14344	14344	14344
lactate dehydrogenase B	AF072455	8	0.00	0.00	2545	2545	2545	2545	2545	2545	2545	2545	2545	2545	2545	2545
gelatinase B (MMP-9)	M10217	6	3.21	0.98	10714	2545	2545	2545	2545	2545	2545	4461	4461	4461	4461	4461
mitochondrial cytochrome c oxidase subunit 1	DB8303	6	1.71	0.59	5524	13551	4102	2545	5524	5524	2545	4058	2545	2545	2545	2545
argininase	DB7689	8	8.26	0.68	161	17	-14	196	21	21	231	97	196	196	196	196
proteasome subunit Y	AF062738	3	0.00	0.40	2545	2545	2545	2545	2545	2545	3924	3444	3444	3444	3444	3444
CSK-3 binding protein	U44894	7	2.14	1.03	5	17	42	156	17	17	107	46	107	107	107	107
hsp 30	U44894	7	2.14	1.03	5	17	42	156	17	17	107	46	107	107	107	107
proteasome subunit XC3	S51111	8	0.75	3.19	9890	2545	9854	2545	9854	9854	2545	3843	14792	3843	3843	3843
myosin heavy chain 3	AF097906	9	0.45	3.41	8339	5591	6620	18464	6620	6620	72122	18464	18464	18464	18464	18464
alpha skeletal actin	X03470	9	0.49	0.62	1367	1436	772	1367	1367	1367	670	1227	1227	749	4814	4814
alpha 1 collagen Type I	AB015440	9	1.12	0.92	5530	4577	10798	70303	54233	54233	20583	54233	54233	54233	54233	54233
alpha 2 collagen Type I	DB8764	9	0.81	1.35	6247	5058	10123	6247	69244	69244	11080	43155	43155	43155	43155	43155
SPARC	X62483	1	0.73	2.93	10759	5007	7883	26002	5072	5072	7152	7152	7152	7152	7152	7152
MAP kinase phosphatase	X83742	3	0.80	1.45	8719	7398	14397	99111	32810	32810	45736	45736	45736	45736	45736	45736
MAP kinase phosphatase	X89476	1	0.00	0.55	2545	2545	2545	2545	2545	2545	3501	2545	2545	2545	2545	2545
cyclin D2	AF105259	3	0.48	0.12	18055	11347	13834	42762	39762	39762	44867	44867	44867	44867	44867	44867
activated protein kinase C	U07176	6	0.36	1.01	13176	11235	15954	53111	99583	99583	53111	45837	53111	53111	53111	53111
lactate dehydrogenase B	AF072455	8	0.88	1.41	7923	8971	15785	8971	12106	4882	5131	5131	5131	5131	5131	5131
gelatinase B (MMP-9)	M10217	6	0.96	8.83	7235	5539	12509	7235	2545	2545	25029	2545	2545	2545	2545	2545
mitochondrial cytochrome c oxidase subunit 1	DB8303	6	1.03	0.55	14447	7862	22707	14447	14447	14447	13111	13111	13111	13111	13111	13111
argininase	DB7689	8	0.43	0.64	136	199	147	147	147	147	1038	1038	1038	1038	1038	1038
proteasome subunit Y	AF062738	3	1.07	0.92	2545	942	8421	5483	59103	59103	601	21840	40471	40471	40471	40471
CSK-3 binding protein	U44894	7	0.63	0.47	942	873	395	489	601	601	369	489	489	489	489	489
hsp 30	U44894	7	0.63	0.47	942	873	395	489	601	601	369	489	489	489	489	489
proteasome subunit XC3	S51111	8	0.68	0.85	4205	4335	7169	9277	6284	6284	14202	9277	9277	9277	9277	9277

Appendix 2.8. 48 h set T₃-responsive genes variance analysis.

Gene Name	GeneBank Accession #	Functional Cite	estimated SD 48h	estimated SD T3G 48h	D/D Mean	48h /17 Mean	48h /19 Mean	48h /20 Mean	T3G Mean	48h /21 Mean	48h /22 Mean	48h /24 Mean	Median
inf serpin Hense	X12948	3	0.90	0.99	2545	2545	2545	2545	2545	6071	3574	2545	3574
C/EBP	S44193	4	1.62	0.52	2545	2797	7052	2545	2797	4789	4069	6567	4789
nuclear factor I-C1	L43149	4	0.40	0.50	2545	3854	4089	3854	4495	3154	2639	3154	3154
RNA pol I transcription factor UBF	X57561	4	1.34	0.35	2545	2545	5994	2573	3689	3230	2545	3230	2545
beta factor 1	AF101387	4	1.56	0.50	2545	2702	6762	2702	6972	4121	3730	5750	3730
NK-2 homolog	S65507	4	0.64	0.41	2011	2545	6821	2011	3418	4021	3061	4021	3061
DLA	L09728	4	0.90	0.31	2545	2545	2545	2545	3579	2545	3579	3579	3579
POU2	U17634	4	1.75	0.28	4196	2731	10066	4196	5671	6110	7484	6110	6110
z/2	U57453	2	2.99	0.26	3482	2545	9805	3482	3482	6081	4675	5378	5378
mitotic phosphoprotein 90	AF097906	2	1.24	0.72	2545	2922	2545	2545	2545	2545	2545	2545	2545
myosin heavy chain 3	AF079161	9	0.15	0.39	2545	2545	2545	2545	2545	2545	2545	2545	2545
alpha skeletal actin	X03470	9	0.40	0.24	287	428	351	351	1483	1042	1133	1133	1133
cytoplasmic beta actin	AF079161	9	0.39	0.88	1190	1715	1328	1328	2814	2230	2417	2417	2417
alpha 1 collagen type I	AB015440	9	0.86	0.29	2545	2807	4972	2807	2807	12627	7201	6464	7201
alpha 2 collagen type I	D88764	9	0.64	0.51	2545	6134	5591	5591	11269	8613	9068	9068	9068
glycyl hormone binding protein	X03878	5	0.00	0.29	2545	2545	2545	2545	2545	4487	7941	7941	7941
SEFRC	X62483	1	1.74	0.02	2545	2545	4436	2545	8092	7941	2545	2545	2545
cyclin D2	X89476	1	1.33	0.00	3092	12589	7165	7165	2545	2545	2545	2545	2545
DAD-1	D15059	8	0.78	0.26	2869	2545	6352	2869	2545	5215	3998	4606	4606
capsase-6	AB018169	8	0.00	0.80	2545	2545	4523	2545	2545	2545	2545	2545	2545
gelsolin B (VAMP-9)	AF072455	8	0.00	0.67	2545	2545	2545	2545	2545	2545	2545	2545	2545
SERC11 fast skeletal muscle	X63009	5	0.36	0.39	2545	2833	2545	2833	2545	6411	2545	5784	5784
iodothyronine deiodinase type II	L42815	5	0.00	0.00	2545	2545	3552	2545	2545	2545	2545	2545	2545
retinoic acid converting enzyme	AF057566	6	0.00	0.66	2545	2545	14112	2545	2545	12510	12064	20263	20263
mitochondrial cytochrome c oxidase subunit I	M10217	6	1.02	0.66	3767	2545	14112	3767	2545	2545	4033	3789	3789
agrinase	D18303	6	1.22	0.46	2545	2545	5647	2545	2545	2013	2545	2545	2545
aldolase B	AF030822	6	0.00	0.15	2545	2545	2545	2545	2545	2013	2545	2545	2545
frizzled 7	AF159106	7	2.37	0.25	2799	2545	9191	2545	2799	538	4820	5298	5298
hsp 30	U44894	7	1.78	0.78	23	52	115	115	107	112	112	112	112
proteasome subunit XC3	S51111	8	3.11	0.23	3337	2300	12943	3337	4423	4423	28	28	28
rat serpin Hense	X12948	3	1.21	0.00	5963	13165	5963	5963	2545	4699	4699	4699	4699
C/EBP	S44193	4	1.21	47.58	4814	10628	4814	4251	2545	3464	12336	2545	2545
nuclear factor I-C1	L43149	4	1.21	21.59	4982	11000	4982	4251	3464	95259	95259	4251	4251
RNA pol I transcription factor UBF	X57561	4	1.21	0.71	9845	4459	4459	3849	7740	9708	7740	85288	85288
beta factor 1	AF101387	4	1.06	1.77	5041	11129	5750	85288	19413	170472	170472	12488	12488
NK-2 homolog	S65507	4	1.21	0.75	4526	9993	4526	12488	3894	13208	13208	44005	44005
DLA	L09728	4	1.21	1.51	4135	9128	4135	44005	10721	70996	44005	44005	44005
POU2	U17634	4	1.21	1.88	6188	13662	6188	20989	6490	45911	20989	79400	79400
z/2	U57453	2	1.21	1.53	6024	13300	6024	78400	4783	124795	45911	34211	34211
mitotic phosphoprotein 90	U95102	2	1.21	1.75	4376	9662	4376	34211	4901	64720	9504	9504	9504
myosin heavy chain 3	AF097906	9	1.19	2.76	17255	38097	17545	2545	28757	9504	9504	9504	9504
alpha skeletal actin	X03470	9	0.55	0.63	1623	1027	1133	1636	1434	752	1434	1434	1434
cytoplasmic beta actin	AF079161	9	0.35	0.37	3165	3174	3165	5438	4105	6885	5438	5438	5438
alpha 1 collagen type I	AB015440	9	0.80	0.82	4878	10769	7201	30217	6881	37277	30217	30217	30217
alpha 2 collagen type I	D88764	9	0.76	1.04	5712	12611	9648	29741	31131	62302	31131	31131	31131
thymidyl hormone-binding protein	U03878	5	1.20	1.20	6004	13258	6042	4558	11307	6302	5446	5446	5446
SPARC	X62483	5	1.13	0.40	7492	18340	8016	6466	7194	5784	5784	5784	5784
SEFRC	X89476	8	0.00	2.34	2545	2545	2545	2545	2545	9019	2545	2545	2545
cyclin D2	D15059	8	1.21	0.00	4822	10646	4822	2545	5082	4495	4788	4788	4788
DAD-1	AB018169	8	1.21	0.12	5081	11217	5081	2916	5082	4495	4788	4788	4788
capsase-6	AF072455	8	1.21	0.15	8184	18069	8184	2916	5082	4495	4788	4788	4788
gelsolin B (VAMP-9)	X63009	3	1.21	0.97	6530	14418	6530	2916	5082	4495	4788	4788	4788
iodothyronine deiodinase type II	L42815	5	1.21	0.62	9365	20677	9365	2916	5082	4495	4788	4788	4788
retinoic acid converting enzyme	AF057566	5	1.08	1.33	4118	9092	4118	2994	5092	4495	4788	4788	4788
mitochondrial cytochrome c oxidase subunit I	M10217	6	1.21	2.03	11198	24724	12510	15868	34817	2545	15868	15868	15868
agrinase	D38303	6	1.21	5.31	4219	9314	4219	12781	75711	7902	12781	12781	12781
aldolase B	AF030822	6	1.21	1.10	4177	9221	4177	24103	19154	24103	24103	24103	24103
frizzled 7	AF159106	7	1.13	0.59	4952	10933	5298	47819	87352	87352	67885	67885	67885
hsp 30	U44894	7	7.23	2.08	268	2203	268	371	48	820	371	371	371
proteasome subunit XC3	S51111	8	1.21	4.52	5384	11887	5384	4078	22537	4085	4085	4085	4085